



TALLINN UNIVERSITY OF TECHNOLOGY

SCHOOL OF ENGINEERING

Department of Civil Engineering and Architecture

**EXAMINING THE SEA LEVEL VARIATION AND
PERFORMANCE OF ALONG TRACK MULTI-MISSION
SATELLITE ALTIMETRY**

**SATELLIITALTIMEETRIA ANDMETEL PÕHINEVA
MEREPINNA KÕRGUSE TÄPSUSE KINDLAKS MÄÄRAMINE
ERINEVATE ANDMESTIKE KOOSMÕJUL**

MASTER'S THESIS

Student:

Lenne-Liisa Heinoja

Student code:

204069EAXM

Supervisors:

Dr. Nicole Delpeche-Ellmann

Prof. Artu Ellmann

Tallinn 2022

AUTHOR'S DECLARATION

Hereby I declare, that I have written this thesis independently.

No academic degree has been applied for based on this material. All works, major viewpoints and data of the other authors used in this thesis have been referenced.

"....." 20....

Author:

/signature /

Thesis is in accordance with terms and requirements

"....." 20....

Supervisor:

/signature/

Accepted for defence

".....".....20... .

Chairman of theses defence commission:

/name and signature/

Non-exclusive licence for reproduction and publication of a graduation thesis¹

I _____ (author's name)

1. grant Tallinn University of Technology free licence (non-exclusive licence) for my thesis

(title of the graduation thesis)

supervised by _____,

(supervisor's name)

1.1 to be reproduced for the purposes of preservation and electronic publication of the graduation thesis, incl. to be entered in the digital collection of the library of Tallinn University of Technology until expiry of the term of copyright;

1.2 to be published via the web of Tallinn University of Technology, incl. to be entered in the digital collection of the library of Tallinn University of Technology until expiry of the term of copyright.

2. I am aware that the author also retains the rights specified in clause 1 of the non-exclusive licence.

3. I confirm that granting the non-exclusive licence does not infringe other persons' intellectual property rights, the rights arising from the Personal Data Protection Act or rights arising from other legislation.

_____ (date)

¹ The non-exclusive licence is not valid during the validity of access restriction indicated in the student's application for restriction on access to the graduation thesis that has been signed by the school's dean, except in case of the university's right to reproduce the thesis for preservation purposes only. If a graduation thesis is based on the joint creative activity of two or more persons and the co-author(s) has/have not granted, by the set deadline, the student defending his/her graduation thesis consent to reproduce and publish the graduation thesis in compliance with clauses 1.1 and 1.2 of the non-exclusive licence, the non-exclusive license shall not be valid for the period.

THESIS TASK

Student: Lenne-Liisa Heinoja, 204069EAXM

Study programme, main speciality: EAXM15/18 - Hooned ja rajatised, ehitusgeodeesia

Supervisor(s): PhD, Nicole Delpeche-Ellmann, (+372) 6204167

Prof. Artu Ellmann, (+372) 6202603

Thesis topic:

Examining the sea level variation and performance of along-track multi-mission satellite altimetry

Satelliitaltimeetria andmetel põhineva merepinna kõrguse täpsuse kindlaks määramine erinevate andmestike koosmõjul

Thesis main objectives:

1. Examine and compare satellite altimetry derived sea level height values for three different satellite missions – Sentinel-3A, Sentinel-6A and Jason-3
2. Examine satellite altimetry derived sea level height for along-track and near coast perspective
3. Evaluate and examine sea level variation in the Gulf of Finland

Thesis tasks and time schedule:

No	Task description	Deadline
1.	Collecting and processing the data	01.03.2022
2.	Preliminary analysis of the results	01.04.2022
3.	Submission of the complete draft	01.05.2022

Language: English **Deadline for submission of thesis:** ".....".....20....a

Student: ".....".....20....a
/signature/

Supervisor: ".....".....20....a
/signature/

Supervisor: ".....".....20....a
/signature/

Head of the study programme:
..... ".....".....20....a
/signature/

Terms of thesis closed defence and/or restricted access conditions to be formulated on the reverse side

Table of Contents

List of Figures	8
List of Tables	10
1. Preface/Research activity	11
2. List of Abbreviations and Symbols	12
3. Introduction.....	14
3.1 Objective and outline of thesis.....	17
4. Study area	19
4.1 The Baltic Sea and the Gulf of Finland	19
4.2 Sea ice	21
4.3 River discharge	22
5. Principles of satellite altimetry, used satellites.....	24
5.1 Sentinel-3.....	26
5.2 Sentinel-6.....	28
5.3 Jason-3	29
6. Geoid models, Hydrodynamic models and tide gauges	31
6.1 Hydrodynamic models	31
6.1.2 Nemo Nordic hydrodynamic model	32
6.1.2 HIROMB- EST	33
6.2 Geoid model NKG2015	34
6.3 Land uplift model NKG2016LU	35
6.4 Tide Gauges.....	36
7. Method	39
7.1 Vertical Datums.....	39
7.2 Time variance	40
7.3 Determining Dynamic Topography	41
7.4 Correcting the vertical datum of Hydrodynamic Models.....	43

7.5 Calculating the Root Mean Square Error.....	45
7.6 Data processing for all the satellite missions	45
8. Satellite Altimetry Corrections	47
9. Results.....	53
9.1 Along-track perspective	53
9.1.1 Sentinel-3A	53
9.1.2 Sentinel-6A	65
9.1.3 Jason-3	69
9.2 Near coast perspective	71
9.2.1 Sentinel-3A	71
9.2.2 Sentinel-6A	73
9.2.3 Jason-3	75
10. Discussion	78
11. Conclusion	81
12. Abstract	83
13. Kokkuvõte (in Estonian)	84
14. References.....	85
15.1 Results for the track of 0511 (Sentinel-3A)	91
15.2 Results for the track of 0397 (Sentinel-3A)	94
15.3 Results for the track of 0083 (Sentinel-3A)	97
15.4 Results for the track of 0414 (Sentinel-3A)	99
15.5 Results for the track of 0528 (Sentinel-3A)	102
15.6 Results for the track of 0739 (Sentinel-3A)	105
15.7 Results for the track of 0197 (Sentinel-3A)	108
15.8 Results for the track of 0311 (Sentinel-3A)	111
15.9 Results for the track of 0625 (Sentinel-3A)	114
15.10 Results for the track of 0425 (Sentinel-3A).....	117
15.11 Results for the track of 0111 (Sentinel-6A and Jason-3).....	120
15.12 Results for the track of 0168 (Sentinel-6A and Jason-3).....	124

15.13 Results for the track of 0187 (Sentinel-6A and Jason-3).....	128
15.14 Results for the track of 0092 (Sentinel-6A and Jason-3).....	132
15.15 Results for the track of 0016 (Sentinel-6A and Jason-3).....	136

List of Figures

Figure 3.1 Involved data types and interrelations between them. Visual of different vertical reference datums (Jahanmard et al., 2021)	16
Figure 4.1 The Baltic Sea and it's sub-basins (BMEPC, n.d.).	20
Figure 4.2 Extreme case of the coverage of sea ice (shown in white) in the Baltic Sea (FMI, n.d.).....	21
Figure 4.3 The Baltic Sea and its seven largest rivers (HELCOM, 2018).	22
Figure 4.4 Gulf of Finland including its largest rivers Neva, Kymi (Kymijoki), Narva and Luga (Emelyanov et al., 2017).....	23
Figure 5.1 Family tree of Sentinel-6 Micheal Freilich including Sentinel-3 and Jason-3. ..	25
Figure 5.2 Satellite tracks of Sentinel-3A, Sentinel-6A and Jason-3 passing over the Gulf of Finland.	26
Figure 5.3 Sentinel-3A tracks over the Gulf of Finland.	27
Figure 5.4 Sentinel-6 tracks over the Gulf of Finland.	29
Time difference of track measurement between Jason-3 and Sentinel-6 is about 2 minutes.	30
Figure 5.5 Jason-3 tracks over the Gulf of Finland.....	30
Figure 6.1 The sea level according to the Nemo-Nordic hydrodynamic model for 03.01.2018 01:00:00 AM.	32
Figure 6.2 The sea level according to the HBM-EST hydrodynamic model for 01.11.2018 01:00:00 AM.	33
Figure 6.3 Section of NKG2015 at the Gulf of Finland and Estonia.	34
Figure 6.4 Land uplift according to NKG2016LU model (Vestøl, et al., 2016).	35
Figure 6.5 Tide gauges at the coast of Gulf of Finland.	37
Figure 7.1 Process of deriving DT for satellite altimetry sea level track of 0083 (Sentinel-3A), passing date: 06.01.2017.....	40
Figure 7.2 a) Process of interpolation for the track of 0414 (Sentinel-3A). The 1 x 1nm gridded data represents a HBM model, whereas satellite pass footprints are denoted with red dots; b) Interpolated (blue arrows) data example to find the hydrodynamic model (blue dots) values along the satellite track (red dots) footprint.	41
Figure 7.3 Data processing to correct VLM to the TG values.	43
Figure 7.4 Example of tide gauges of both Estonian (vertical datum: EH2000) and Finnish (vertical Datum: N2000) coast as well as corresponding original HDM at the same moment with corrected HDM.	44

Figure 7.5 Data processing using satellite missions, tide gauges, hydrodynamic models, marine geoid and land uplift model for general processing (green) and unique to this thesis (orange).	46
Figure 8.1 Satellite altimetry corrections (Snaith et al., 2006).	47
Figure 8.2 Dynamic atmosphere correction of track 0625 (Sentinel-3A).	49
Figure 8.3 Ocean tide correction for the track of 0625 (Sentinel-3A).	50
Figure 8.4 a) Wet Tropospheric Correction for the track of 0111 (Sentinel-6A); b) Dry Tropospheric Correction for the track of 0111 (Sentinel-6A).	51
Figure 9.1 a) Tide gauge values throughout the year of 2018. TGs used are Heltermaa, Helsinki, Kunda and Hamina; b) Tracks of Sentinel-3A.	55
Figure 9.2 Example of a track of 0425 at the date of 19.05.2018. The height represents DT in the vertical axis.	55
Figure 9.3 Example of a track of 0083 at the date of 27.07.2018. The height represents DT in the vertical axis.	56
Figure 9.4 a) Track 0625 and used stations of Pirita and Helsinki; b) Track 0425 and station Kronstadt.	57
Figure 9.5 Ice-chart from 23.03.2018 which possibly explains why there were large RMSE values during March 2018.	58
Figure 9.6 Tracks of (left to right) 0414, 0197, 0528 and 0311 and the stations of Kunda, Narva-Jõesuu, Kronstadt and Hamina.	59
Figure 9.7 a) Tracks of 0528 on 25.12.2018, when the minimum RMSE occurred. The height represents DT in the vertical axis.	60
Figure 9.7 b) Tracks of 0414 on 21.12.2018, when the minimum RMSE occurred. The height represents DT in the vertical axis.	60
Figure 9.8 a) Tide gauge values throughout the year of 2021-2022. TGs used are Heltermaa, Helsinki, Kunda and Hamina.	66
Figure 9.8 b) Tracks of Sentinel-6A and Jason-3.	66
Figure 9.9 Tracks of Sentinel-6A and Jason-3, which pass over the Gulf of Finland. The track of 0111 is marked by yellow marker.	67
Figure 9.10 Example of a track of 0016 at the date of 29.12.2021. The height represents DT in the vertical axis.	68
Figure 9.11 Example of a track of 0111 at the date of 02.01.2022. This example shows how the tracks were analysed to all passes.	69
Figure 9.12 Example of the track of 0625 with usable and unusable datapoints.	72
Figure 9.13 Example of the track of 0016 with usable and unusable datapoints.	74

List of Tables

Table 5.1 Satellite mission of Sentinel-3A, Sentinel-6A and Jason-3 and their key characteristics.	25
Table 6.1 Summary of types of data used for each satellite mission.	31
Table 8.1 All corrections which are added to the satellite mission tracks.	52
Table 9.1 Values gathered from analysing root mean square error from the satellite mission of Sentinel-3A from 2018.	60
Table 9.2 Values gathered from analysing root mean square error from the satellite mission of Sentinel-6A from November 2021 – February 2022.....	61
Table 9.3 Values gathered from analysing root mean square error from the satellite mission of Jason-3 from November 2021 – February 2022.	62
Table 9.4 Values gathered from analysing tide gauges and hydrodynamic model from the satellite mission of Sentinel-3A from 2018.....	63
Table 9.5 Values gathered from analysing tide gauges and hydrodynamic model from the satellite mission of Sentinel-6A from November 2021 – February 2022.	64
Table 9.6 Values gathered from analysing tide gauges and hydrodynamic model from the satellite mission of Jason-3 from November 2021 – February 2022.....	64
Table 9.7 Values gathered from analysing data points from the satellite mission of Sentinel-3A from 2018.	73
Table 9.8 Values gathered from analysing data points from the satellite mission of Sentinel-6A from November 2021 – February 2022.....	75
Table 9.9 Values gathered from analysing data points from the satellite mission of Jason-3 from November 2021 – February 2022.	76
Table 10.1 Summary of the values gathered during data processing.	79

1. Preface/Research activity

First and foremost, I would like to thank my supervisors Dr. Nicole Delpeche-Ellmann and Prof. Artu Ellmann, who were very supportive and helpful during writing this thesis. I would also like to thank them for providing me an opportunity to present my first results of this research as a poster presentation at the Gulf of Finland Science Days 2021, organized by the Estonian Academy of Sciences in November 2021 in Tallinn.

This study was supported by the Estonian Research Council grant for Development of an iterative approach for near-coast marine geoid modelling by using re-tracked satellite altimetry, in-situ and modelled data (Grant no. PRG330) and PRG 1129.

2. List of Abbreviations and Symbols

Abbreviations:

ASL	Absolute Sea Level
BMEPC	Baltic Marine Environment Protection Commission
BSCD2000	Baltic Sea Chart Datum 2000
BSH	Bundesamt Für Seeschifffahrt und Hydrographie
DORIS	Doppler Orbitography and Radiopositioning Integrated by Satellite
DT	Dynamic Topography
EEA	European Environmental Agency
EM	electromagnetic
ETRS 89	European Terrestrial Reference System 1989
EUMETSAT	The European Organisation for the Exploitation of Meteorological Satellites
EVRS	European Vertical Reference System
FMI	Finnish Meteorological Institute
GNSS	Global Navigation Satellite System
HBM	HIROMB-BOOS
HBM-EST	Estonian implementation of the HIROMB-BOOS model
HBV	river run-off model Hydrologiska Byråns Vattenbalansavdelning
HDM	Hydrodynamic Model
Lev	leveled
LRM	low resolution mode
LU	land uplift
NAP	Normaal Amsterdam Peil
NEMO	Nucleus for European Modelling of the Ocean
NKG	Nordic Geodetic Commission (Nordiska Kommissionen för Geodesi)
NRT	Near-Real Time
NTC	Non Time Critical
RMSE	root mean square error

SA	Satellite Altimetry
SAR	Synthetic Aperture Radar
SLA	Sea-Level Anomaly
SRAL	Synthetic Aperture Radar Altimeter
STC	Short Time Critical
SSH	Sea Surface Height
T/P	Topex-Poseidon
TG	Tide Gauge
VLM	Vertical Land Motion

3. Introduction

The Earth's climate is changing due to both natural and anthropogenic causes, this results in rising Earth's temperature both on land and sea to rise. There are two major causes, which affect the warming of the ocean – thermal expansion and increased land-based ice melting, such as glaciers and ice sheets (NOAA, n.d.). As a result of these climate changes, it is now imperative that sea level is determined with the best accuracy possible.

Sea level can be interpreted in many ways, for example through absolute sea level, global sea level, mean sea level etc. Two main terminologies used is that of: (i) absolute sea level which represents height of the ocean surface above the center of the Earth (e.g., above a mathematically determined reference ellipsoid) and (ii) relative sea level which represent height of the ocean relative to the land at a particular location. It has been stated by the European Environment Agency (EEA) in 2021, that there is an average of 3 to 5 millimeters relative sea level rising in the Baltic Sea. However due to post-glacial rebound the land uplift is still occurring around northern Europe (e.g., such as Norway and Sweden), and the relative sea level along the coastlines of Finland, Sweden and Norway continue to decrease at a rate of around 4 mm/year. Meanwhile, relative sea level around the Baltic countries (Estonia, Latvia and Lithuania) has been rising on average 3-4 millimeters/year. In general, the projected relative sea level change during 21st century is varying around 0.4-0.6 m (EEA, 2021). Thus, depending on the perspective one can obtain quite contrasting sea level results. Also, accurate quantification of sea level relies not only on relative versus absolute and the vertical reference datum used but also on the limitations of different sources.

Various sources of sea level data are often utilized such as tide gauge records (TG), satellite altimetry (SA) and hydrodynamic models (HDM). These sources however are often limited in their capabilities by different resolutions (in both space and time) and dissimilar or unknown vertical reference datums (Jahanmard et al., 2021). Tide gauges are typically (and also in this study) referenced to a geoid or chart datum. With respect to hydrodynamic models the vertical datum is often undisclosed.

Satellite altimetry however is an advancing technology, which is being constantly updated and perfected over different satellite missions and novel technology. It also happens to be one of the most accessible data sources for sea level with the vertical reference being that of the ellipsoid.

The basic methodology of satellite altimetry measurement is that the distance of the altimeter to the target (liquid) surface is determined by radar pulses transmitted towards the sea surface and records of the time which it takes for the pulses to return (NOAA, n.d.).

Satellite altimetry has been used for the last 29 years and the SA is still a continuously developing technology. Currently (as of year 2022), there are 8 satellites altimeter missions observing the Earth (CryoSat-2, HY-2A, SARAL, Sentinel-3, Jason-3, HY-2B, Sentinel-6, SWOT) (Grgic & Bašić, 2021). With satellite missions being operational and with new advanced features, it is important to examine the performance of some of the newest satellite missions to determine if the new advances implemented actually improves the accuracy and quality of sea level data. In particular this thesis focuses on examination of the Sentinel-3A, Jason-3A and the recently (in 2020) launched Sentinel-6A mission. It should be noted that these chosen satellite missions have different characteristics and corrections that are applied. A more detailed description is presented in chapters 5 and 8 of this thesis.

As mentioned above, the sea level variation can be interpreted in many ways (e.g., absolute and relative) and also various sources often refer to different vertical reference surface (e.g., ellipsoid mean sea level (MSL) etc.). To actually obtain realistic variation in sea level requires a more stable and practical vertical reference, like the geoid is recommended (Fig 3.1). The geoid represents the shape of the equipotential ocean surface under the influence of the gravity and rotation of Earth alone (i.e., without the influence of winds, tides etc.). The importance of accurately defining the geoid is that the dynamic topography (DT) can now be derived by using satellite altimetry instantaneous sea surface height (SSH). This can be calculated by subtracting the satellite range from the geoid (N). This concept is illustrated in Fig. 3.1. Using DT information about the changes in ocean circulation, eddies, influence of winds and waves can be extracted as signals from both low- and high-frequency (GGOS, n.d.).

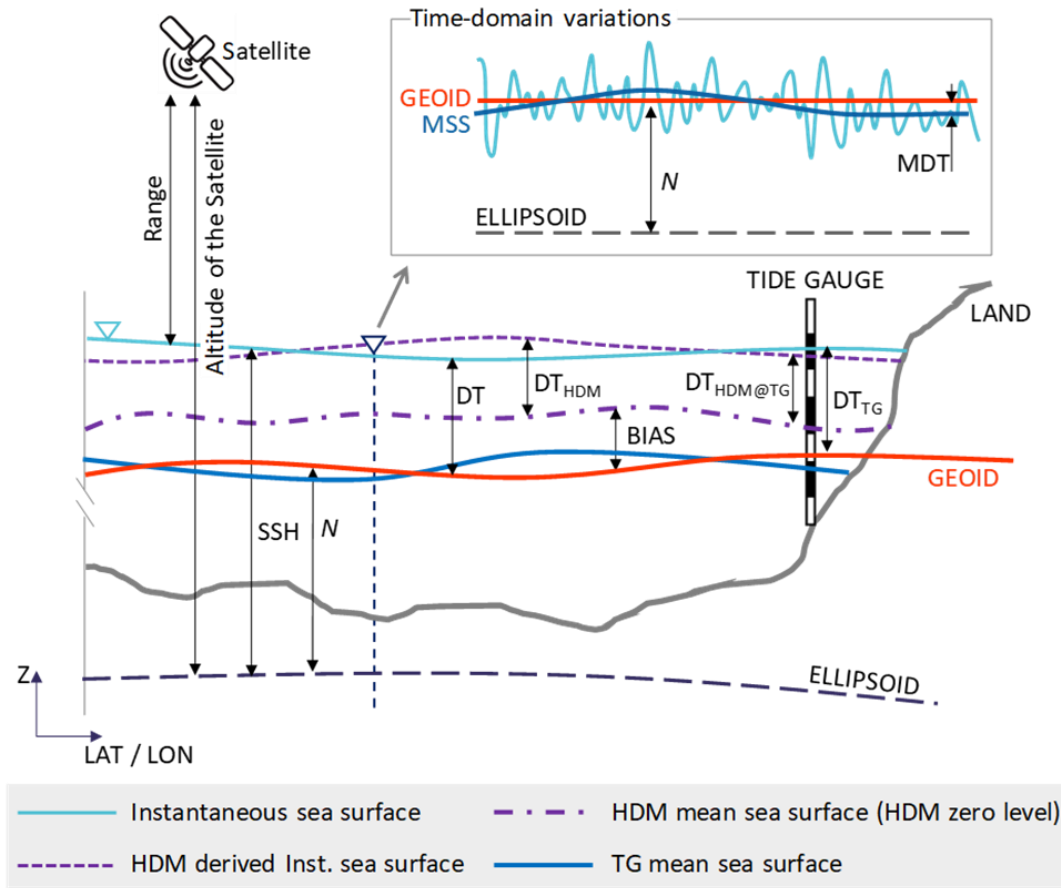


Figure 3.1 Involved data types and interrelations between them. Visual of different vertical reference datums (Jahanmard et al., 2021)

It should be considered that many sea level studies often do not have access to an accurate and high-resolution geoid so instead of determining DT a sea-level anomaly *SLA* is often derived. This *SLA* defined as the height of water over the mean sea surface in a given time and region (ECMWF Support Portal, n.d.) i.e., $SLA = SSH - MSS$, where *MSS* is some determined mean sea surface (GGOS, n.d.).

DT and *SLA* are quite different terms. With *SLA*, the inclusion of *MSS* implies that small scale variations in sea levels are smoothed out, whilst with DT they are still included. This implied that from using DT it is possible to obtain sub-mesoscale dynamics of the ocean.

In this thesis the eastern Baltic Sea is used as a study site. The Baltic Sea is semi-closed sea and is located in Northern Europe and is surrounded by nine countries. It's northern and coastal regions have seasonal sea-ice coverage and it has irregular coastlines with many islands and islets (Passaro et al., 2021). Due to these characteristics and varying sea level

dynamics of the Baltic Sea, it is important to assess how accurate is the SA derived sea level data in the region. Thus, this research focuses on examining the performance of multi-mission satellite altimetry data in the eastern section of Baltic Sea – the Gulf of Finland.

Previous studies have examined satellite altimetry derived data and sea surface height. For instance, Mostafavi et al. (2021) reported the accuracy for JA3 was 8.5-7.7 cm and for S3 re-tracker was 3.9-5.0 cm. Whilst in Birgiel et al. (2019) reported that Sentinel-3 an accuracy that varied from 5.2-19.9 cm and 6.4-13.5 cm. These studies used different time periods and also different technological advances in satellite processing. Regardless the Sentinel-3A results shows promising results at near-coast marine areas. This study utilizes a somewhat similar method but instead of using SSH we now derive the DT to actual examine the realistic sea level variation, in addition this study also explores one of the newest satellite altimetry missions i.e., the Sentinel-6.

Satellite Sentinel-6 Micheal Freilich has been measuring the Earth from the ending of 2020, but its high-resolution data was only available from November 2021 (ESA, n.d.). There has not been a wide research or studies on the performance and accuracy of Sentinel-6 satellite altimetry derived dynamic topography and it is expected that the results of this study can be used for further improvements in sea level determination.

3.1 Objective and outline of thesis

This thesis examines the performance of three different satellite missions, Sentinel-3A, Jason-3 and Sentinel-6A, at two different time periods – for Sentinel-3A the year of 2018 and for the Sentinel-6A and Jason-3 the ending of the year 2021 and beginning of 2022. With the newest contribution being examining the latest Sentinel-6A satellite mission and compare the results to Jason-3 satellite mission because they pass over the Gulf of Finland at the same track with around 2 minutes apart. To compare the performance of all three satellite missions two aspects are explored:

1. Along-track perspective – compare satellite altimetry and hydrodynamic models to determine the realistic sea level data (i.e., DT) and the accuracy of the satellite altimetry.

2. Near coast perspective – to examine tide gauges and satellite altimetry sea level heights performance at near coast areas in terms of accuracy and quality of satellite data points on approaching the coast.

Scientific Questions

1. What is the sea level variation in the Gulf of Finland using satellite altimetry?
2. Do new satellite missions and re-trackers improve the accuracy of sea level data?
3. Do different satellite missions give better near coast performance in terms of quality of data points and distance to coast?
4. How well do satellite data compare to TG?

This research is examining the Gulf of Finland with three satellite missions; therefore, this thesis is sectioned as follows: Section 4 discusses the study area which is The Baltic Sea, specifically the Gulf of Finland, Section 5 and 6 provide further overview about each satellite mission and used geoid, land uplift, hydrodynamic models and tide gauges. Sections 7 and 8 concentrate on methodology and corrections. Section 9 shows viewer the results and summarizes the answers to these aforementioned questions.

4. Study area

In this thesis the Gulf of Finland located in the Baltic Sea is chosen as the study site to examine the multi-mission satellite altimetry sea level data. The Baltic Sea is an estuarine environment with numerous rivers flowing into it. Salt water usually infiltrates from the Atlantic Ocean via narrow Danish straits. The study site is a challenge for satellite altimetry for it contains many small islands and archipelagos that may contaminate the SA data. Sea ice is also present in the winter months and in some years can even almost completely cover the whole sea area.

4.1 The Baltic Sea and the Gulf of Finland

The Baltic Sea is located at northern Europe and is a semi-closed sea, which is surrounded by nine countries (Denmark, Germany, Poland, Lithuania, Latvia, Estonia, Russia, Finland and Sweden). The Baltic Sea has high density of marine traffic as well as coastal activities. The sea is divided into multiple sub-basins such as Bothnian Bay, Bothnian Sea, Northern Baltic Proper, Eastern and Western Gotland Basin, Gulf of Riga, Gulf of Gdansk, Gulf of Finland (Fig 4.1) etc. This study focuses on the Gulf of Finland, which is the most eastern sea section of the Baltic Sea. It is narrow and elongated – its length approximately 400km and width 48-135 km, mean water depth is around 38 meters and maximum water depth is 123 meters (Mostafavi et al., 2021).

Gulf of Finland sea level dynamics are affected by changes in water balance, which can be caused by different atmospheric conditions such as winds, river runoff from the countries that surround the Gulf of Finland as well as the presence of sea ice. Seasonal and short-term variability are also affected by storm surges, coastal upwellings etc. The Gulf of Finland has a higher mean sea level which is influenced by prevailing southwest wind, river discharge (influenced mostly by the Neva River, which is also the largest river in the BS). Mean sea surface topography in the GOF is from 20-29 centimeters (averaged over 2014-2019) and occurs mostly in the eastern section of the GOF (Kollo & Ellmann, 2019) and extreme sea level has been measured 4.21 meters and was recorded in 1824 (Wolski et al., 2014). The

largest differences in standard deviation of spatial accuracy occurs in the winter and spring. The variability of Mean Dynamic Topography (MDT) across the GOF from west to east was -12.7 to -8.2 centimeters (Jahanmard et al., 2021). Wave height is typically ranging from 0.5-0.8 m, maximum wave height being 5.2 meters (Soomere et al., 2008).

The Gulf of Finland is surrounded by three countries – Estonia, Finland and Russia. The GOF has cliff-like or low-lying coastline with multiple peninsulas. Coastal area has several archipelagos, islands and rocks within 10 km from the coast. The Gulf of Finland has precise tide gauge (TG) network, which has high-quality geodetic infrastructure. All together the GOF is surrounded by 8 tide gauges (Mostafavi et al., 2021).

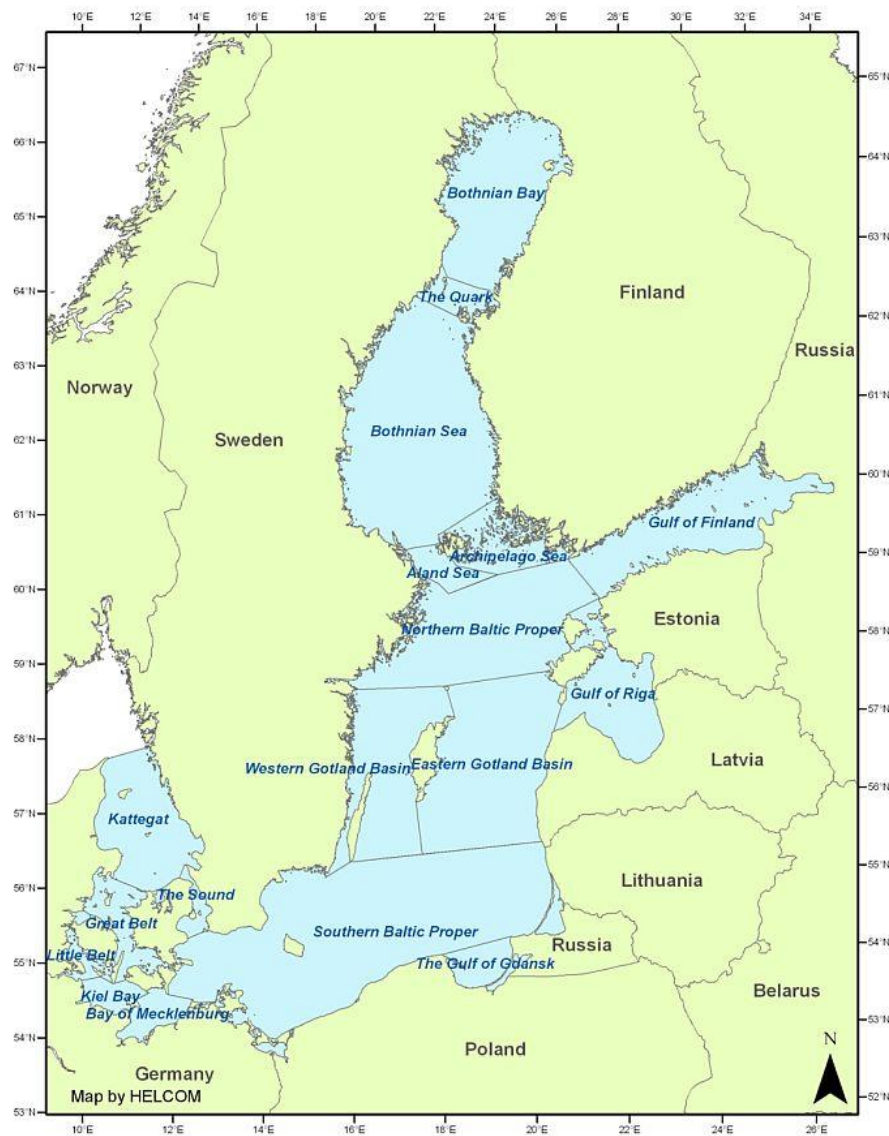


Figure 4.1 The Baltic Sea and it's sub-basins (BMEPC, n.d.).

4.2 Sea ice

Due to its shape, the Baltic Sea has diverse sea ice conditions. The area of BS ice cover in January until March is the largest. On average, almost 40% of the Baltic Sea area (422 000 km², including Kattegatt and Skagerrak near Danish straits (Fig. 4.1)) is covered in ice, which is approximately 170 000 km² (FMI, n.d.).

The sea first freezes in October-November along the coasts of the northern Bothnian Bay and inner Gulf of Finland. Then the freezing spreads towards the Quark (between Bothnian Bay and Bothnian Sea). Normally, the ice also covers the rest of the Bothnian Sea, the Archipelago Sea and whole Gulf of Finland and some parts of the northern Baltic Proper (FMI, n.d.). For some extreme cases, the whole Baltic Sea can be mostly covered by ice (Fig. 4.2), for example in 2011 it was recorded that over 309 000 km² of the Baltic Sea was covered with ice. There are different types of sea ice present during the winter, e.g., very open ice, open ice, close ice, very close ice, rotten ice, level ice, fast ice and new ice. These terms are based on the concentration of the ice at the sea – open water is defined as concentration less than 1/10 to compact ice which is defined as concentration of 10/10. New ice is ice, which is newly frozen; fast ice is fastened along the coast and rotten ice is ice, which is disintegrating and starting to melt. An example is provided in the section of “Results” in the Figure 9.6.

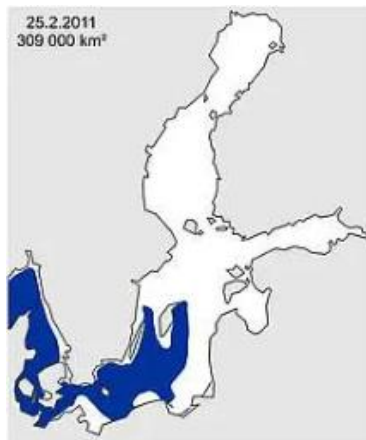


Figure 4.2 Extreme case of the coverage of sea ice (shown in white) in the Baltic Sea (FMI, n.d.).

For the year of 2018 the maximum ice extent in the Baltic Sea was 170 000 km² (FMI, n.d.). Currently there is no information about the year of 2021-2022.

4.3 River discharge

There are numerous rivers that flow to the Baltic Sea, the seven largest are Göta (Sweden), Kemi (Finland), Daugava (Latvia), Nemunas (Lithuania), Oder (Germany), Vistula (Poland) and Neva (Russia) (Fig. 4.3). Around 112 km^{3/a} river water is estimated that Gulf of Finland receives (GOF Team, 2014).



Figure 4.3 The Baltic Sea and its seven largest rivers (HELCOM, 2018).

The Neva River at the eastern end of the Gulf of Finland is the largest single freshwater river which flows into the Baltic Sea. River Neva’s average discharge is 2432 m³/s (from 1996 to 2014) with the range variation of 861-3650 m³/s. Neva’s contribution to the river runoffs to the Gulf of Finland is about 67%. The minimum river discharge is in the winter and maximum is in the spring, which could be caused by the ice freezing and melting. Other major rivers with significant river discharge are Kymi, Narva and Luga (Fig. 4.4). 89% of total river runoff

to the Gulf of Finland is by the rivers of Neva, Kymi, Narva and Luga and average discharge by mentioned rivers all together is about $100 \text{ km}^3/\text{a}$. When examining the results and evaluating them it is important to consider river discharge as well as a major contributor to the coastal and offshore area (GOF Year 2014 Team, 2014).

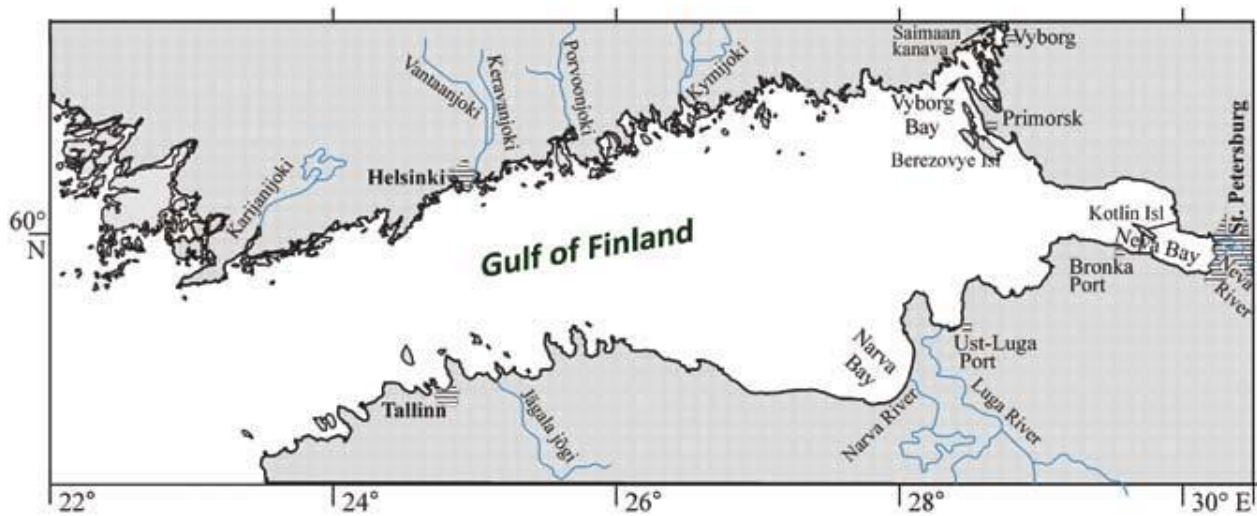


Figure 4.4 Gulf of Finland including its largest rivers Neva, Kymi (Kymijoki), Narva and Luga (Emelyanov et al., 2017).

The 2017/2018 hydrological year started with a lot of precipitation, but the spring high water remained rather modest. The flow of the spring high water period is less than the long-term average flow of the high-water period. The summer was characterized by low rainfall and high air temperatures (Estonian Environmental Agency, 2018). For the year of 2021/2022 there has been no annual report of river discharge.

5. Principles of satellite altimetry, used satellites

Altimetry satellites have an onboard tracker, which calculates the echo from the target surface to the altimeter. The distance, which the tracker calculates, is first approximation – actual sea surface height might be mistaken by the influence of rocks, marine traffic, land and infrastructure etc. Coastal re-trackers are specially developed to determine and eliminate any possibility of land contamination or other interference from the actual sea surface height in near coast areas. Those re-trackers are tuned according to local conditions and are expected to deliver more accurate near-coast sea surface height (Mostafavi et al., 2021). SAR-altimetry is a method to process and examine altimetry data and was first operated on CyroSat-2 mission, which launched in 2010 (Aviso+, n.d.). This technique has multiple benefits in which one of the best improvements lays in the resolution of the system along the satellite track. This benefit comes from improving the Doppler effect in the altimeter (Egido & Smith, 2017). The Synthetic Aperture Radar Altimeter is always operated by two modes – high-resolution mode and low-resolution mode (LRM). Satellite missions are also equipped with two different bands of wavelengths – Ku (13.575 GHz, bandwidth=350 MHz) and C (5.41 GHz, bandwidth=320 MHz) bands. Ku being the main frequency band used is being transmitted with complementing C band frequency, which is being used to correct delay errors due to varying density of electrons in the ionosphere (ESA, n.d.).

There are three different types of data products used to derive observations – near-time time (NRT), short time critical (STC) and non-time critical (NTC). In this thesis the NTC type of data product is used, because it has the highest quality data intended for climate studies and research and products are split by pass (from pole to pole) (ESA, n.d.).

The Sentinel-6A is processed in Level-2 SAR mode. Level-2 mode objective is to provide re-tracked altimeter ocean, coastal zones, ice sheet and sea-ice elevation estimates. It also provides geophysical corrections and environmental parameters as well as significant wave height and backscatter coefficient (ESA, n.d.).

Sentinel-6A and Jason-3 mean sea surface height is derived with two solutions. In this thesis the solution used is MSS_CNES_CLS2015. The CNES_CLS15 models are based on altimeter measurements from the open ocean. As a consequence, it is not defined in all regions where measurements are not available (Pujol, et al., 2018).

In this research Sentinel 3A, Sentinel 6A and Jason 3 satellite mission data is used (Table 5.1). Used satellites vehicles can be viewed in Figure 5.1, where the used satellite missions are circled in yellow (NASA, 2020) .

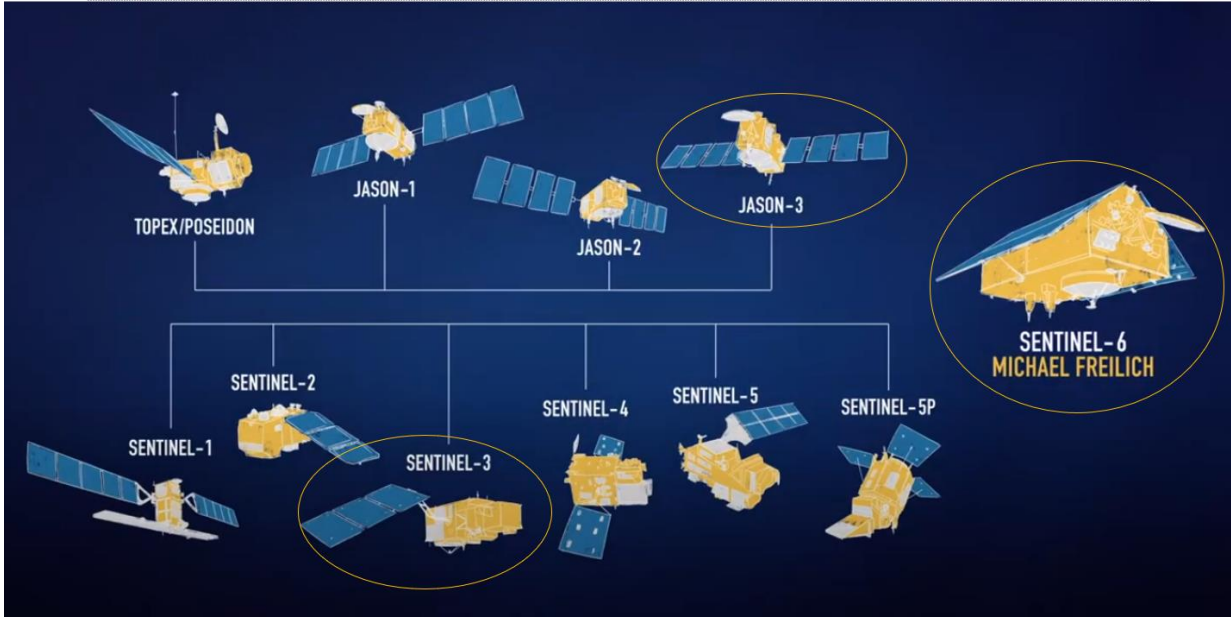


Figure 5.1 Family tree of Sentinel-6 Micheal Freilich including Sentinel-3 and Jason-3.

Table 5.1 Satellite mission of Sentinel-3A, Sentinel-6A and Jason-3 and their key characteristics.

Mission	Alti- meter	Mode	Re- tracker	Altitu- -de (km)	Incli- na- tion	Cycle pe- riod (days)	Along- track resolu- tion	Across- track resolu- tion
Sentinel-3A	SRAL	SAR	ALES+S AR	814.5	98.65°	27	~300 m	1.64 km
Sentinel-6A	Posei- don-4	SAR	Level-2	1336	66°	9.91	~300 m	10 km
Jason-3	Posei- don- 3B	LRM	Ocean ML4	1336	66.64°	9.91	~300 m	10 km

Figure 5.2 is an example of the Gulf of Finland and the mentioned satellite tracks, where red lines belong to the tracks of Sentinel-3A and blue tracks for Sentinel-6A/Jason-3.

5.2 Sentinel-6

Copernicus Sentinel-6 Michael Freilich is a new satellite which first launched at the end of 2020. There will be another satellite launched sequentially in 2025. Sentinel-6 is Earth Observation satellite mission, which main objective is to provide and continue to provide stable time series of mean sea level measurements and observations. Sentinel-6 is derived from Topex-Poseidon mission, which is continued by the Jason-1, Jason-2 and Jason-3 satellite missions. The satellite was designed, built and operated by European organizations, while NASA provided the launch of the vehicle (ESA, n.d.).

Copernicus Sentinel-6 Micheal Freilich mission has multiple objectives. One of them is to continue to provide data for Copernicus services and to overlap Jason satellite series. Also contribute to marine meteorology and provide observations of significant wave height and wind speed in near-real time which could be available and delivery timeliness. One of the objectives worth mentioning is also to support coastal oceanography and to build new techniques in radar altimetry and enhance the quality of measurements – especially in the near-coast areas (ESA, n.d.). Reprocessed standard data can be downloaded from EUMETSAT Earth Observation Portal <https://eoportal.eumetsat.int/>.

Sentinel-6A is a new satellite, which was launched in November 2020. Sentinel-6's Poseidon-4 altimeter provides high- and low-resolution mode measurements. The low-resolution are matched with Sentinel-6 mission's predecessor Jason-3 and it is to ensure the continuity of Jason satellite missions and the enhanced high-resolution data can be provided with absolute confidence (ESA, 2021). Poseidon-4 radar altimeter is equipped with a microwave radiometer (ESA, n.d.), which is derived from SAR altimeter mode of Sentinel-3 SRAL and CyroSat-3 SIRAL (isardSAT, n.d.). This means, that Sentinel-6A satellite holds improved re-tracker which should derive better results of measuring sea surface height.

Two products were released of the Sentinel-6: low-resolution and high-resolution data. Low-resolution data was released in the July of 2021 (over 60m/pixel), high-resolution data was released in the November of 2021 (30cm-5m/pixel) (ESA, 2021). In this research the high-resolution data is used and compared to the low-resolution mode data to assess the quality.

Sentinel-6 satellite pass cycle is in every 10 days and 5 tracks cover the Gulf of Finland. Since the high accuracy data of Sentinel-6 became available from November 2021, there has been only used 5 or 6 passes over the Gulf of Finland at the period on November 2021 – February 2022.

6. Geoid models, Hydrodynamic models and tide gauges

List of types of data

Hereby is a mention of all different types of data which has been processed to analyse the accuracy of SA dynamic topography (Table 6.1).

Table 6.1 Summary of types of data used for each satellite mission.

Data used for processing/Satellite	Sentinel – 3	Sentinel – 6–/ Jason - 3
Hydrodynamic Model	Nemo Nordic	HBM-EST
Geoid Model	NKG2015	NKG2015
Land uplift model	NKG2016 (for vertical land motion)	NKG2016 (for vertical land motion)
Tide Gauges	Estonian and Finnish	Estonian and Finnish
Year observed	01-12/2018	November, December 2021; January, February 2022
Number of tracks, that pass the Gulf of Finland	10	5
Repeat period	27 days	10 days

6.1 Hydrodynamic models

Hydrodynamic model gives sea level data in the sea area, but vertical datum is often unknown. By comparing tide gauges and hydrodynamic model, the HDM data can be corrected for the vertical datums issue. Comparison to corrected satellite altimetry data with the marine geoid model allows to determinate dynamic topography, which can be compared to the corrected hydrodynamic model data. In current thesis, it is called “corrected HDM” (more mentioned and analyzed in the “9. Results” section). Depending on the satellite mission different hydrodynamic models are used (Table 6.1).

6.1.2 Nemo Nordic hydrodynamic model

Nemo-Nordic hydrodynamic model is NEMO based ocean model, which is designed for the Baltic and North Sea and can be used for study of climate and oceanographic process and operational oceanographic applications. This specially designed model takes into account the variability of dynamics of the Baltic Sea and North Sea at various scales - taking into account the basins and sub-basins, overflows and sea ice (Hordoir, et al., 2019). The ocean model also includes the sea-ice module LIM3, which simulates ocean and sea-ice processes at various time and space scales (Rjazin et al., 2019).

Nemo-Nordic hydrodynamic model is used to visualize and analyse Sentinel-3 derived dynamic topography. Nemo-Nordic hydrodynamic model is calculated hourly; therefore, it is also important to choose the correct time of hydrodynamic model calculation depending on the satellite passing time (Fig. 6.1).

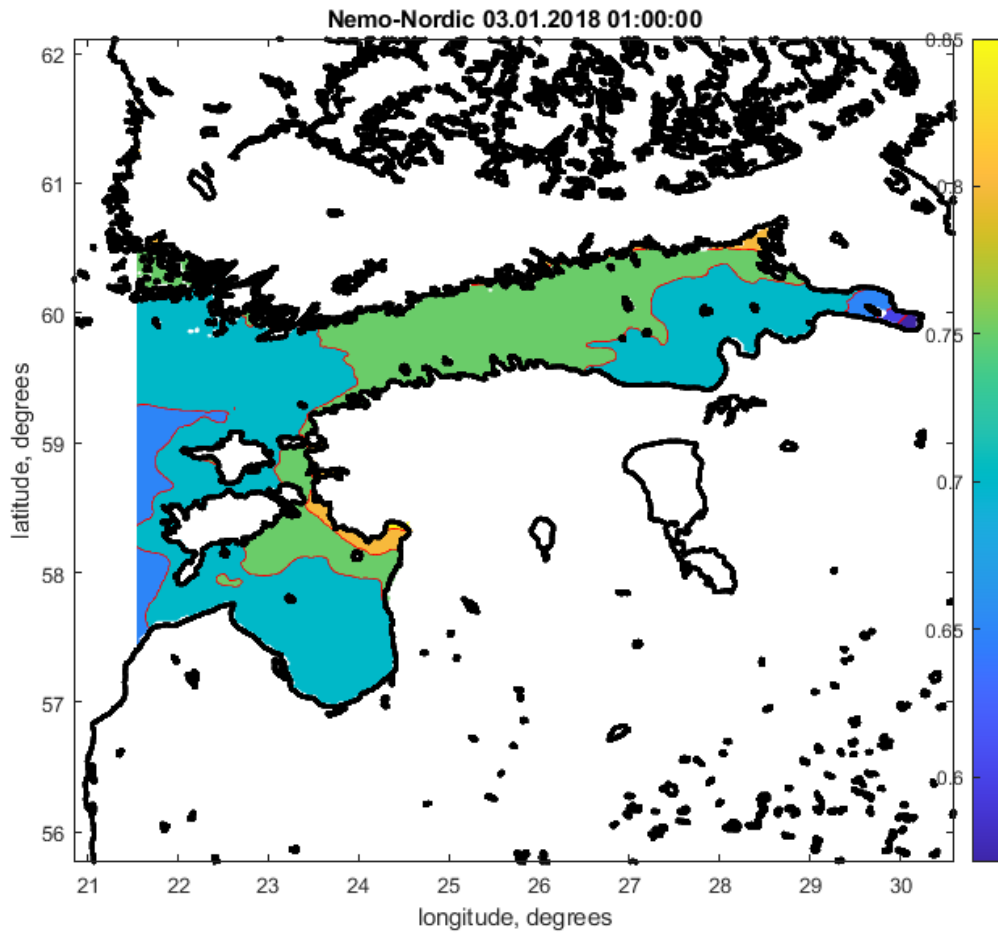


Figure 6.1 The sea level according to the Nemo-Nordic hydrodynamic model for 03.01.2018 01:00:00 AM.

6.1.2 HIROMB- EST

Another HDM used in this study is HIROMB-EST.

HIROMB-Boost HDM (HBM-EST) is developed in the Marine System Institute in Tallinn University of Technology. It is a three-dimensional baroclinic eddy-resolving circulation model and it is specially tuned to the Estonian waters. The horizontal resolution of the model is of 0.5 nautical miles. HBM-EST models open boundary is located at the Danish Straits. There are two models used to accurately correct the HDM model – a high resolution limited area model to examine atmospheric forcings (HIRLAM) and for freshwater inflow the daily data from the river runoff model HBV. Sea ice data was obtained from Louvain-la-Neuve sea ice model (LIM3) (Mostafavi et al., 2021). The HBM-EST data was retrieved from <http://emis.msi.ttu.ee>.

HBM-EST hydrodynamic model is used to visualize and analyze Sentinel-6 and Jason-3 derived dynamic topography. HBM-EST hydrodynamic model is calculated hourly; therefore, it is also important to choose the correct time of hydrodynamic model calculation depending on the satellite passing time (Fig. 6.2).

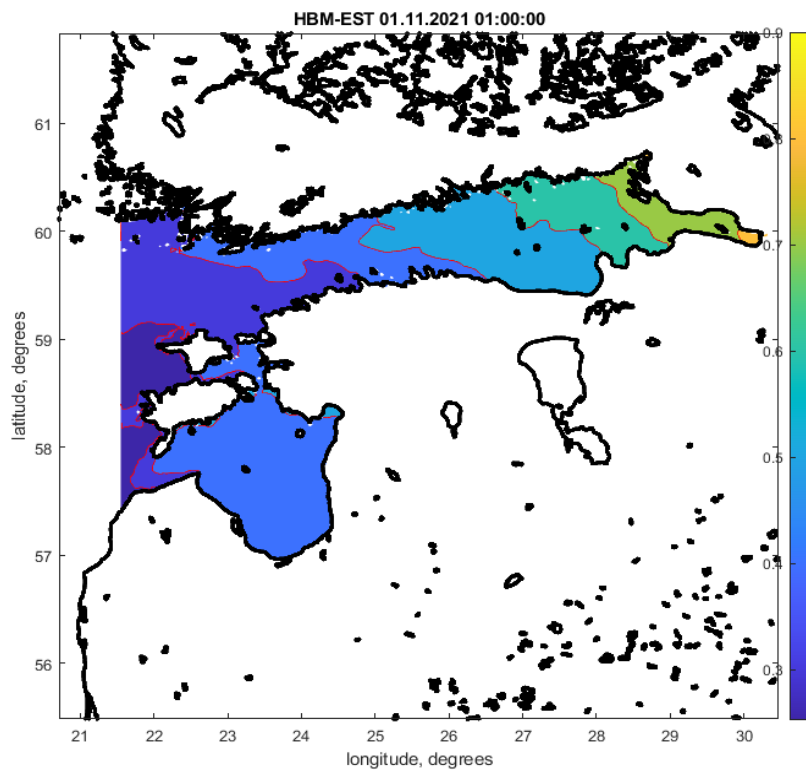


Figure 6.2 The sea level according to the HBM-EST hydrodynamic model for 01.11.2018 01:00:00 AM.

6.2 Geoid model NKG2015

In the present study NKG2015 geoid (Fig. 6.3) is used to calculate dynamic topography from Sentinel-3A, Jason-3 and Sentinel-6 satellite altimetry.

The NKG2015 geoid's horizontal positions and heights are transformed to national ETRS 89 and EVRS realisations. It has been updated with quality checked and new data from all the Nordic and Baltic countries. Data transformed is to zero permanent tide system and epoch 2000.0 (Ågren, et al., 2016).

These transformations from NKG2008 geoid model consist of a 7-parameter part and a postglacial land uplift correction part (NKG2005LU). The GNSS-heights have been transformed to the common ETRS 89 realisation ETRF2000 epoch 2000.0 using the so-called NKG2008 transformations. The standard deviation in the 1-parameter fit to GNSS/levelling is 2.85 cm and the resolution for the whole model model is 3"x3" (Ågren, et al., 2016).

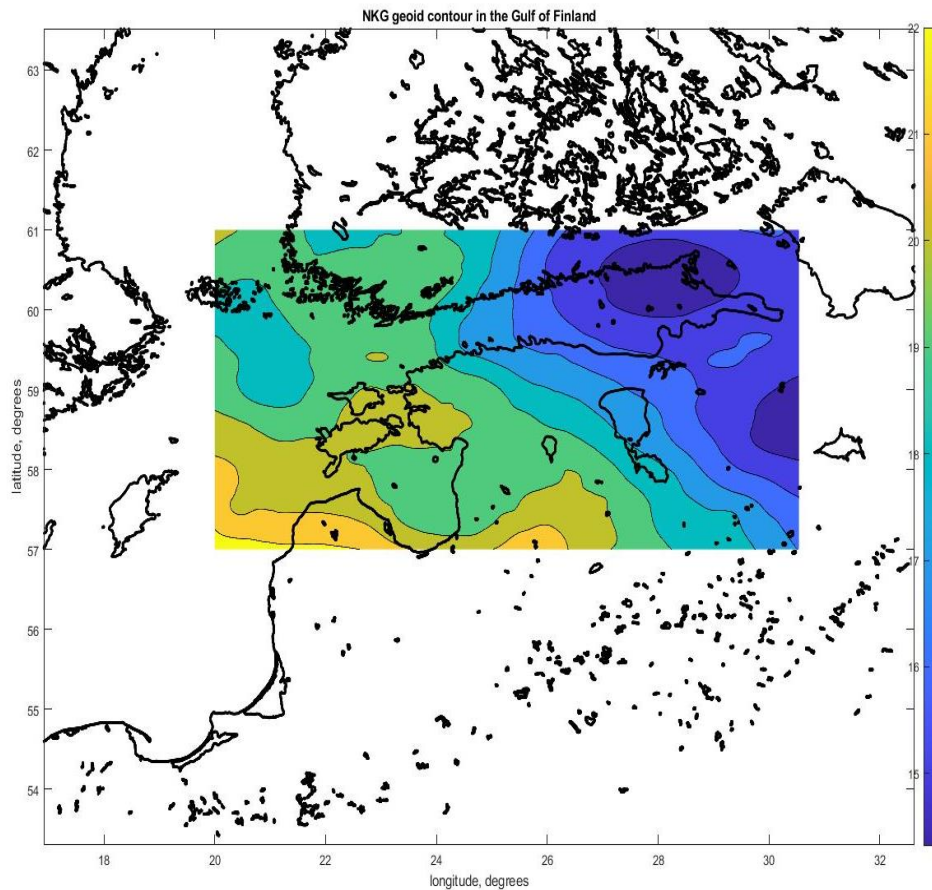


Figure 6.3 Section of NKG2015 at the Gulf of Finland and Estonia.

6.3 Land uplift model NKG2016LU

In the Baltic Sea the official land uplift model NKG2016LU is used to describe land uplift. The model is made by the Nordic Commission of Geodesy (NKG). The model was released in 2016 and covers an area from 49° to 75° latitude and 0° to 50° longitude (Fig. 4.3). The NKG2016LU model is an empirical model, which is computed from observations using for example the least squares collocation. In this thesis, the uplift leveled model is used – the levelled uplift (relative to geoid) is then computed by subtracting the GIA model geoid rise from the absolute uplift model. Model consists of geodetic observations, NKG levelling and also GNSS observations although no tide gauges are used to receive the model. NKG2016LU final levelled model is independent from any tide gauges or other sea level related sources. Model can be adapted to different time periods depending on the year observed (Vestøl, et al., 2016).

The land uplift at the Gulf of Finland is around 1-5 mm/a. The maximum land uplift is located at the Bothnian Bay (around 11 mm/a), lowest land uplift is in the Danish straits, Southern Baltic Proper and Gulf of Gdansk (around 0-1 mm/a) (Fig. 6.4).

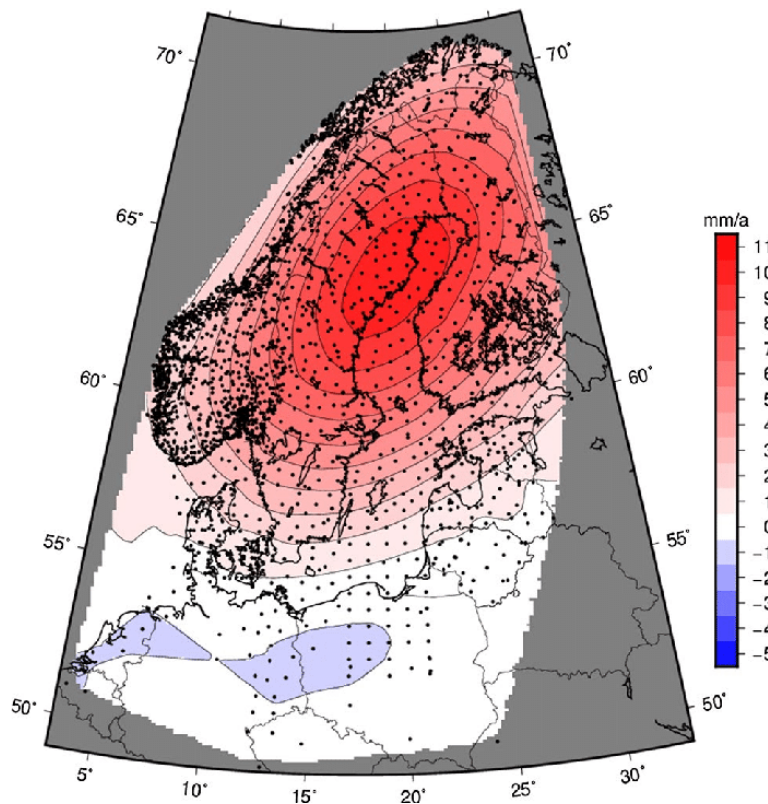


Figure 6.4 Land uplift according to NKG2016LU model (Vestøl, et al., 2016).

6.4 Tide Gauges

Tide gauges records have been used to measure changes in sea water level for centuries. A locally installed tide gauge is land-bound, which mean that it does not take into account the Earth's movement or land uplift (Guerova & Simeonov, 2021). Therefore, the vertical land motion (VLM) has to be taken account. VLM has been taken to account depending on the satellite mission and time period and VLM added to the tide gauge value (Eq. 7.4).

In certain countries TG data are often referred to Theoretical Mean Sea level (TMSL) (e.g., Finland) or Mean Sea level, Lowest Astronomical tide LAT (e.g., United Kingdom, Australia) or some varying datum. In this study the TG data are referred to theoretical mean sea level (Finnish TGs) and EH2000 (Estonian TGs). Since theoretical mean sea level is an arbitrary value, a conversion is needed to add to convert the values to N2000 (Finnish height system). The N2000 and EH2000 are corresponding to Baltic Sea Chart Datum 2000 (BSCD2000) and therefore to the geoid.

The Baltic Sea Chart Datum 2000 (BSCD2000) is a specially delivered geodetic reference system to be used to explain the changes for example in sea level in the Baltic Sea. BSCD2000 can be used to hydrographic surveying and engineering. BSCD2000 is based on the EVRS, the zero level of which is in accordance to NAP and height reference system is Earth's gravity field's equipotential surface (BSHC Chart Datum Working Group, n.d.). According to the article of (Varbla et al., 2022), the BSCD2000 will be compatible with the national height system realizations of the Baltic Sea countries (e.g., EH2000, N2000, and RH 2000) and will coincide with national geoid models to allow height transitions.

In this thesis the Estonian, Finnish and Russian tide gauges are used (Fig. 6.5).

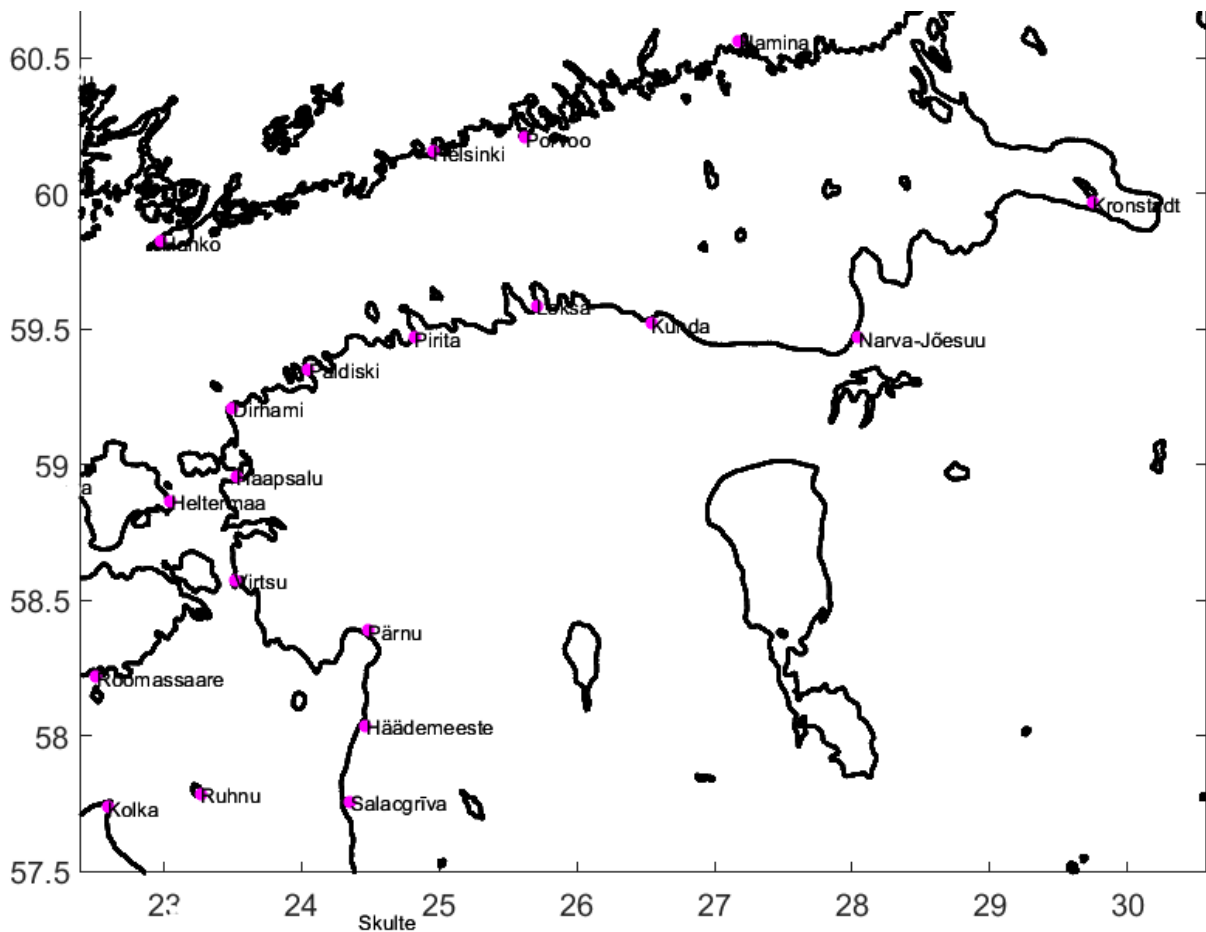


Figure 6.5 Tide gauges at the coast of Gulf of Finland.

Russian tide gauge station

The only Russian tide gauge used in this thesis is the station of Kronstadt. Russian tide gauges are usually presented in BK77 height system, though for this thesis the station of Kronstadt is corrected to EH2000 system by adding 18 cm to the Kronstadt station records.

Estonian tide gauges

Estonian tide gauges information is operated by the Estonian Environmental Agency. Pirita, Narva-Jõesuu, Lohka, Kunda, Heltermaa, Dirhami and Paldiski tide gauge data are used in

this thesis and analysis. These are established in local harbours. Each tide gauge station is equipped with instantaneous sea level levelling staff enabling visual measurements and pressure sensors, which records continuously (Kollo & Ellmann, 2019).

Previously the sea surface height measurement results were presented with respect to the BK77 height system. From 2018 the sea surface height measurement results are presented according to the new Estonian height system EH2000, which is derived from NAP (Normaal Amsterdams Peil).

Finnish tide gauges

Finnish tide gauges information is obtained from the Finnish Meteorological Institute (FMI). Hamina, Porvoo, Helsinki, Hanko and Turku tide gauge data are used in this thesis and analysis.

Until 2021 the theoretical mean sea level as a reference level was commonly used in Finland. Also, depth data in nautical charts have been given in relation to the theoretical mean sea level. Now the data has been also given commonly in N2000-system. The height system N2000 is based on the Third Levelling of Finland (1978–2006). It is a Finnish realization of the common European height system, and its datum is derived from NAP (Normaal Amsterdams Peil) (FMI, n.d.).

Conversion tables are used in the thesis to transfer annual theoretical mean sea levels on the Finnish coast to the referenced geodetic height system (FMI, n.d.).

Difference between EH2000 and N2000 is around 1cm, which is also taken to account.

7. Method

7.1 Vertical Datums

To obtain realistic sea level from SA and to evaluate its performance the dynamic topography is derived. Note that reasoning for this is that the SA data are normally expressing Sea Surface Height (SSH) where the vertical reference is a reference ellipsoid. The ellipsoid is a mathematical approximation of the Earth's shape and it does not realistically represent the sea surface. Instead, the geoid is an equipotential surface of the Earth and it coincides with the mean sea level over the ocean. This means that the geoid is an ideal component that can be used for describing the changes of sea level. Also, the geoid model is static which means, that it does not have a time variable compared to other vertical reference datums such as mean sea level etc. It is a reasonable option to reference and correct all used data (Satellite Altimetry (SA), Hydrodynamic Models (HDM), tide gauges (TG)) to a geoid (Fig. 7.5). Figure 7.1 illustrates an example of SA along track (for track 0083 of Sentinel-3A mission (Fig 5.1)) displaying the difference between SSH (referenced to an ellipsoid) and DT when it is referenced to a geoid. The example also shows where the outliers are – they appear as steep peaks and valleys throughout the track. These outliers are removed with two different methods, which are described later on in section “7.3 Determining Dynamic Topography”.

The utilization of satellite altimetry derived data is also limited by various data sources, which use different vertical data. For example, hydrodynamic models commonly do not use any vertical data and therefore it is important to correct the hydrodynamic model to be able to compare the hydrodynamic model to satellite altimetry data.

The methodology employed in this study is a comparison of the SA derived DT with that TG and HDM. The TG data are also land bounded and representative of sea level in the vicinity of the TG location. This implies that it is practical to compare with SA data points that are close by to TG location. To obtain DT in the offshore areas requires the hydrodynamic models to be utilized. The HDM models are however often referred to some other datum (e.g., MSL or unknown).

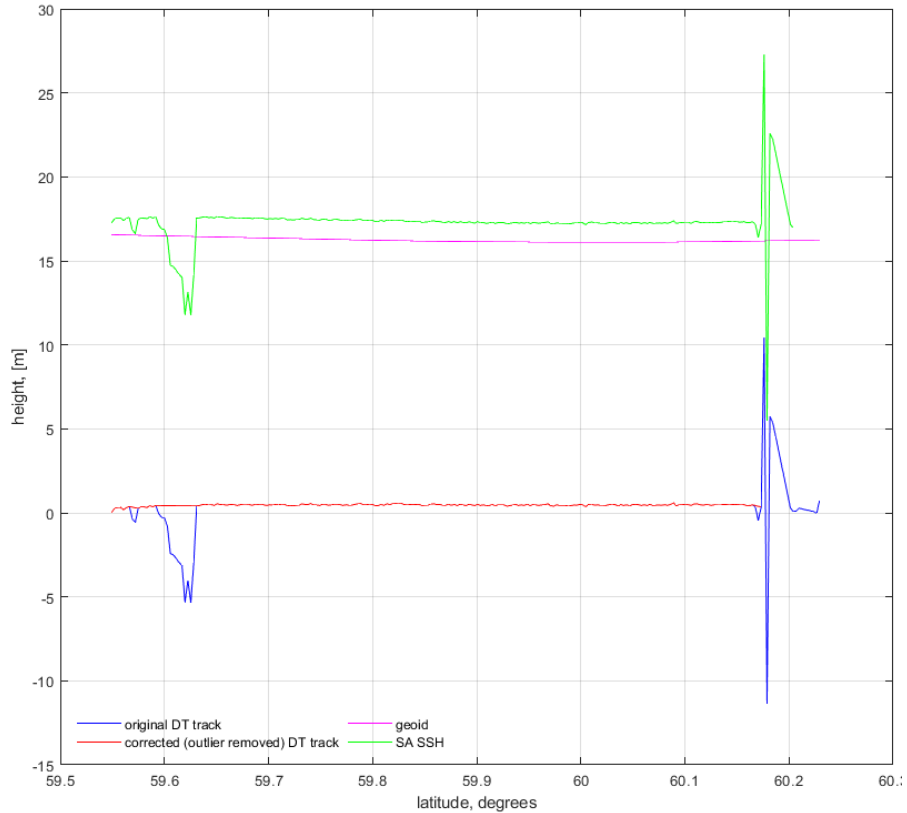


Figure 7.1 Process of deriving DT for satellite altimetry sea level track of 0083 (Sentinel-3A), passing date: 06.01.2017.

7.2 Time variance

The method used in this study, to compare the SA derived DT in the offshore, combines the tide gauges and hydrodynamic models. Only then the evaluation can be done in the offshore. Note that the evaluation of DT depends on the passing SA track location and time. Thus, both TG and HDM are adjusted for this. The TG and HDM data have hourly temporal resolution, but the satellite passes over the study area only mere seconds. Therefore, the TG and HDM data is interpolated according to satellite passing time instant, to obtain the closest time of the satellite passing. The height values of the TG and HDM are also linearly interpolated according to two closest time instants (Fig. 7.2a and Fig. 7.2b).

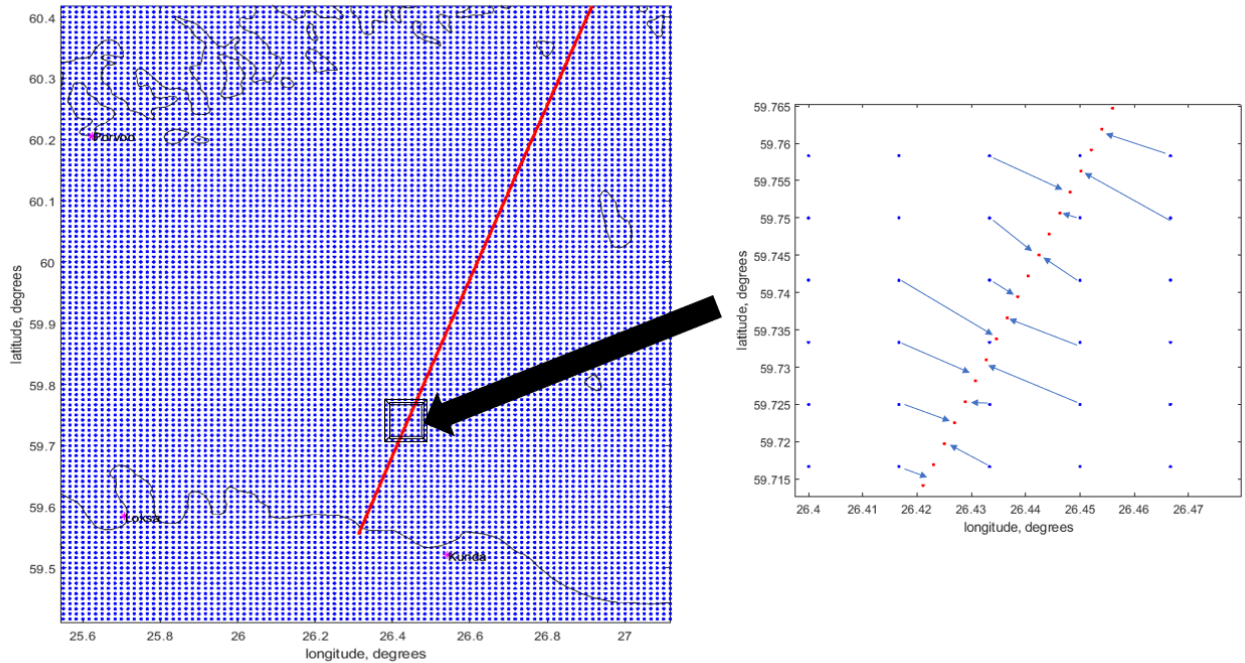


Figure 7.2 a) Process of interpolation for the track of 0414 (Sentinel-3A). The 1 x 1nm gridded data represents a HBM model, whereas satellite pass footprints are denoted with red dots; b) Interpolated (blue arrows) data example to find the hydrodynamic model (blue dots) values along the satellite track (red dots) footprint.

7.3 Determining Dynamic Topography

A step-by-step description of the overall methodology is described below. With respect to SA – the satellite altimeter transmits a pulse of known power towards the sea surface. On interacting with the sea surface, the pulse is reflected to altimeter where the two-way travel time is determined, yielding the range of the satellite (Fig. 3.1). Several other corrections are also applied for example instrumental, atmospheric refraction, external geophysical and sea-state bias corrections. This gives the term SSH, which is presented in coordinates and the corresponding time instant:

$$SSH(\varphi, \lambda, t) = H_{altitude} - (R + \text{atmospheric and geophysical corrections}) \quad (7.1)$$

, where $H_{altitude}$ is the height between the satellite and the ellipsoid and $SSH(\varphi, \lambda, t)$ is sea surface height, which depends on coordinates (φ for latitude and λ for longitude) and time

(t). Atmospheric and geophysical corrections include various types of corrections, for example range (R), wet and dry tropospheric corrections etc. A detailed description of correction for each satellite mission is described in the section of "8. Satellite Altimetry Corrections".

The geoid represents the vertical datum, to which tide gauges for this study also are referenced to. Dynamic topography (DT) is calculated by subtracting geoidal height (N) from the instantaneous sea surface height (SSH):

$$DT(\varphi, \lambda, t) = SSH(\varphi, \lambda, t) - N \quad (7.2)$$

DT represents information about the changes in ocean circulation, eddies, winds and waves as signals from both low- and high-frequency (GGOS, n.d.).

In this study two other corrections are applied – first being the ellipsoidal correction dh , which corrects the SSH data due to usage of different reference ellipsoid. This correction is taken into account while calculating SSH_{SA} for Sentinel-3 (due to Sentinel-3A data being referred to Topex-Poseidon reference ellipsoid, whereas the rest of SA data and geoid are referred to GRS-80).

The second correction is Dynamic Atmosphere Correction (DAC). This correction is automatically removed from the SA data when downloading the data from the source, therefore for this study it is de-corrected. The reason for this is to compare the instantaneous data from various sources. An example of the DAC can be viewed in Figure 8.2.

The SA derived SSH is then obtained:

$$SSH_{SA}(\varphi, \lambda, t) = SSH(\varphi, \lambda, t) + DAC - dh \quad (7.3)$$

, where $SSH_{SA}(\varphi, \lambda, t)$ is SA derived sea surface height. Due to SA footprint being contaminated by different causes such as islands and coastal marine traffic the outliers need to be removed. Outliers appear as steep peaks and valleys along the track (Fig. 7.1). Outliers are removed by two outlier steps – firstly by every data point which is over 40cm than the average value of all data points, secondly by *rmoutliers* function (using MatLab 2020 to process the data), which removes outliers from the remaining data.

The TG records and HDM data have been used to validate the DT in this study. As mentioned above the TG measurements commonly refer to the zero of national vertical datum. TG records are valid only at the near-shore and may not represent adequately the offshore DT . Note that in this study the TG data is assumed to represent the almost true DT at the coast.

Used TGs of both Estonian and Finnish coast are corrected for the vertical land motion (VLM) that are estimated from the NKG2016LU model (see Fig. 7.3). Vertical land motion describes the land uplift/down lift in coordinates and a time period of the change need to be added to the change. The Absolute Sea Level (ASL) is calculated:

$$ASL(\varphi, \lambda, t) = RSL(\varphi, \lambda, t) + VLM(\varphi, \lambda, t) * (t - t_0) \quad (7.4)$$

where $RSL(\varphi, \lambda, t)$ is relative sea level measured by TG sea level and $VLM(\varphi, \lambda, t)$ is vertical land motion, where the vertical land motion is calculated in the time epoch of interest t and the reference time-epoch t_0 (Varbla et al., 2022). Time epoch t for this study is either 2018 or 2022 depending on the satellite mission examined and the reference time-epoch t_0 is for the year of 2000. The annual VLM values used for this study are below 1 cm. Since the land uplift value is positive, then this correction increases the TG DT values (Fig. 7.3).

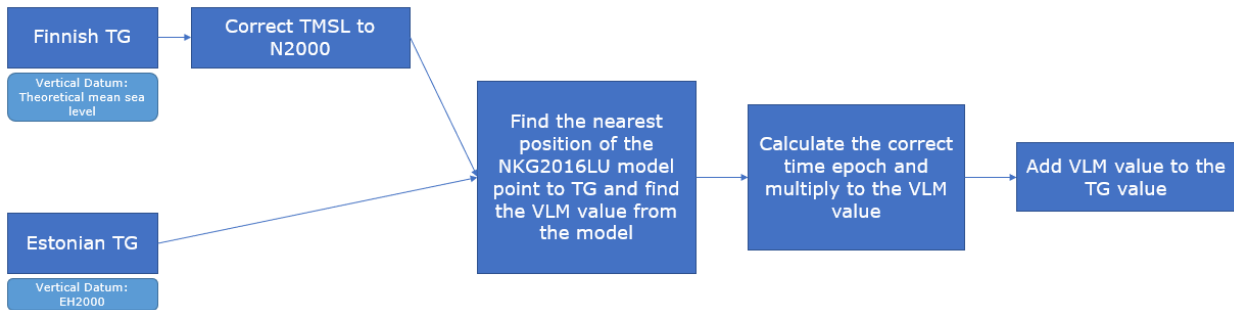


Figure 7.3 Data processing to correct VLM to the TG values.

7.4 Correcting the vertical datum of Hydrodynamic Models

To validate the SA offshore points a regionally computed hydrodynamic model (HDM) is used (see section “6.1 Hydrodynamic Models” for more details). The HDM is based on Navier-Stokes mathematical equations that are driven by meteorological and hydrological data to model actual sea surface and state. Even though the HDM model may not exactly portray reality for many of its initial driving conditions are based on other models (e.g., atmosphere, sea ice, river discharge) – it is still the best available data sources to describe offshore sea level variation both spatially and temporally. Essentially, the results of HDMs used in this study are equivalent to DT, but not referred to the geoid. The HMD usually provides hourly

estimation of gridded DT for a time period (see section "6.1 Hydrodynamic Models" for specifics of the HDM use). Due to an unknown vertical datum in the HDM, a shift between tide gauges of both Estonian and Finnish coast and hydrodynamic model is found. This shift ($Shift_{HDM}$) essentially marks the difference between TG and HDM model values (Fig. 7.4) and the shift value depends on the coordinates of viewable time period of the TG:

$$Shift_{HDM}(\varphi_{TG}, \lambda_{TG}, t_{TG}) = DT_{HDM}(\varphi_{TG}, \lambda_{TG}, t_{TG}) - DT_{TG}(\varphi_{TG}, \lambda_{TG}, t_{TG}) \quad (7.5)$$

If the shift ($Shift_{HDM}$) is found, it is applied to the original HDM model through linear interpolation to match with the TG values. In the figures the shift marked as a blue line. It is named as corrected HDM (DT_{HDM}^{corr}) (Fig. 7.4):

$$DT_{HDM}^{corr}(\varphi, \lambda, t) = DT_{HDM}(\varphi_{TG}, \lambda_{TG}, t_{TG}) - Shift_{HDM}(\varphi_{TG}, \lambda_{TG}, t_{TG}) \quad (7.6)$$

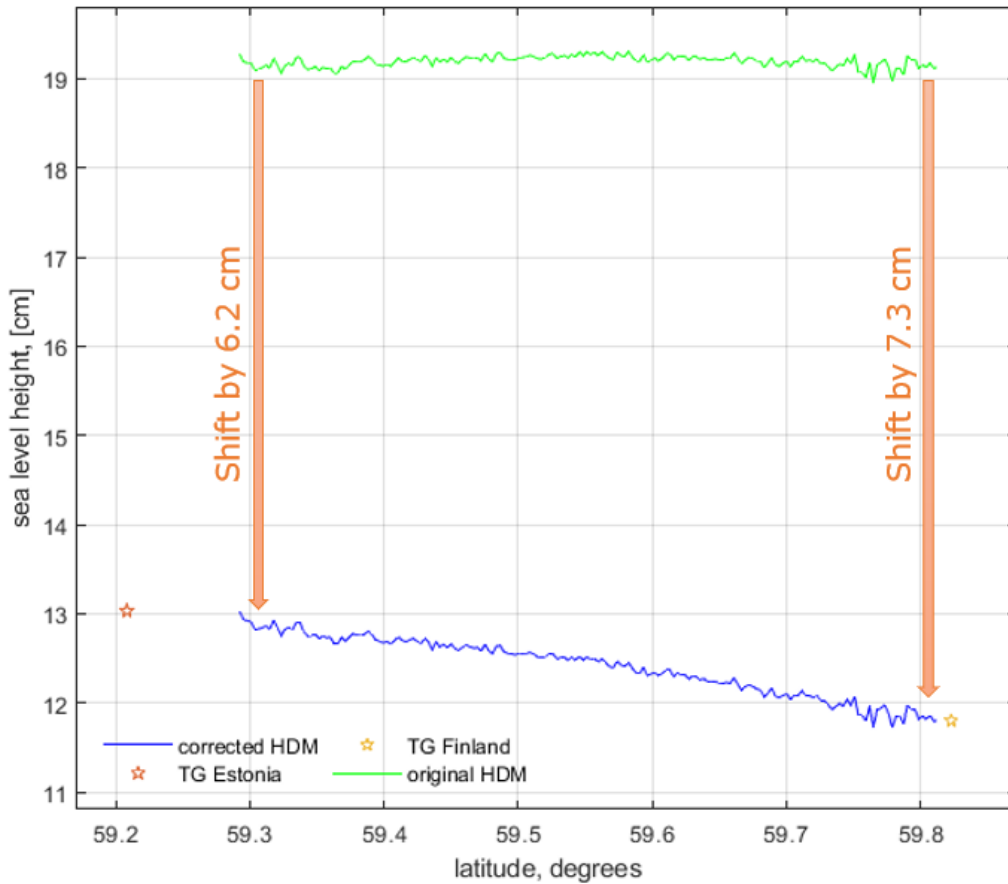


Figure 7.4 Example of tide gauges of both Estonian (vertical datum: EH2000) and Finnish (vertical Datum: N2000) coast as well as corresponding original HDM at the same moment with corrected HDM.

7.5 Calculating the Root Mean Square Error

Difference between SA derived DT ($DT(\varphi, \lambda, t)$) and corrected HDM ($DT^{HDM}_{corr}(\varphi, \lambda, t)$) at a location and time instant φ, λ, t is found by:

$$\Delta DT(\varphi, \lambda, t) = DT(\varphi, \lambda, t) - DT^{HDM}_{corr}(\varphi, \lambda, t) \quad (7.7)$$

This is the basic quantity that is used for evaluating the accuracy and performance of each SA data-set.

Root mean square error (RMSE) is used to measure difference between values of corrected HDM and the values observed from SA. In this study, the root mean square error ($RMSE(\#track, t)$) explains the difference between satellite derived DT and corrected HDM ($\Delta DT(\varphi, \lambda, t)$):

$$RMSE(\#track, t) = \sqrt{((\sum \Delta DT(\varphi, \lambda, t))/n)} \quad (7.8)$$

where n stands for number of data points in the cycle.

7.6 Data processing for all the satellite missions

So, the difference between two mentioned values is determined for every track and cycle passing over the Gulf of Finland – altogether there are 15 satellite tracks and 194 passings were examined. The number of data points in the Gulf of Finland is for Sentinel-3A varies within 181-487 data points, for Jason-3 within 49-67 data points and for Sentinel-6A within 50-69 data points. The data processing flowchart for each satellite and satellite track Fig. 7.5, where green boxes express general data processing in other studies and orange boxes express data processing unique to this thesis:

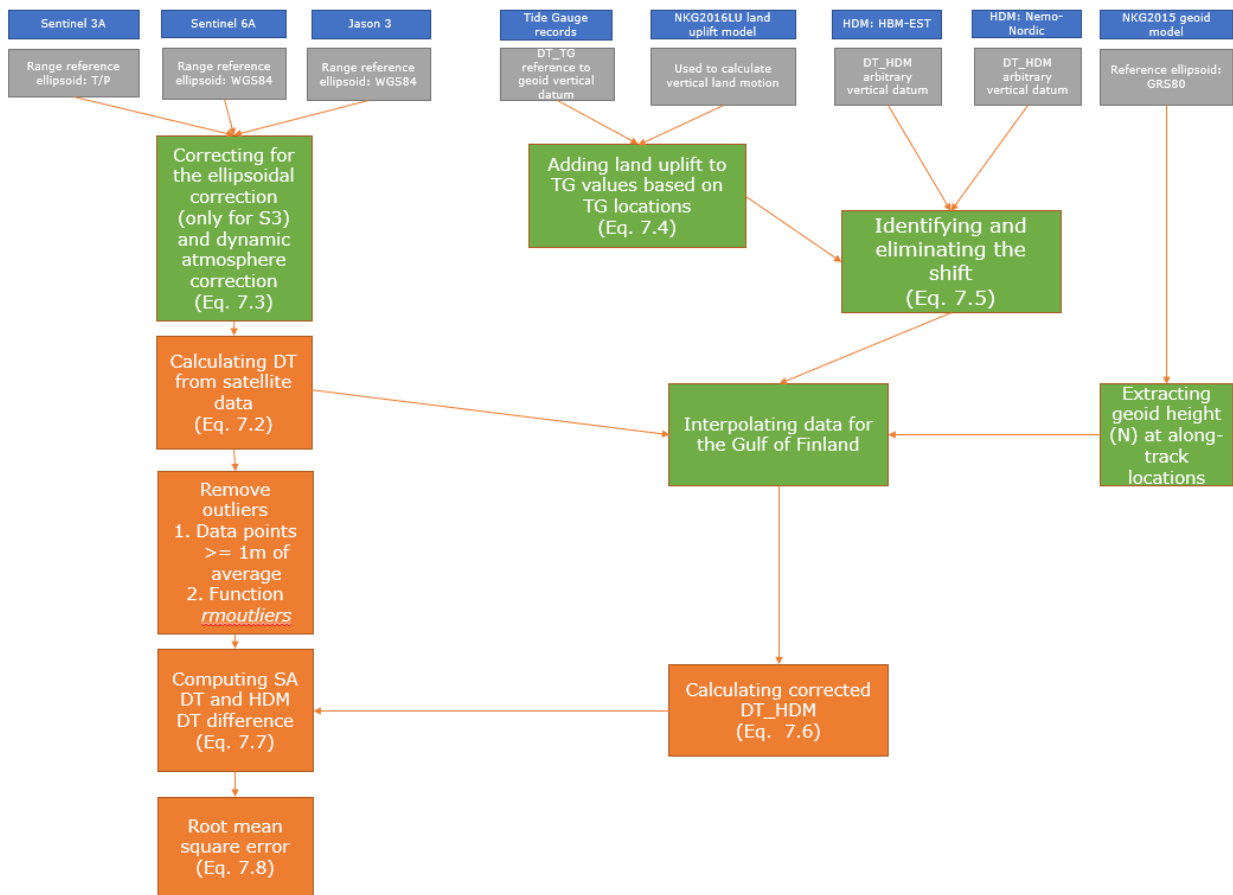


Figure 7.5 Data processing using satellite missions, tide gauges, hydrodynamic models, marine geoid and land uplift model for general processing (green) and unique to this thesis (orange).

8. Satellite Altimetry Corrections

In this thesis, three main satellite missions are used – Sentinel-3A, Jason-3 and Sentinel-6A. To derive the sea surface height (Fig. 3.1) several corrections are implemented.

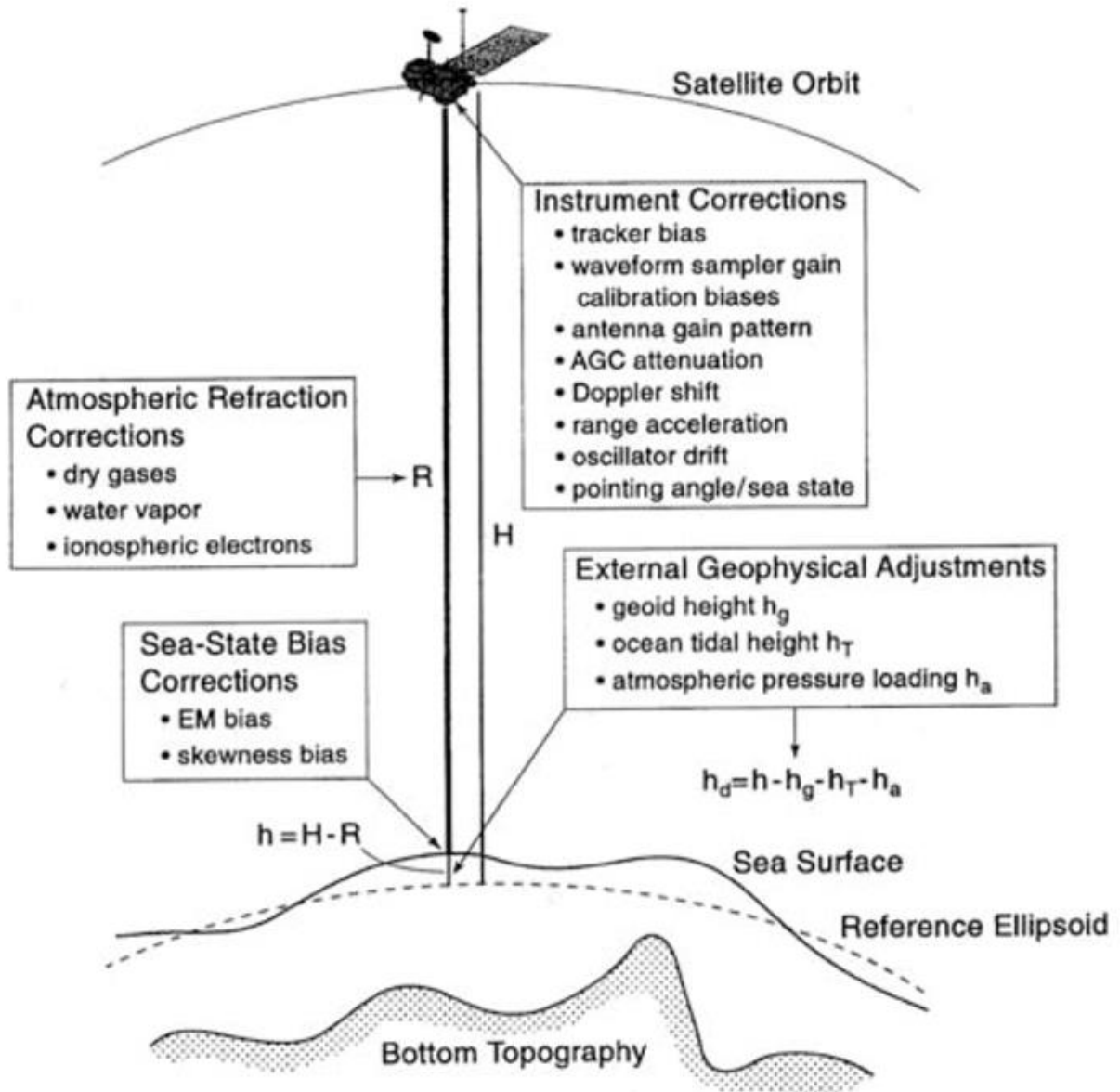


Figure 8.1 Satellite altimetry corrections (Snaith et al., 2006).

Corrections are usually divided into three groups – range, instrumental and geophysical. Range corrections (in the Fig. 8.1 mentioned as Atmospheric Refraction Corrections) depend on the radar pulse and its scattering. The geophysical corrections depend on different

geophysical aspects such as ocean tide, atmosphere pressure etc. To receive the highest possible accuracy over sea, altimeters downlink the waveforms to Earth and final geophysical parameters retrieval from the waveforms is performed on the ground (Vignudelli et al., 2011). Instrumental corrections are usually automatically applied to the satellite, when it is producing results (Fig. 8.1). These corrections include tracker bias, Doppler shift, range acceleration, oscillator drift etc. There are also corrections based on sea-state, which include EM and skewness bias.

To apply corrections correctly, they must be in the same fixed coordinate system and also tide system. Sentinel-3A is in Topex-Poseidon system, Sentinel-6A and Jason-3 are in GRS80. All missions are in zero-tide permanent tide system, which means that all used data including the geoid model and tide gauges are corrected to be tidal free (Varbla et al., 2022).

Sentinel-3A corrections

From knowing the satellite orbit height ($H_{altitude}$) and satellite altimeter range (R) there is a need to apply different atmospheric and geophysical corrections to derive sea surface height. Following equation displays the algorithm which is implemented by default to the Sentinel-3A products:

$$SSH = H_{altitude} - (R + WT + DT + iono + SSB + DAC + SET + PT + ROC) \quad (8.1)$$

where SSH is obtained by default from the S3A data (Baltic+ SEAL project). The wet tropospheric (WT), dry tropospheric (DT), and ionospheric ($iono$) are atmospheric propagation corrections due to radar pulse passing through Earth's atmosphere. Sea state bias (SSB), dynamic atmospheric correction (DAC), solid Earth tide (SET), along with pole tide (PT) are classified in the geophysical corrections, which refer to the systematic geophysical effects that can be modelled and corrected. The radial orbit error (ROC) is a new correction, that was derived and is based on multi-mission cross-calibration. This correction was developed to ensure a consistent combination of all different altimetry missions. The default dynamic atmosphere correction (DAC) that was included in the SSH was de-corrected from the SA data (by adding it back to SSH) because it is needed in order to compare the instantaneous data from various sources (Mostafavi et al., 2021).

An example of a dynamic atmosphere correction of a track passing over the Gulf of Finland is shown below. These are an example of the DA-corrections of the Sentinel-3A track 0625 for 2018 in the Gulf of Finland area latitude wise (Fig. 8.2). Dynamic atmosphere correction visualizes the weather – the impact of snow, ice and storms in the water, therefore the along-track DAC individual range varies between maximum 0.4...-0.3m. Compared to the other corrections mentioned, the DAC is one of the largest corrections applied reaching up to -30 cm to 40 cm.

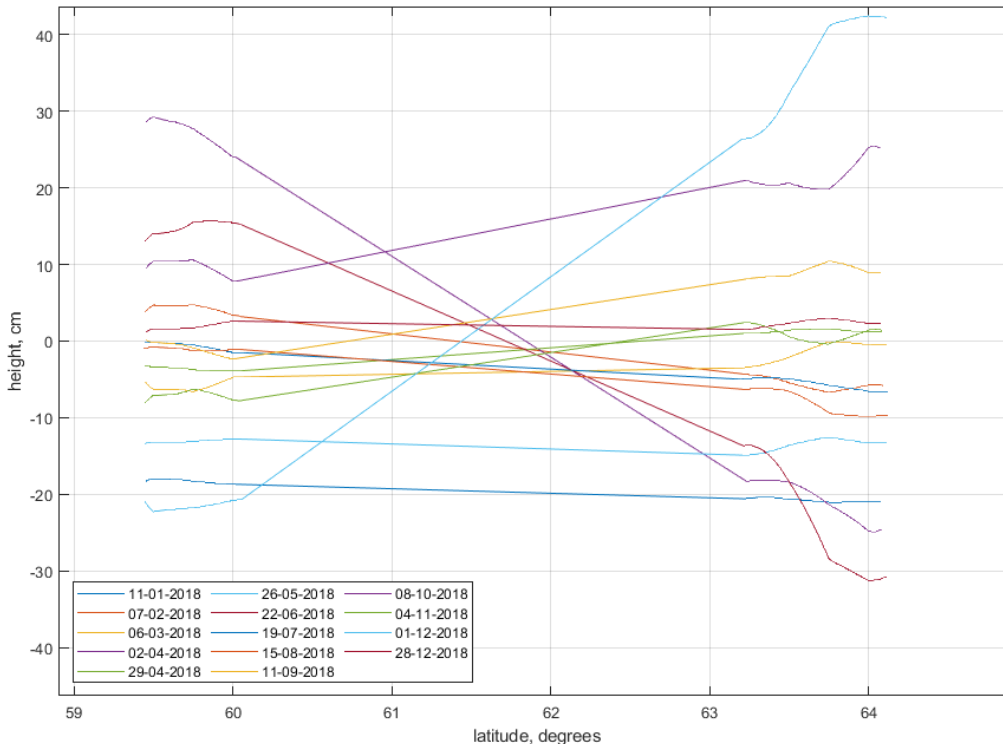


Figure 8.2 Dynamic atmosphere correction of track 0625 (Sentinel-3A).

Other corrections include different solutions of ocean tide corrections. Ocean tide correction is corrected automatically with geophysical corrections for all of the researched satellite passings.

Ocean tides represent more than 80% of the variability of the surface in the open ocean. In most regions of the world oceans, the tides periods are shorter than the repeat periods of an altimeter satellite orbit. Tidal corrections are very important for oceanographic studies because tidal signals contaminate the low-frequency part of raw altimetric signals (Zwaly & Berner, 2001). For the track of 0625 the ocean tide corrections and their values are between -8 cm to 5cm for the year of 2018 in the Gulf of Finland area (Fig. 8.3). This figure also

shows how ocean tide correction depends on the seasons – in winter months and late autumn, the correction along coastlines is very erratic, but in summer its quite smooth. This visualizes the sea state in the Gulf of Finland and along coastlines.

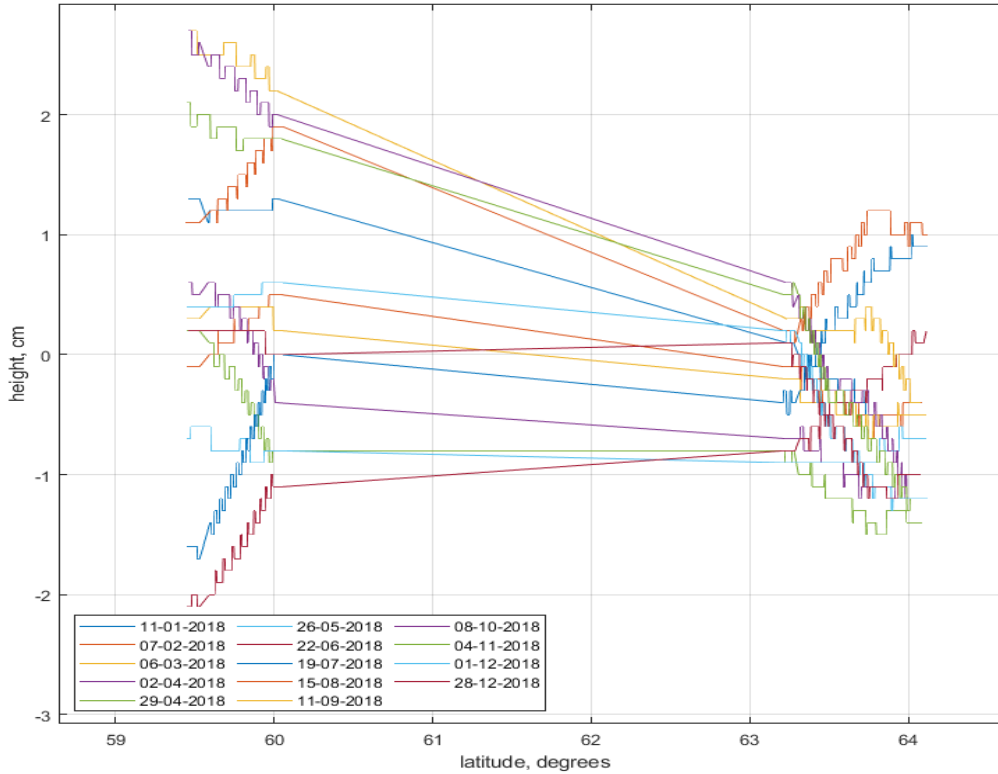


Figure 8.3 Ocean tide correction for the track of 0625 (Sentinel-3A).

Sentinel-6 corrections

Similarly, to Sentinel-3A corrections, from knowing the satellite orbit height ($H_{altitude}$) and satellite altimeter range (R) there is a need to apply different atmospheric and geophysical corrections to derive sea surface height. Following equation displays the algorithm which is implemented by default to the Sentinel-6A products:

$$SSH = H_{altitude} - (R + WT + DT + iono + SSB + DAC + SET + PT + ROC + OT2 + OTA + IT) \quad (8.2)$$

where compared to Sentinel-3A corrections also include geocentric ocean tide height solution ($OT2$), non-equilibrium long-period geocentric ocean tide height (OTA) and internal tide (IT)

(EUMETSAT, 2021). Example of Sentinel-6A track 0111 wet tropospheric correction (*WT*) and dry tropospheric correction (*DT*) are presented in Figures 8.4a and 8.4b.

Ocean-tide height (OT2) correction contains short- and long period load tide height for the geocentric ocean tide. Non-equilibrium (unbalanced) long-period geocentric ocean tide height (OTA) is a correction, which contains two separate corrections for the long-period ocean tide and the long-period load tide (EUMETSAT, 2021).

The dynamic atmosphere correction is also decorrected for this satellite mission.

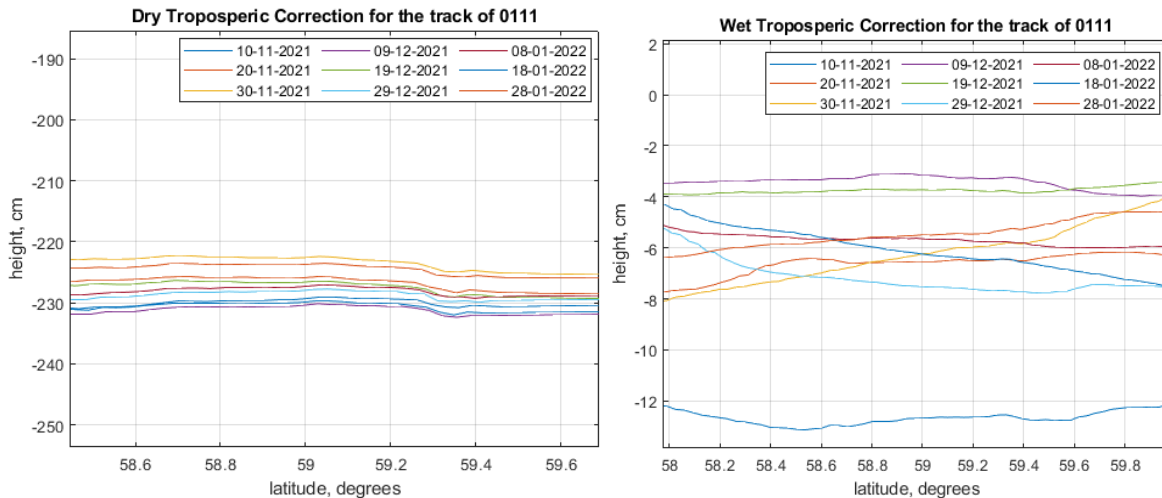


Figure 8.4 a) Wet Tropospheric Correction for the track of 0111 (Sentinel-6A); b) Dry Tropospheric Correction for the track of 0111 (Sentinel-6A).

Jason-3 corrections

Similarly, to Sentinel-3A, from knowing the satellite orbit height ($H_{altitude}$) and satellite altimeter range (R) there is a need to apply different atmospheric and geophysical corrections to derive sea surface height. Following equation displays the algorithm which is implemented by default to the Jason-3 products:

$$SSH = H_{altitude} - (R + WT + DT + iono + SSB + DAC + SET + PT + ROC) \quad (8.3)$$

The dynamic atmosphere correction is also de-corrected for this satellite mission. The dynamic atmosphere correction also includes inversive barometric height correction, which is computed from interpolation of 2 meteorological fields at the altimeter time-tag.

All corrections are shown in Table 8.1. Note, that all satellite missions included the same correction, although only Sentinel-6A had 3 more corrections added – geocentric ocean tide height, geocentric ocean tide height and internal tide.

Table 8.1 All corrections which are added to the satellite mission tracks.

Correction / Satellite mission	Sentinel-3A	Sentinel-6A	Jason-3
Wet Tropospheric correction	+	+	+
Dry Tropospheric correction	+	+	+
Ionospheric correction	+	+	+
Sea state bias correction	+	+	+
Dynamic Atmospheric correction	De-corrected	De-corrected	De-corrected
Solid Earth Tide	+	+	+
Pole tide	+	+	+
Radial orbit error	+	+	+
Geocentric ocean tide height solution	-	+	-
Geocentric ocean tide height	-	+	-
Internal tide	-	+	-

9. Results

The results are presented into two main sections – along-track perspective which is described in Section 9.1 and near coast perspective which is described in Section 9.2.

The section of along-track perspective examines (i) the SA derived Dynamic Topography (DT) and how it changes along the Gulf of Finland and also (ii) the results of root mean square error (RMSE) and its variation with different SA tracks at different times. Recall that the DT explains the highs and lows of the sea level (along the satellite track), with respect to the geoid representing the zero level. Therefore, it is the most realistic method to describe changes in sea level surface height. Eq. 7.7 is used to identify differences of the SA derived DT and the ground truth, the root mean square error of these residuals ΔDT is a basic mathematical method to identify the quality and performance of SA data-sets. The RMSE (Eq. 7.8) helps to explain the error (variety and differences) in results – if the value of RMSE is considered large, that means that the SA track data are either biased (with respect to the ground truth) or more erratic than average or both.

The section of near coast perspective examines the quality and quantity of data points on approaching coast area as well as nearest TG. In this section it is also show that islands are affecting the quality of SA datapoints and how far to the coast of islands or inland should the considered when calculating the SA DT.

9.1 Along-track perspective

9.1.1 Sentinel-3A

Dynamic Topography of Sentinel-3A

For this study 10 tracks of Sentinel-3A, that crossed over Gulf of Finland, were examined. Tracks 0414 and 0528 are descending, all other tracks are ascending (see Fig. 9.1 b)). These tracks of Sentinel-3A are viewed and analyzed for the whole year of 2018 with respect to the derived dynamic topography for the SA, HDM and TG data. Since Sentinel-3A passes

over one placer every 27 days, this calculates that for every track there is around 13 to 14 passes. Figure 9.3 shows an example of DT results for track 0083 passing 27th July 2018. Such procedure was performed for all of the tracks and their passes; thus, these figures can be viewed in the appendices (sections 15.1-15.10 in Appendices).

In general, these figures (sections 15.1-15.10 in Appendices) show that in most of the cases the DT for the original HDM were overestimated (for example most of the cases for the track of 0511 (Fig. 15.1.1-15.1.14), 0397 (Fig. 15.2.1-15.2.14), 0083 (Fig. 15.3.1-15.3.12), 0414 (Fig. 15.4.1-15.4.14), 0739 (Fig. 15.6.1-15.6.13), 0311 (Fig. 15.8.1-15.8.13), 0425 (Fig.15.10.1-.15.10.14)) or underestimated (for example most of the cases for the track of 0528 (Fig. 15.5.1-15.5.14), 0197 (Fig. 15.7.1-15.7.13), 0625 (Fig. 15.9.1-15.9.14)). This overestimation/underestimation varied throughout the year (minimum -55.10 cm to maximum 90.58 cm in range). As expected, the HDM results are more or less smooth compared to the varying SA data. This demonstrates the difference in quality of results due to the different methods used to collect sea level data. With HDM being smoother due to the mathematical equations utilized to simulate DT whilst the SA sensor measures the real sea surface and its environment.

The TG from both Estonia and Finland serves as a base truth in the methodology applied. The distance between the TG from Estonia to Finland within the selected time-span varied from 69.9–156.5 km. As expected, the DT from both sides were not the same. On the Estonian side the range of DT was within the range -60.4–151.2 cm whilst in the Finland it was -66.6–149.6 cm. The difference between both sides (from Estonia to Finland) varied at times from 1.0–50.0 cm. Also, along the Gulf the DT varied from west to east -40.5–108.5 cm and north to south -64.7–151.8 cm. An example of the difference throughout the year can be also viewed from the Figure 9.1a, where line yellow is for the date of 15th October 2018 12:00, line red is for the date of 15th July 2018 12:00, line green is for the date of 15th April 2018 12:00 and line blue is for the date of 15th January 2018 12:00. As expected, the TG DT values also vary depending on the season – in the winter months the TG DT values are lower than in the summer and autumn, in the middle of the spring is also quite low, which can mean, that most of the melting and large quantities of water has been balanced throughout the GOF. This variety of values depend on the weather, storms and marine traffic.

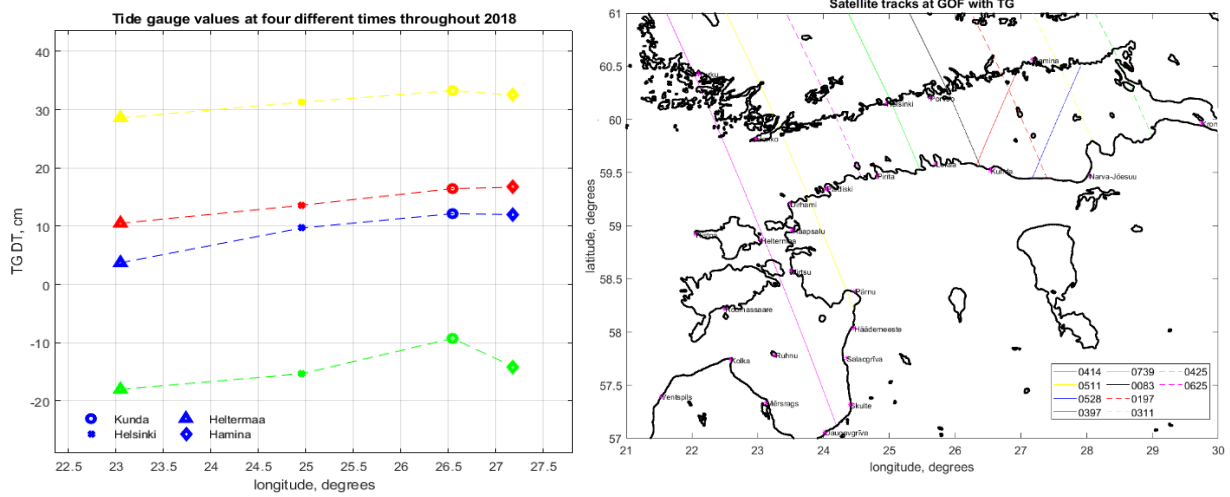


Figure 9.1 a) Tide gauge values throughout the year of 2018. TGs used are Heltermaa, Helsinki, Kunda and Hamina; b) Tracks of Sentinel-3A.

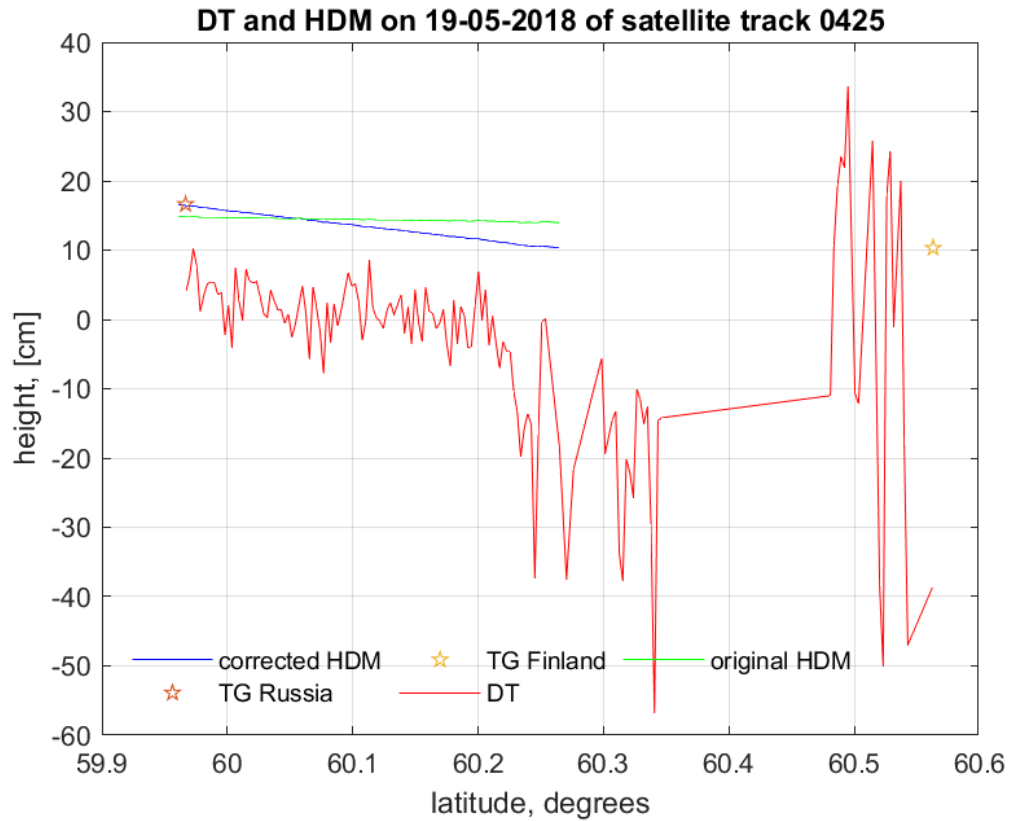


Figure 9.2 Example of a track of 0425 at the date of 19.05.2018. The height represents DT in the vertical axis.

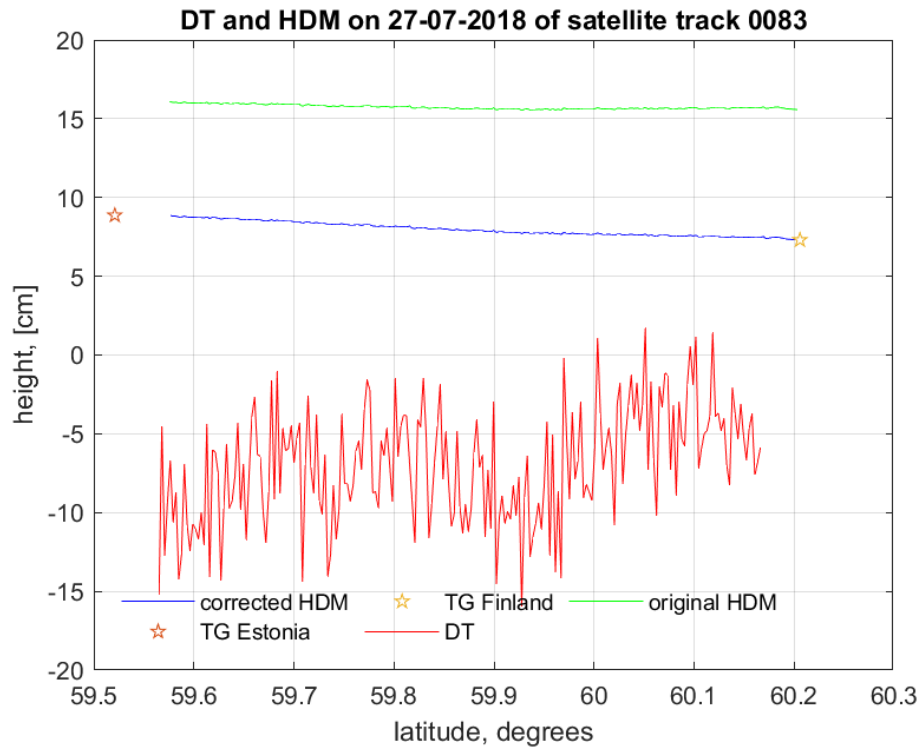


Figure 9.3 Example of a track of 0083 at the date of 27.07.2018. The height represents DT in the vertical axis.

Root Mean Square Error of Sentinel-3A

A compilation of RMSE results is displayed in Table 9.1. The general range for the RMSE for Sentinel-3A tracks is from minimum to 2.8–13.15 cm and maximum 14.7–46.2 cm, so the general range is between 2.8–46.5 cm. The lowest RMSE values range is for the 0625 track (Fig. 15.9.1-15.9.14), which is an ascending track in the middle of the GOF and passes over island Naissaar (Estonia) (Fig. 9.4a). This also happened to be shortest track length in this data of 60.6 km. The highest RMSE values range is for the 0425 track (Fig. 15.10.1-15.10.14), which is an ascending track at the end of the GOF (last track to pass over the GOF) and it passes over multiple of islands such as Beryozovye (Russia) islands (Fig. 9.4b). An example of the DT values is also displayed in Fig. 9.2 showing the presence of islands/land contamination on the data. From latitude 60.35° and further (i.e., the near Finnish coast archipelago) the effects of islands/land contamination is noticeable. This example shows how the tracks were analysed for all passes.

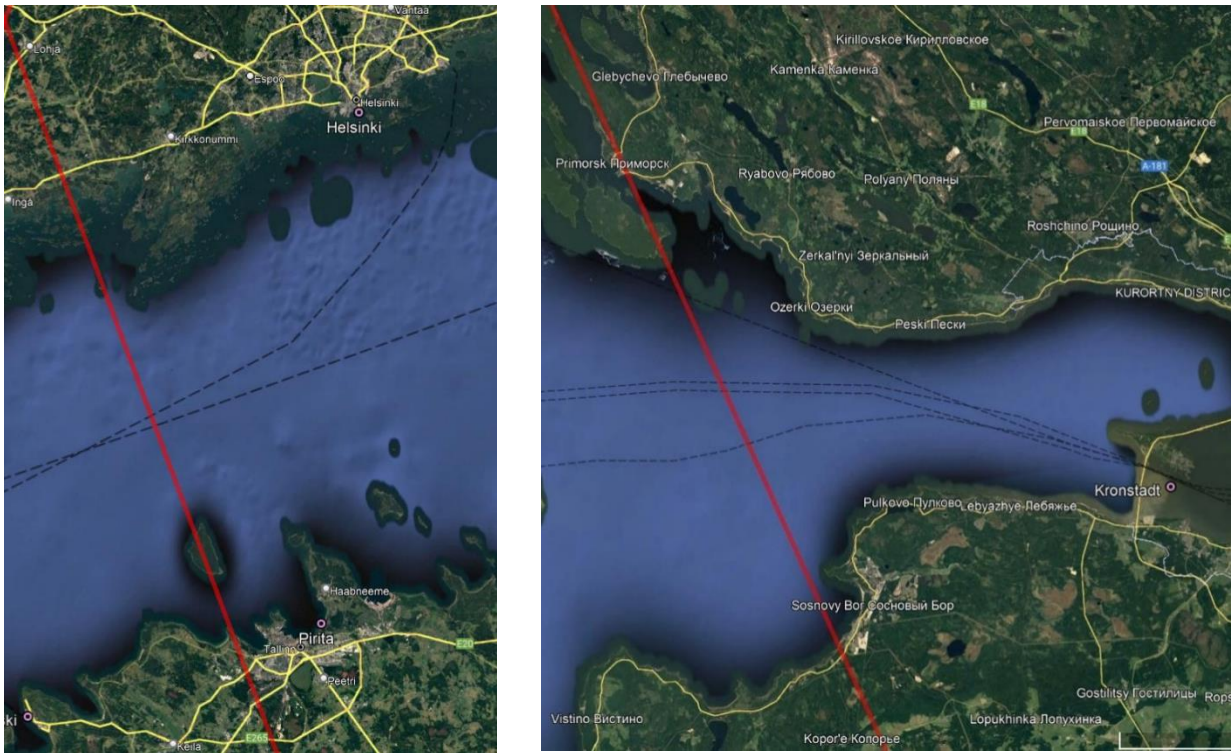


Figure 9.4 a) Track 0625 and used stations of Pirita and Helsinki; b) Track 0425 and station Kronstadt.

Examination of the results of shows that there seems to be no correlation between minimum RMSE (2.8–13.15 cm) and date/season of the minimum value, for the minimum value varied each month. This at first hints that the performance may not be influenced by environmental conditions of the study area (e.g., seasons with ice, river discharge etc.). On the contrary however there seems to be a correlation between maximum RMSE of 14.7–46.2 cm and date of the maximum value occurring - for most of the maximum RMSE values are calculated in March 2018. According to Leibniz Institute for Baltic Sea Research (Siegel & Gerth, 2018) examination March was the coldest month in 2018 and the coldest day of the year was in the first week of March. Also, the late winter led to negative anomalies in March and April 2018 (Table 9.1).

Another article by EUMETSAT states, that through satellite imaging we can view the extent of sea ice and its thickness. They also show, that at the end of March 2018, the sea ice was present at the Gulf of Finland as well. In fact, its thickness was maximum of 50cm in the Gulf of Finland near Hamina (Finland) station (Nietosvaara & Prieto, 2018). The sea ice reports and ice charts can be accessed through Bundesamt Für Seeschifffahrt und Hydrographie (BSH) webpage, which also explains the maximum RMSE value occurrence in March 2018. In the figure (Fig. 9.5) below, we can examine that sea ice was present in the Gulf of Finland (BSH, n.d.). This suggests that the satellite performance may not be the best

Also, in the results it is found, that most of the highest RMSE values appear at the end of the GOF using Narva-Jõesuu, Kronstadt and Hamina stations. This could be affected due to large quantity of islands in the end of the GOF such as Vaindloo (Estonia), Gogland (Russia), Malõi Tjuters (Russia) etc. Tracks 0197 (Fig. 15.7.1-15.7.13) and 0311 (Fig. 15.8.1-15.8.13) also pass over some of the mentioned islands (Fig. 9.7). This could also explain the difference between 0528 (Fig. 15.5.1-15.5.14) and 0414 (Fig. 15.4.1-15.4.14), the only descending tracks used in this thesis, minimum RMSE values. Track 0528 crosses over Kilpisaari (Finland) and track 0414 does not cross any islands in the middle of the GOF (Fig. 9.7a and 9.7b). These four passes locate near the largest rivers that run off to GOF – Narva, Kemi, Luga and Neva.

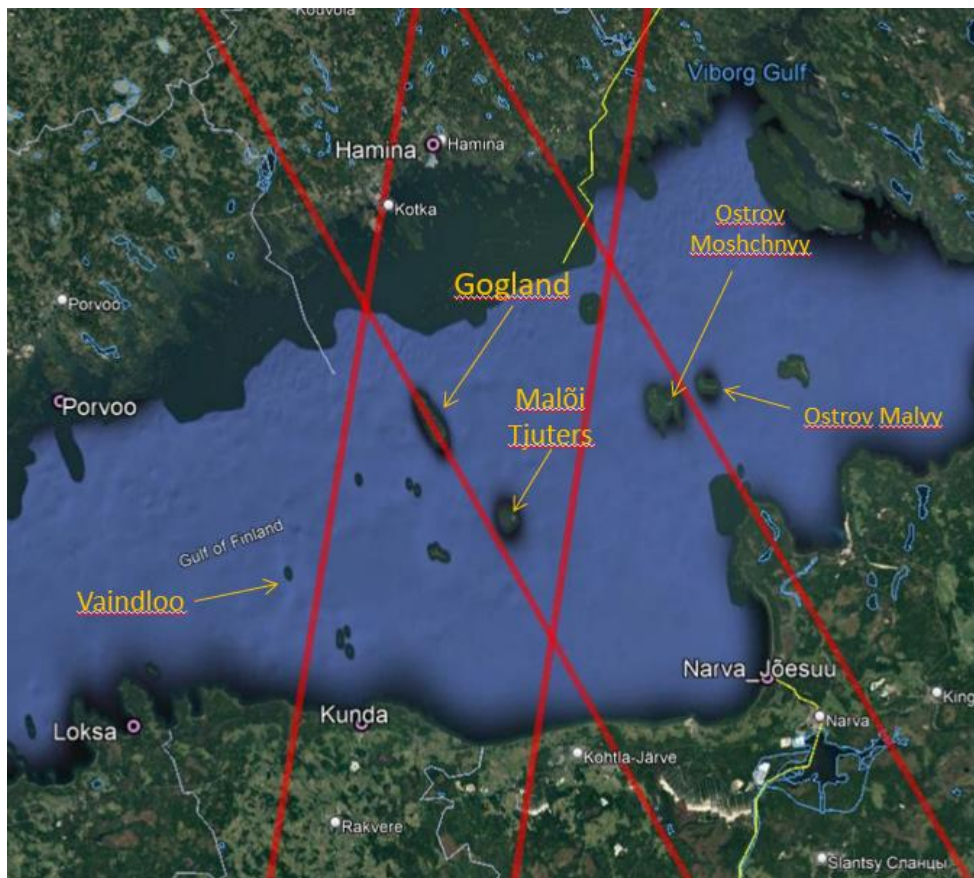


Figure 9.6 Tracks of (left to right) 0414, 0197, 0528 and 0311 and the stations of Kunda, Narva-Jõesuu, Kronstadt and Hamina.

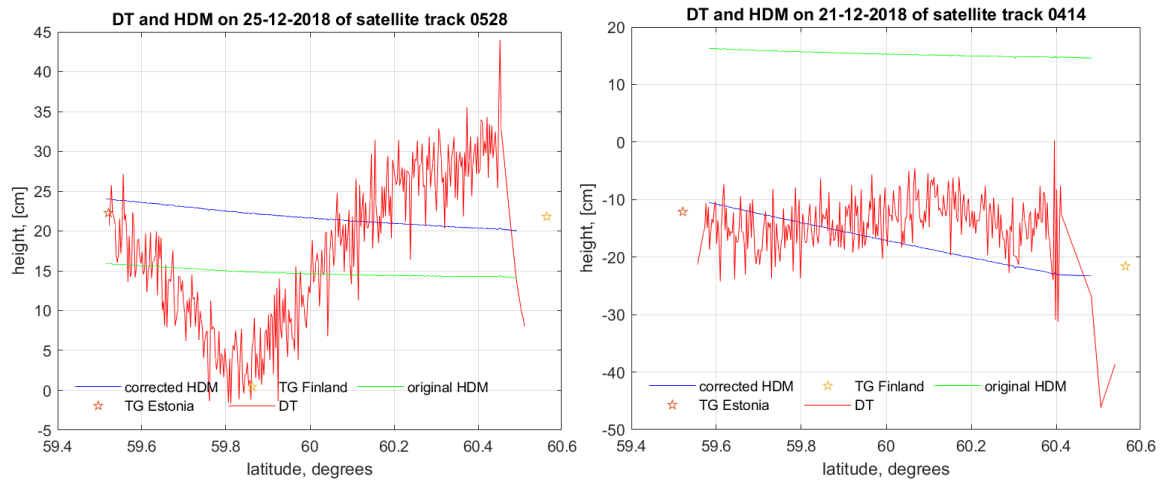


Figure 9.7 a) Tracks of 0528 on 25.12.2018, when the minimum RMSE occurred. The height represents DT in the vertical axis.

Figure 9.7 b) Tracks of 0414 on 21.12.2018, when the minimum RMSE occurred. The height represents DT in the vertical axis.

The methodology employed depended partly on how close to the TG the SA data points are located. Table 9.1 shows that the closest SA data point was within 8.87 – 85.97 km from the TG stations. With the closest TG station being at Kunda (ascending track) with a distance of 8.87 km and the furthest at Kronstadt with a distance of 46.33 km and also Turku of 85.92 km. The biggest difference did not appear to affect the RMSE.

Table 9.1 Values gathered from analysing root mean square error from the satellite mission of Sentinel-3A from 2018.

Sentinel-3 track	Estonia TG	Finland TG	Distance bet-ween Estonian TG and closest SA point to TG (km)	Root mean square error minimum along the track (cm)	Date of the RMSE minimum value	Root mean square error maximum along the track (cm)	Date of the RMSE maximum value	Mean root mean square error (cm)
0625	Pirita	Helsinki	17.41	2.83	02.04. 2018	14.78	22.06. 2018	8.8
0311	Narva-Jõesuu	Hamina	39.75	13.15	11.06. 2018	36.59	22.03. 2018	24.87
0197	Narva-Jõesuu	Hamina	38.66	3.20	14.04. 2018	22.96	18.03. 2018	13.08
0739	Loksa	Helsinki	18.2	4.49	03.05. 2018	20.67	06.04. 2018	12.58

0528	Kunda	Hamina	38.4	11.13	25.12. 2018	29.19	04.02. 2018	20.16
0414	Kunda	Hamina	13.52	6.68	21.12. 2018	30.30	26.03. 2018	18.49
0397	Heltermaa	Turku	85.92	4.79	26.02. 2018	20.14	27.10. 2018	12.46
0511	Dirhami	Hanko	14.11	5.20	15.07. 2018	19.19	02.03. 2018	12.19
0083	Kunda	Porvoo	8.871	5.23	19.01. 2018	22.20	16.10. 2018	13.71
0425	Kronstadt (Russia)	Hamina	46.33	9.19	21.12. 2018	46.27	31.01. 2018	27.73

Table 9.2 Values gathered from analysing root mean square error from the satellite mission of Sentinel-6A from November 2021 – February 2022.

Sentinel-6 track	Estonia TG	Finland TG	Distance between Estonian TG and closest SA point to TG (km)	Root mean square error minimum along the track (cm)	Date of the RMSE minimum value	Root mean square error maximum along the track (cm)	Date of the RMSE maximum value	Mean root mean square error (cm)
0111	Heltermaa	Porvoo	92.95	3.50	02.01. 2022	43.90	11.02. 2022	23.7
0016	Paldiski	Hanko	18.99	4.29	29.12. 2021	39.39	07.02. 2022	21.84
0092	Kunda	Helsinki	23.62	5.28	01.01. 2022	37.08	13.11. 2021	21.18
0187	Kunda	Hamina	19.61	7.04	06.12. 2021	37.60	16.11. 2021	22.32
0168	Narva-Jõesuu	Hamina	67.49	5.39	15.12. 2021	32.64	13.02. 2022	19.01

Table 9.3 Values gathered from analysing root mean square error from the satellite mission of Jason-3 from November 2021 – February 2022.

Jason-3 track	Estonia TG	Finland TG	Distance between Estonian TG and closest SA point to TG (km)	Root mean square error minimum along the track (cm)	Date of the RMSE minimum value	Root mean square error maximum along the track (cm)	Date of the RMSE maximum value	Mean root mean square error (cm)
0111	Heltermaa	Porvoo	92.95	1.68	11.02.2022	50.14	22.01.2022	25.91
0016	Paldiski	Hanko	18.99	11.13	17.02.2022	41.01	07.02.2022	26.07
0092	Kunda	Helsinki	23.62	6.59	12.12.2021	29.85	10.02.2022	18.22
0187	Kunda	Hamina	19.61	4.62	26.12.2021	38.81	25.01.2022	21.71
0168	Narva-Jõesuu	Hamina	67.49	8.81	25.12.2021	29.86	03.02.2022	19.33

Tables 9.1, 9.2 and 9.3 examine Sentinel-3A, Sentinel-6A and Jason-3 results in terms of RMSE and the date of its maximum and minimum occurrence. As mentioned, most of the maximum RMSE values occurred in March 2018 for Sentinel-3A, in November 2021 and in February 2022 for Sentinel-6A and in the end of January and beginning in February for Jason-3. More in depth for Sentinel-6A and Jason-3 is examined in “9.1.2 Sentinel-6A” and “9.1.3 Jason-3”.

Table 9.4 summarizes some important attributes of TG, HDM and SA data. These results show that difference between HDM and TGs varied greatly – range difference can differ from -12 cm to 90 cm. This could be also related to seasons and/or storms, because as mentioned previously, the HDM describes a mathematical model, which does not have a known vertical reference. The difference between HDM and Estonian and Finnish TGs was around the same size - although, the tracks that pass at the end of the GOF had larger difference, that pass over or pass near several islands. This also explains the high average difference in corrected and uncorrected HDM DT values.

This phenomenon also occurs in the difference between corrected HDM DT and satellite derived DT for the same mentioned tracks. As seen in the table 9.4 difference is mostly negative valued which means, that the HDM in most of the cases overestimated the value in comparison to the TGs. The biggest difference is for the track of 0425, which is located at the end of the GOF and passes over several islands. The largest differences appear on the tracks which are located at the end of the GOF, for example track 0311, 0528, 0414. This difference is also shown in the column of average difference between corrected and uncorrected HDM DT.

Table 9.4 Values gathered from analysing tide gauges and hydrodynamic model from the satellite mission of Sentinel-3A from 2018.

Sentinel-3 track	Estonia TG	Range of difference closest HDM point to Estonian TG (cm)	Finland TG	Range of difference closest HDM point to Finnish TG (cm)	Average difference between corrected and uncorrected HDM DT (cm)	Range of difference between corrected HDM DT and satellite DT (cm)
0625	Pirita	-53.23...66.85	Helsinki	-45.97...66.37	-0.86	-13.70...1.75
0311	Narva-Jõesuu	-12.08...90.58	Hamina	-21.63...77.93	10.07	-33.17...-7.16
0197	Narva-Jõesuu	-30.24...54.88	Hamina	-31.89...54.52	14.85	-21.24...0.31
0739	Loksa	-27.81...37.30	Helsinki	-25.65...27.30	-0.13	-19.98...0.39
0528	Kunda	-34.28...60.48	Hamina	-38.94...74.69	5.48	-27.22...-4.60
0414	Kunda	-55.10...53.53	Hamina	-64.87...47.49	-2.32	-23.75...2.93
0397	Heltermaa	-29.78...52.81	Turku	-25.87...43.46	-5.51	-17.73...3.13
0511	Dirhami	-45.31...77.51	Hanko	-36.98...52.91	-3.25	-14.98...0.59
0083	Kunda	-14.21...36.51	Porvoo	-18.70...28.12	-0.36	-21.51...7.79
0425	Kronstadt (Russia)	-50.93...46.81	Hamina	-51.25...48.19	-2.19	-44.01...-7.09

Table 9.5 Values gathered from analysing tide gauges and hydrodynamic model from the satellite mission of Sentinel-6A from November 2021 – February 2022.

Sentinel-6 track	Estonia TG	Range of difference of closest HDM point to Estonian TG (cm)	Finland TG	Range of difference of closest HDM point to Finnish TG (cm)	Average difference between corrected and uncorrected HDM DT (cm)	Range of difference between corrected HDM DT and satellite DT (cm)
0111	Heltermaa	-6.53...9.38	Porvoo	-61.1...37.24	-0.90	-40.48...2.88
0016	Paldiski	-33.64...12.63	Hanko	-49.1...63.96	-5.26	-40.83...1.93
0092	Kunda	7.87...84.78	Helsinki	10.78...80.12	49.74	-31.4...13.30
0187	Kunda	26.92...75.50	Hamina	21.04...62.52	45.46	-40.65...-8.92
0168	Narva-Jõesuu	-22.71...11.26	Hamina	-57.8...42.70	-7.26	-38.25...8.07

Table 9.6 Values gathered from analysing tide gauges and hydrodynamic model from the satellite mission of Jason-3 from November 2021 – February 2022.

Jason-3 track	Estonia TG	Range of difference of closest HDM point to Estonian TG (cm)	Finland TG	Range of difference of closest HDM point to Finnish TG (cm)	Average difference between corrected and uncorrected HDM DT (cm)	Range of difference between corrected HDM DT and satellite DT (cm)
0111	Heltermaa	-6.53...9.38	Porvoo	-61.12...37.24	-0.90	-50.14...9.7
0016	Paldiski	-33.64...12.63	Hanko	-49.16...63.96	-5.26	-40.99...1.0
0092	Kunda	7.87...84.78	Helsinki	10.78...80.12	49.74	-33.7...20.2
0187	Kunda	26.92...75.50	Hamina	21.04...62.52	45.46	-38.8...4.55
0168	Narva-Jõesuu	-22.71...11.26	Hamina	-57.88...42.70	-7.26	-28.6...7.48

Tables 9.4, 9.5 and 9.6 examine Sentinel-3A, Sentinel-6A and Jason-3 results in terms of range between hydrodynamic models and tide gauge records in comparison both in the

Estonian and Finnish coastlines. The range of difference for closest HDM point to Estonian TG varied -55.10...90.58 cm, largest differences occurring for the Sentinel-3A data results. The range of difference for closest HDM point to Finnish TG varied -64.87...80.12 cm, the lowest differences occurring for the Sentinel-3A data results and highest differences occurring for the Sentinel-6A and Jason-3 data results. Note, that Sentinel-3A and Sentinel-6A/Jason-3 data has been processed by two different HDM models. More in depth for Sentinel-6A and Jason-3 is examined in "9.1.2 Sentinel-6A" and "9.1.3 Jason-3".

9.1.2 Sentinel-6A

Dynamic Topography of Sentinel-6A

5 tracks of Sentinel-6 that crossed over Gulf of Finland, were examined. Tracks 0111 and 0187 are descending, tracks 0168, 0092 and 0016 are ascending for this satellite mission (Fig. 9.8b).

Since Sentinel-6 high resolution data is available from November 2021, the months of November and December 2021 and January and February 2022 were processed and compared to the same time instance of Jason-3 satellite mission passings. The time difference between two satellite mission passings at the same track is about 2 minutes. Therefore, both satellite mission tracks and results are highly comparable.

In general, the results (Table 9.5) of HBM-EST derived DT show that in most of the cases the DT for the original HDM were overestimated (for example most of the cases for the track of 0016 (Fig. 15.15.1-15.15.11)), underestimated (for example most of the cases for the track of 0187 (Fig. 15.13.1-15.13.11), 0092 (Fig. 15.14.1-15.14.11)) and/or quite even compared (for example most of the cases for the track of 0111 (Fig. 15.11.1-15.11.10), 0168 (Fig. 15.12.1-15.12.11)) to the TG values throughout the months (minimum -33.64 cm to maximum 84.78 cm in range).

The TG from both Estonia and Finland serves as a base truth in the methodology applied. The distance between the TG from Estonia to Finland varied from 69.9 – 156.5 km. The DT

from both sides were not the same. On the Estonian side the range of DT was -33.6–84.7 cm whilst in the Finland it was -61.1–80.1 cm. The difference between both sides (from Estonia to Finland) varied at times from 1.0–50.0 cm. Also, along the Gulf the DT varied from west to east -33.6–75.5 cm and north to south 10.7–84.7 cm. The difference throughout the year can be also viewed from the Figure 9.8a, where line yellow is for the date of 15th February 2022 12:00, line red is for the date of 15th January 2022 12:00, line green is for the date of 15th December 2022 12:00 and line blue is for the date of 15th November 2022 12:00.

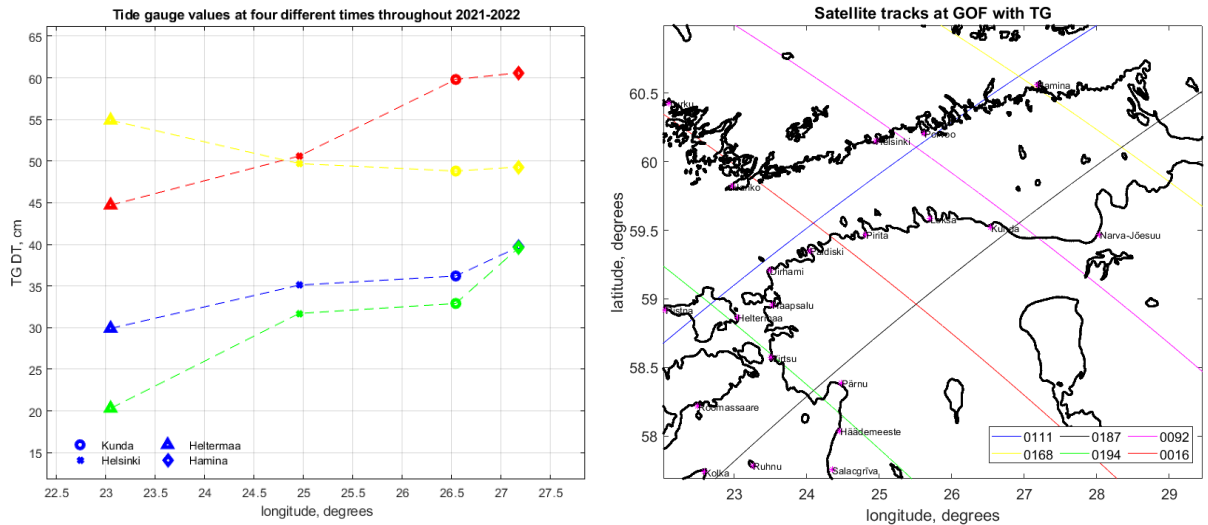


Figure 9.8 a) Tide gauge values throughout the year of 2021-2022. TGs used are Heltermaa, Helsinki, Kunda and Hamina.

Figure 9.8 b) Tracks of Sentinel-6A and Jason-3.

Root Mean Square Error of Sentinel-6A

Examination of table 9.2 shows that there seems to be no correlation between minimum RMSE and date/season of the minimum value. Similar observation was also made with S3 results. The minimum RMSE is between 3.5–7.0 cm and maximum RMSE is between 32.6–43.9 cm. Minimum as well as a maximum RMSE occurred for the track of 0111 (Fig. 15.11.1-15.11.10), which is descending track that begins in the opening of the GOF and crosses over the GOF almost all the way from west to east. Track 0111 is the longest track of Sentinel-

6A which crosses over the GOF. This track also crosses over island of Osmussaare (Estonia) (Fig. 9.9).

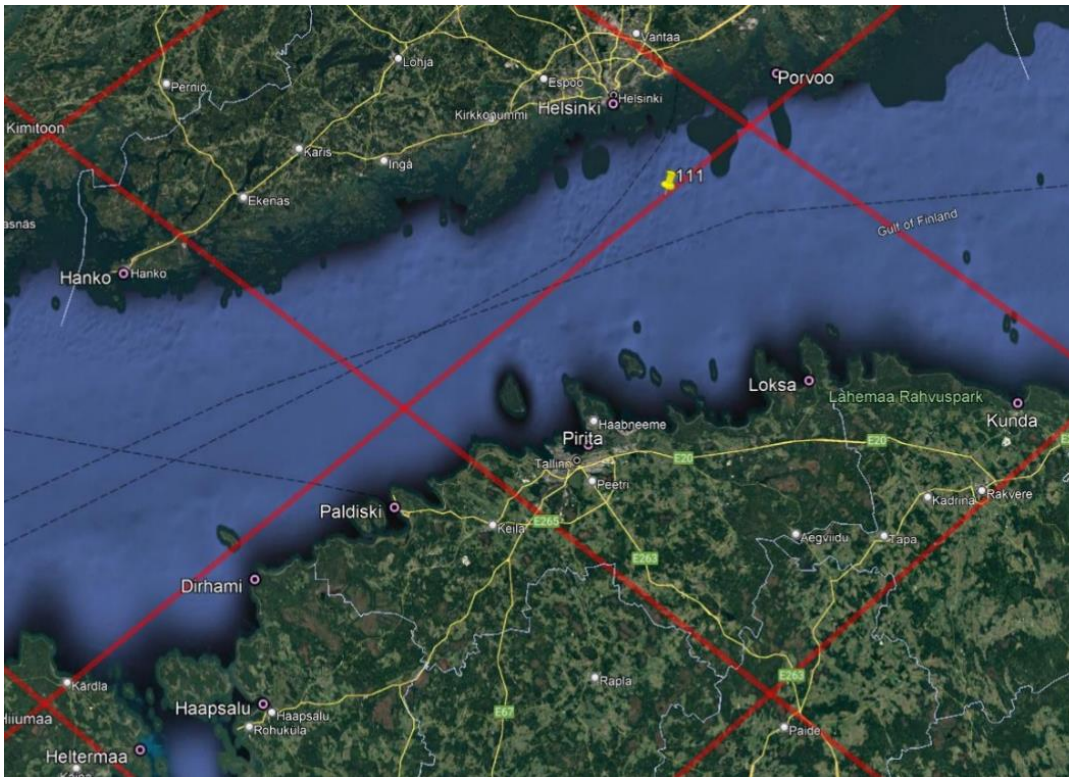


Figure 9.9 Tracks of Sentinel-6A and Jason-3, which pass over the Gulf of Finland. The track of 0111 is marked by yellow marker.

From the Table 9.2 there seems to be a correlation between maximum RMSE and date of the maximum value – for the tracks of 0111 (Fig. 15.11.1-15.11.10), 0016 (Fig. 15.15.1-15.15.11) and 0168 (Fig. 15.12.1-15.12.11) maximum RMSE was recorded at the same week of 07th-13th of February, for the tracks of 0092 (Fig. 15.14.1-15.14.11) and 0187 (Fig. 15.13.1-15.13.11) maximum RMSE was recorded at the same week of 13th-16th of November. The maximum RMSE is between 32.6–43.9 cm. Note, that there are around 90.5% less data points for Sentinel-6A than Sentinel-3A, which means that the RMSE calculation is stricter and highly depends on the quality of the data points.

Table 9.5 shows, that difference between HDM and TGs vary greatly. Most of the largest range differences occur for the tracks of 0111 and 0016. Both of these tracks are located at each side of the Gulf, so there seems to be no correlation due to usage of different tide gauges. Although there seems to be a correlation between the values and the dates they occurred – the minimum RMSE occurred on the same week (27.12.2021-02.01.2022) (Fig. 9.10 and Fig. 9.11). The same for the maximum RMSE values. This underestimating can be

visually also examined in the figures in the Appendices (Fig. 15.11.1-15.11.10 and Fig. 15.15.1-15.15.11).

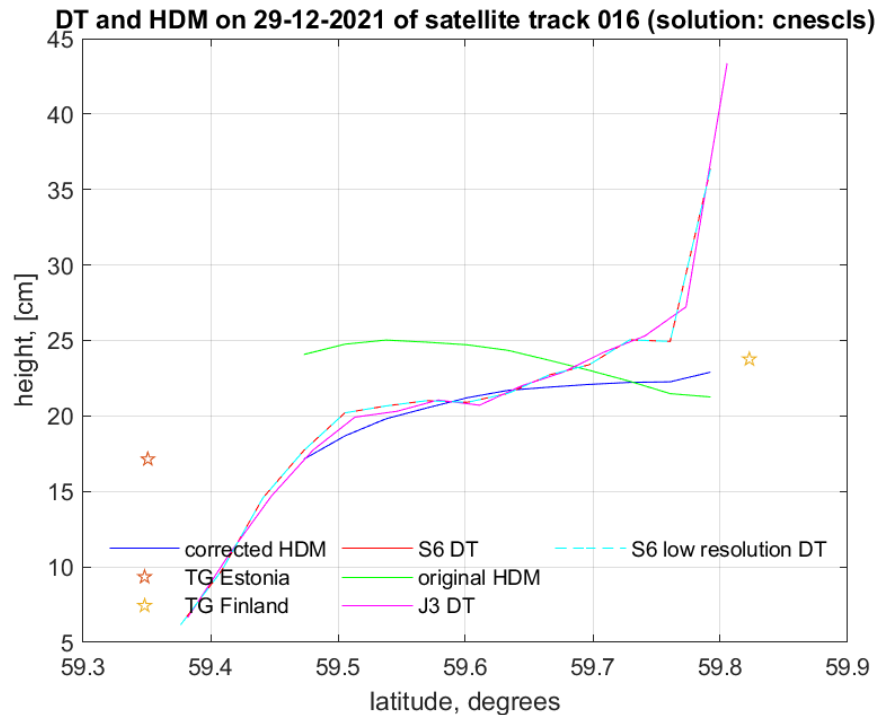


Figure 9.10 Example of a track of 0016 at the date of 29.12.2021. The height represents DT in the vertical axis.

Hereby is shown a graph of track 0111 passing by 02.01.2022 in the Gulf of Finland (Fig. 9.10). In the example is shown the correlation between low- and high-resolution Sentinel-6A data. As mentioned in the section "5.2 Sentinel-6", the difference between two resolutions lies in the waveform bands used. For almost all the tracks, which are presented and delivered for this thesis, the SA DT is always lower than the tide gauge recorded data. This means that SA data under-estimates the results, which could be caused by the presence of sea-ice and/or added corrections. Sea ice in the year of 2022 was present until early March, therefore sea-ice could be one of the aspects which hinder the RMSE values as well as the DT of SA. This could not be a technical problem regarding the satellite because then the Sentinel-6A and Jason-3 derived SSH would not be so comparable.

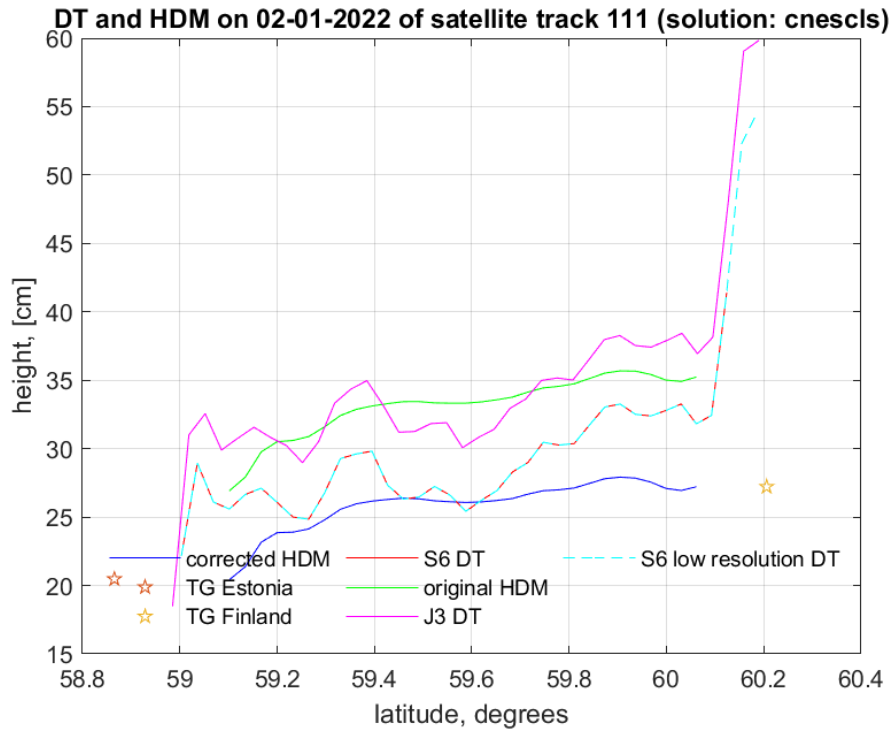


Figure 9.11 Example of a track of 0111 at the date of 02.01.2022. This example shows how the tracks were analysed to all passes.

9.1.3 Jason-3

Dynamic Topography of Jason-3

5 tracks of Sentinel-6 that crossed over Gulf of Finland, were examined. Tracks 0111 and 0187 are descending, tracks 0168, 0092 and 0016 are ascending for this satellite mission (Fig. 9.8b).

In general, the results of HBM-EST derived DT show that in most of the cases the DT for the original HDM were overestimated and/or quite even compared to the TG values throughout the months (minimum -33.64 cm to maximum 84.78 cm in range) (Table 9.6).

The TG from both Estonia and Finland serves as a base truth in the methodology applied. The distance between the TG from Estonia to Finland varied from 69.9 – 156.5 km. The DT

from both sides were not the same. On the Estonian side the range of DT was -33.6–84.7 cm whilst in the Finland it was -61.1–80.1 cm. The difference between both sides (from Estonia to Finland) varied at times from 1.0–50.0 cm. Also, along the Gulf the DT varied from west to east -33.6–75.5 cm and north to south 10.7–84.7 cm. The difference throughout the year can be also viewed from the Figure 9.9a.

Root Mean Square Error of Jason-3

Examination of Table 9.3 shows that there seems to be no visual correlation between minimum RMSE and date of the minimum value. The minimum RMSE is between 1.6–11.1 cm and maximum RMSE is between 28.8–50.1 cm. Minimum as well as a maximum RMSE occurs for the track of 0111 (Fig. 15.11.1-15.11.10), which is descending track that begins in the opening of the GOF and crosses over the GOF almost all the way from west to east. Track 0111 is the longest track of Sentinel-6A which crosses over the GOF. This track also crosses over island of Osmussaare (Estonia) (Fig. 9.9).

There seems to be visual correlation between maximum RMSE and date of the maximum value – for all of the tracks the maximum RMSE was recorded at the period of two weeks at the end of January and in the beginning of February 2022. The maximum RMSE is between 29.8-50.1 cm. Note, that there are around 90.5% less data points for Jason-3 than Sentinel-3A, which means that the RMSE calculation is affected by the quality and quantity of the data points.

Comparing Sentinel-6A and Jason-3 results, the most of the minimum RMSE occurred in December 2021 (in range of 4.29-8.81 cm). Range of minimum RMSE values is smaller for Sentinel-6A than Jason-3. For both satellite missions the maximum RMSE mostly occurred in the month of February 2022 (in range of 29.86-43.9 cm). Range of maximum RMSE values is smaller for Sentinel-6A than Jason-3. By these results we can say that Sentinel-6A results are more stable than for the Jason-3.

Table 9.6 shows, that difference between HDM and TGs vary greatly. Most of the largest range differences occur for the tracks of 0092 and 0187. Both of these tracks have been examined in Kunda station. Both of mentioned tracks also have a large average difference between corrected and uncorrected HDM. This means, that uncorrected HDM was mostly

greatly underestimating the dynamic topography. This underestimating can be visually also examined from the Appendices (Fig. 15.14.1-15.14.11 and Fig. 15.13.1-15.13.11). Comparing Sentinel-6A and Jason-3, the largest range of differences between corrected HDM and SA DT for Sentinel-6A is for the tracks of 0016, 0187 and 0168 and for Jason-3 is for 0111 and 0092 (-50.14...20.2).

9.2 Near coast perspective

One of the objectives of the thesis was to examine near coast perspective. In this study calculations are made with respect to a coastline that was generated from the Matlab adapted software that was produced over 5 years previous (Artu Ellmann, personal communication). In the Figure 9.12 is shown an example of the track 0625, which passes over the center of the Gulf of Finland. This track also passes over Naissaar island (Estonia). In the Figure 9.13 is shown an example of the track 0016, which passes over the Gulf of Finland at the opening. In mentioned figures is shown DT points, which are taken into account (a.k.a. the good points) and which are not (a.k.a. the bad points). The "bad data points" are removed by two outlier removal steps – firstly by every data point which is over 40cm than the average value of all data points, secondly by *rmoutliers* function (using MatLab 2020 program function), which removes outliers from the data. *Rmoutliers* function uses removes outliers, which are more than three scaled median absolute deviations (MAD) away from the median.

9.2.1 Sentinel-3A

Table 9.7 shows that for Sentinel-3A the bad data points vary track-wise greatly from 13 to 242 points. As mentioned, bad data points refer to outliers along such tracks, which can be caused by hindrances of coastal activity, marine traffic, island, turbulent waters etc. The

worst quality data points occur on the tracks of 0739, 0528, 0397 and 0425. These tracks locate at the different ends of the Gulf and also their length (number of data points available) is different. This occurs near the rivers of Neva, Narva, Kemi and Luga (see more in section “4.4 River discharge”) and their river-runoff can be a major influencer to cause outliers.

Average difference between Estonian TG value and averaged ten closest satellite DT points is also calculated for each satellite track. As seen in the Table 9.7, all of the values between TG and averaged ten closest satellite DT points are negative – which means, that SA DT greatly underestimates the DT compared to TG. The largest averaged offset occurred for the track of 0311 (result of -33.12 cm), which locates at the end of the Gulf and near rivers Narva and Luga. The smallest averaged offset occurred for the track of 0511 (result of -9.31 cm) and this track passes over the Gulf of Finland at the opening.

The same patterns seem to follow for the nearest points to coast and nearest TG – the best (smallest in value) results seem to appear for the track, which locate at the opening of the GOF, for example 0511, 0625 and 0311. There appears an anomaly along the results – at the opening of the GOF the 0397 passes by and it has the largest value considering the distance for both near coast and near TG. This might be explained by the location of the passing, nearest TGs are Heltermaa and Turku, which have lots of island nearby and therefore this distance might be affected due to outliers.

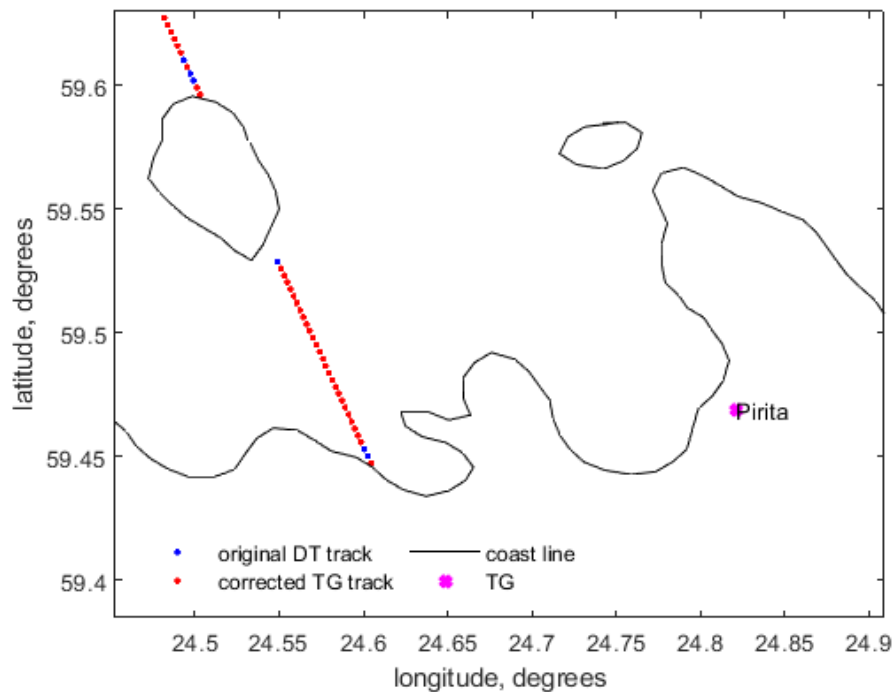


Figure 9.12 Example of the track of 0625 with usable and unusable datapoints.

Table 9.7 Values gathered from analysing data points from the satellite mission of Sentinel-3A from 2018.

Sentinel-3 track	Data points available in the Gulf of Finland	Good data points in the Gulf of Finland	Bad data points in the Gulf of Finland	Nearest good point distance to nearest coast (m)	Nearest good point distance to TG (km)	Average difference between Estonian TG value and averaged ten closest satellite DT points (cm)
0625	181...191	96...177	14...85	56.41	17.41	-16.95
0311	252...255	93...230	25...159	34.19	39.75	-33.12
0197	308...321	259...286	35...49	45.66	38.66	-15.46
0739	226...231	23...192	39...203	165.53	18.2	-15.48
0528	376...383	58...370	13...218	30.58	38.4	-11.79
0414	321...334	178...302	32...143	48.78	15.52	-18.66
0397	478...487	236...391	96...242	1236.34	85.92	-15.75
0511	230...232	172...192	40...58	58.12	14.11	-9.31
0083	236...253	107...216	37...129	125.05	8.87	-11.09
0425	201...234	16...145	89...185	66.45	46.33	-15.48

9.2.2 Sentinel-6A

For the Sentinel-6A bad data points vary from 25 to 49 points for each track and pass. As mentioned, bad data points refer to outliers along the track, which can be caused by hindrances of coastal activity, marine traffic, island, turbulent waters etc. The worst quality data points occur on the tracks of 0016 and 0092. These tracks locate in the middle of the GOF, both of these tracks are ascending. These tracks do not pass over large islands and

their distance to nearest TG and coast was the best concerning all Sentinel-6A tracks, however near the Finnish coast they pass over multiple small islands.

Average difference between Estonian TG value and averaged ten closest satellite DT points is also calculated for each satellite track. As seen in the Table 9.8, all of the values between TG and averaged ten closest satellite DT points are negative – which means, that SA DT greatly underestimates the DT compared to TG. The largest averaged offset occurred for the track of 0168 (result of -48.15 cm), which locates at the end of the Gulf and near the opening of river Neva. The smallest averaged offset occurred for the track of 0111 (result of -21.24 cm) and this is one of the longest tracks to pass over The Gulf of Finland.

The best (smallest in value) results seem to appear for the track, which locate at the middle of the GOF, for example 0016, 0092 and 0168. There seems to be pattern for nearest good data point to coast with descending track of 0187 and 0111 – considering the other Sentinel-6A tracks examined in this study, they have the largest value for the nearest good point distance to nearest coast. This value is between 1900-2600 m. This pattern seems to follow the track 0111 for the nearest good point to nearest TG as well, the value being 92.95 km. This behavior does not correspond to other descending track of 0186, which has one of the smallest values of 19.61 km.

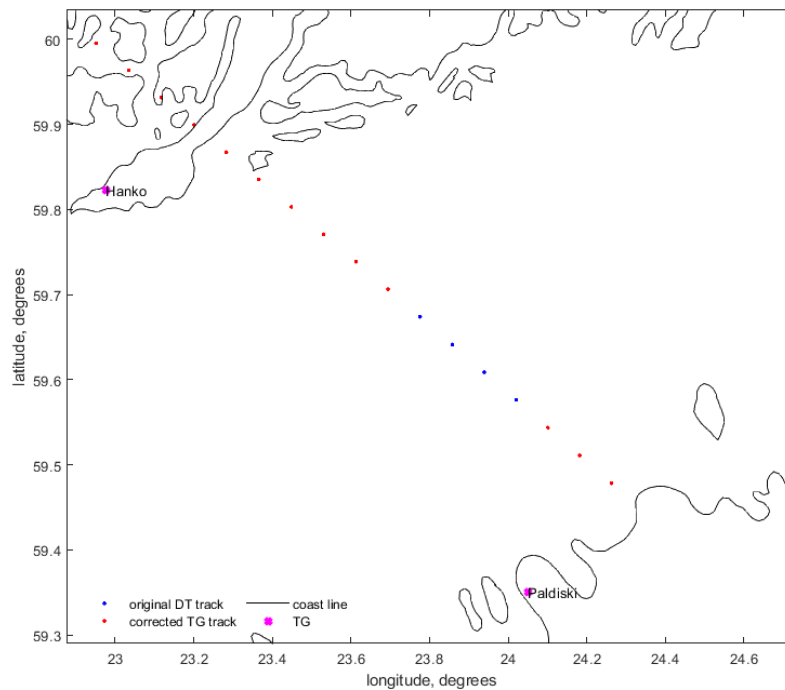


Figure 9.13 Example of the track of 0016 with usable and unusable datapoints.

Table 9.8 Values gathered from analysing data points from the satellite mission of Sentinel-6A from November 2021 – February 2022.

Sentinel-6 track	Data points available in the Gulf of Finland	Good data points in the Gulf of Finland	Bad data points in the Gulf of Finland	Nearest good point distance to nearest coast (m)	Nearest good point distance to TG (km)	Average difference between Estonian TG value and averaged ten closest satellite DT points (cm)
0111	68..69	34..39	30...34	1900	92.95	-21.24
0016	58...59	14..15	44	100	18.99	-39.68
0092	68...69	20	48...49	200	23.62	-45.36
0187	58...59	33...34	25	2600	19.61	-44.82
0168	50...68	19..38	30...31	200	67.49	-48.15

9.2.3 Jason-3

For the Jason-3 bad data points vary from 24 to 47 points for each track and pass. As mentioned, bad data points refer to outliers along the track, which can be caused by hindrances of coastal activity, marine traffic, island, turbulent waters etc. The worst quality data points occur on the tracks of 0016 and 0092. These tracks locate in the middle of the gulf, both of these tracks are ascending. These tracks do not pass over large islands and their distance to nearest TG and coast was the best concerning all Jason-3 tracks, however near the Finnish coast they pass over multiple small islands.

Average difference between Estonian TG value and averaged ten closest satellite DT points was also calculated for each satellite track. As seen in the Table 9.9, all of the values between TG and averaged ten closest satellite DT points are negative – which means, that SA DT greatly underestimates the DT compared to TG. The largest averaged offset occurred for the

track of 0168 (result of -48.15 cm), which locates at the end of the Gulf and near the opening of river Neva. The smallest averaged offset occurred for the track of 0111 (result of -21.24 cm) and this is one of the longest tracks to pass over The Gulf of Finland.

The best (smallest in value) results seem to appear for the track, which locate at the middle of the GOF, for example 0016, 0092 and 0168. There seems to be pattern for nearest good data point to coast with descending track of 0187 and 0111 – considering the other Jason-3 tracks examined in this study, they have the largest value for the nearest good point distance to nearest coast. This value is between 584-1014 m. This pattern seems to follow the track 0111 for the nearest good point to nearest TG as well, the value being 92.95 km. This behavior does not correspond to other descending track of 0186, which has one of the smallest values of 19.61 km.

Table 9.9 Values gathered from analysing data points from the satellite mission of Jason-3 from November 2021 – February 2022.

Jason-3 track	Data points available in the Gulf of Finland	Good data points in the Gulf of Finland	Bad data points in the Gulf of Finland	Nearest good point distance to nearest coast (m)	Nearest good point distance to TG (km)	Average difference between Estonian TG value and averaged ten closest satellite DT points (cm)
0111	67	35..41	26..32	1014	92.95	-21.24
0016	57...58	14...15	43	3	18.99	-39.68
0092	66...67	19...20	47	6	23.62	-45.36
0187	57	32..33	24..25	584	19.61	-44.82
0168	49..67	27..38	29...22	72	67.49	-48.15

Tables 9.7, 9.8 and 9.9 examine Sentinel-3A, Sentinel-6A and Jason-3 results in terms of quantity and quality of data points available. The data points quality is assessed to good and bad data points in terms of outliers. In the tables there are also examined the nearest good

data point to coast and to nearest TG. The results are varying greatly between the results of Sentinel-3A data and Sentinel-6A/Jason-3. The average difference between Estonian TG value and averaged ten closest satellite DT points is also calculated for all three missions and the results value for all three missions are negative – meaning, that the SA DT greatly underestimates the DT compared to TG records. Largest difference occurred for the track of 0168 (Sentinel-6A and Jason-3), smallest difference occurred for the track of 0511 (Sentinel-3A).

10. Discussion

This thesis examines three different satellite missions, Sentinel-3A, Jason-3 and the recently operated Sentinel-6A, at two different time periods. One of the main objectives was to examine Sentinel-6A satellite mission and compare the results to Jason-3 satellite mission because they pass over the Gulf of Finland at the same track. To compare the results two aspects of mentioned satellite missions and satellite altimetry sea level data is examined:

1. Along-track perspective – compare satellite altimetry and hydrodynamic models to determine the realistic sea level data (i.e., DT) and the accuracy of the satellite altimetry.
2. Near coast perspective – to examine tide gauges and satellite altimetry sea level heights performance at near coast areas in terms of accuracy and quality of satellite data points on approaching the coast.

Concerning the along-track perspective, the root mean square error (RMSE) results for all the satellite missions was between 1.68...50.14 cm. With the largest difference occurring in values for the Jason-3 mission and smallest difference in values being for the Sentinel-6A mission. Difference between uncorrected and corrected hydrodynamic model is between - 5.51 to 49.74 cm. Large RMSE values near the end of the GOF could be caused by the location of the satellite passings – rivers Neva, Narva and Luga discharge could affect the results.

Based on the results of this study our assessment show (RMSE values) the most accurate and reliable satellite mission seems to be Sentinel-6A. Although it has some large distances between closest coast point and TG, the overall values seem to be consistent and the RMSE values are also dependable. Summarized values can be seen in the Table 10.1. The value range between minimum and maximum RMSE is the smallest and for dynamic topography it would be ideal that the values are consistent throughout the GOF.

Table 10.1 Summary of the values gathered during data processing.

Satellite mission	Most minimum RMSE (cm)	Most minimum RMSE track	Most maximum RMSE (cm)	Most maximum RMSE track	Allover nearest good point distance to nearest coast (m)	Allover nearest good point distance to TG (km)
Sentinel-3A	2.83	0625	46.27	0425	30.58	8.87
Sentinel-6A	3.50	0111	43.90	0111	3	18.9
Jason-3	1.68	0111	50.14	0111	3	18.9

With respect to the near coast perspective, the results were corrected by two iterations for different outlier removals. Nearest good point distance to nearest coast was from 3 meters to 2.6 kilometers, nearest good point distance to nearest tide gauge was from 8.8 to 92.9 kilometers. The farthest nearest point to the coast was detected from Sentinel-6A and Jason-3 descending tracks (from track 0111 and 0187). Farthest nearest data point to tide gauge was detected using tracks with Heltermaa (Estonia) tide gauge at the opening of the Gulf, which largest distance was 92.9 kilometers. This result occurred for all three satellite missions.

Comparing the results to previous studies on this matter, there is a large difference concerning the distance to coast perspective. According to the study of (Mostafavi et al., 2021), the closeness to coastline was 2-3 kilometers, but in this thesis the closeness to the coast was obtained only 3 meters for the Jason-3 satellite mission. Also as mentioned, the nearest good point distance to nearest coast was from 3 meters to 2.6 kilometers, which is well below the results according to mentioned previous study. The difference in coastline used in this study may attribute for the differences, for coastline changes over time and different sources of coastline may give different results. It is worth mentioning, that bias between hydrodynamic model and tide gauge as well as bias between hydrodynamic model and satellite altimetry derived dynamic topography for satellite tracks of 0016 and 0092 of Jason-3 (which closest good data point was recorded 3 and 6 meters) was the greatest. The bias between HDM and TG varied around -49.16...63.96 cm and the bias between HDM and SA DT varied around -40.99...20.22 cm. This could indicate that different sources utilized may also contain some errors.

Main hindrances concerning SA results is that the results highly depend on the season and weather observed – main high values errors occurred when there was sea-ice present. Some of the high valued results occurred also in the middle of summer or autumn, that could be the results due to storms or other unpredictable coastal processes. This aspect also is mentioned in the study of (Birgiel et al., 2019). This might be also a possible reason for large difference in RMSE values for Sentinel-6A, because the used Sentinel-6A data are mostly from late autumn until late winter. Future examination how sea-ice affects the SA values needs to be performed as well as derived techniques employed. In this study Baltic Seal for Sentinel-3A data set was used, which was intended to improve the performance with sea ice, now including machine learning algorithms. From our analysis this can still be improved.

Mentioned limitations also include quantity and quality of data - the resolution in the Gulf of Finland is for Sentinel-3A 181-487 data points, for Jason-3 49-67 data points and for Sentinel-6A 50-69 data points. This is also critical for both objectives mentioned, because due to the large difference of available data points, the RMSE of all the satellite missions might be affected by the quantity and quality of the data points. The occurrence of the satellite passing – Sentinel-3A being every 27 days and for Sentinel-6A/Jason-3 being every 10 days – is also a reason for data limitations as well as it's access.

For some of the tracks, which crossed islands in the Gulf of Finland had high values of RMSE. So, the presence of islands still influences the performance of SA derived data even though the outliers caused by islands were automatically and manually removed. This could be an issue with estimate sea level with re-tracker or the processing of outliers in this study.

The distance of TG from SA point varied between 0-80 km and this does not appear to influence the results in this study area. Some of the smallest RMSE values occurred where the distance between TG and SA DT was the largest. This occurred for the tracks of 0397 and 0197 of Sentinel-3A.

11. Conclusion

In this thesis using three satellite missions the satellite altimetry derived dynamic topography was examined in two aspects – along-shore perspective and near coast perspective.

Concerning the along-shore perspective, the largest variations occurred in sea level during spring and autumn. This could be affected due to ice melting, storms and river discharge.

Also, the root mean square error (RMSE) results for all the satellite missions was between 2...50 cm as largest difference in values being for the Jason-3 mission and smallest difference in values being for the Sentinel-6A mission. Difference between uncorrected and corrected hydrodynamic model is between -5 to 50 cm. Considering the RMSE values and RMSE values range of all satellite missions, the most accurate and reliable satellite mission seems to be Sentinel-6A. Although it has some large distances between closest coast point and TG, the overall values seem to be consistent and the RMSE values are also dependable. The value range between minimum and maximum RMSE is the smallest and for dynamic topography it would be ideal that the values are consistent throughout the Gulf of Finland. This could mean, that new re-tracker, which Sentinel-6A uses, Poseidon-4 has been improved in technicality and in deriving better results. Also as mentioned in the "8. Satellite Altimetry Corrections", Sentinel-6A uses three more corrections in deriving SSH. If the same corrections were to apply to other satellite missions, then also their results and values could improve.

Concerning the near coast perspective, the results were corrected in two steps by different outlier removals. Nearest good point distance to nearest coast was from 3 meters to 2.6 kilometers, nearest good point distance to the nearest tide gauge was from 8.8 to 92.9 kilometers. The farthest nearest point to the coast was detected from Sentinel-6A and Jason-3 descending tracks (from track 0111 and 0187). Farthest nearest data point to tide gauge was detected using tracks with Heltermaa (Estonia) tide gauge at the opening of the Gulf of Finland, which largest distance was 92.8 kilometers. This result occurred for all three satellite missions. Different satellite missions give a variety of good quality of data points and distance to coast in terms of near coast perspective. The most reliable results seemed to still have for Sentinel-3A but only because the quantity of data points, which is 90.5% larger than for the Sentinel-6A and Jason-3. Otherwise in terms of the near coast perspective, the

Sentinel-6A satellite missions has the best variation of results in good quality data points and distance to coast.

Examining the results for this study it appeared, that presence of sea ice is greatly affecting the results of SA DT and its accuracy. But the sea ice alone is not the only reason – the influence of islands, land contamination and river run-off seem to influence the results of satellite altimetry accuracy. This occurred mostly at the end of The Gulf of Finland, where there are multiple different sizes of islands and 4 largest rivers of Gulf of Finland (and one for the Baltic Sea) flow.

The method employed relied on tide gauges being the ground truth. The distance from SA data points to TG within the range of 8.82 to 92.5 km does not seem to affect the results. The satellites mostly under-estimated the DT value, which is occurring on most of the satellites and their passings in compared to the TG values.

12. Abstract

Satellite altimetry is one of the most known and available data sources to examine and evaluate changes in sea level, especially offshore. There are multiple challenges and hinderances in determining the quality and accuracy of satellite altimetry data along-track and near the coast.

In this thesis, three satellite missions of Sentinel-3A, Jason-3 and Sentinel-6A were examined in two perspectives (i) along-track perspective in determining the accuracy and sea level variation and (ii) the near coast perspective with respect to how much good data points actually approach the coast and how accurate these points are compared to within the vicinity of the nearest tide gauge. Previous studies have been examining Sentinel-3A and Jason-3, but for Sentinel-6A, which was released in November 2020, there has not been many studies to determine its accuracy and/or quality.

To determine the accuracy of satellite altimetry derived dynamic topography a method is developed that utilizes a synergy of different sources that consists of tide gauges of Estonian and Finnish coast, hydrodynamic models (Nemo Nordic and HIROMB-EST), NKG2015 marine geoid model as well as a land uplift model (NKG2016LU). From satellite altimetry derived sea surface height, the dynamic topography was found, which was referenced to a marine geoid. To determine the accuracy of SA DT, the hydrodynamic models were taken into account and corrected based on the value of tide gauges. The method highly depended on the quality of tide gauges where they were considered as ground truth. Comparing the results of corrected HDM and SA DT a bias and root mean square error (RMSE) were calculated and examined.

Considering the RMSE values and RMSE values range of all satellite missions, the most accurate and reliable satellite mission seems to be Sentinel-6A. Although it has some large distances between closest coast point and TG, however the overall values seem to be consistent and the RMSE values are also dependable.

Examining the results for this study it appeared, that presence of sea ice is greatly affecting the results of SA DT and its accuracy. But the sea ice alone is not the only cause – the influence of islands, land contamination and river run-off seem to hinder the results of satellite altimetry accuracy. This occurred mostly at the extreme eastern end of the Gulf of Finland, where there are multiple different sizes of islands and one of the largest rivers flows into the Gulf of Finland.

13. Kokkuvõte (in Estonian)

Satelliitaltimeetria on üha tuntust koguvamaid ja kättesaadavamaid andmekogumikke, mille abil uurida ja hinnata meretaset, eriti avamere aladel. Mitmed väljakutsed ja takistused ilmnevad satelliitaltimeetria andmete kvaliteedi ja täpsuse hindamisel nii satelliidi liikumise rajal kui ka rannikuäärsetel aladel.

Antud magistritöös on uuritud kolme satelliidi – Sentinel-3A, Jason-3 ja Sentinel-6A – missiooni kahel olukorral: (i) satelliidi liikumise rajal eesmärgiga määrata kindlaks meretaseme täpsus ja variatsioon ja (ii) hea kvaliteediga andmepunktide hindamisel rannikuäärsetel aladel ja kui täpsed need punktid on hinnates neid lähimate rannikujaamadega. Eelnevad uurimused on uurinud Sentinel-3A ja Jason-3 satelliidimissioone aga Sentinel-6A missioon, mis käivitati 2020. aasta novembris, pole uuritud täpsuse ja andmekvaliteedi tulemuste osas.

Satelliitaltimeetria andmete põhjal tuletatud dünaamilise topograafia täpsuse kindlaks määramisel on kasutatud meetodit, mis hõlmab erinevate andmete vastastikust võrdlemist näiteks Eesti ja Soome rannikujaamade mõõtetulemused, hüdrodünaamilised mudelid (Nemo Nordic ja HIROMB-EST), NKG2015 meregeoidi mudel kaasaarvatud maapinna kerke mudel (NKG2016LU). Satelliitaltimeetria (SA) andmetest tuletatud merepinna kõrgusest on arvatud merepinna dünaamiline topograafia, mille referentsaluseks on võetud meregeoid. SA dünaamiline topograafia täpsuse hindamiseks on võetud arvesse ka hüdrodünaamilisi mudeleid, mille tulemusi on parandatud vastavalt rannikujaamadele. Kasutatud meetod sõltus rannikujaamade mõõtmisandmete kvaliteedist, kuna neid arvestati kui alustõde. Võrreldes parandatud hüdrodünaamiliste mudelite tulemusi SA dünaamilise topograafia tulemustega vahe ja ruutkeskmise viga arvutati ja uuriti.

Arvestades ruutkeskmise viga tulemusi kõikidel satelliidi missioonidel leiti, et kõige täpsemaid ja usaldavatamaid tulemustega satelliidi missioon on Sentinel-6A. Kuigi esines suuri vahemaid satelliidi andmepunktide ja ranniku ja rannikujaamade vahel oli üleüldine väärtuste tulemus järjepidev ja ruutkeskmise vea väärtused usaldatavad.

Uuringutest ilmnas, et merejää olemasolu mõjutab tugevasti dünaamilise topograafia tulemusi ja täpsust. Merejää pole aga ainukene mõjur – samuti mõjutab satelliitaltimeetria andmete täpsuse tulemusi ka saared, reostus ja jõgede äravool. Selline nähtus ilmus peamiselt Soome lahe idapoolses lõpus, kus on mitmeid väikseid saari ja üks suuremaid Läänemere suurima äravooluga jõge voolavad.

14. References

- Ågren, J., Strykowski, G., Bilker-Koivula, M., Omang, O., Mårdla, S., Forsberg, R., . . . Valsson, G. (2016). *The NKG2015 gravimetric geoid model for the Nordic-Baltic region*. Nordic Geodetic Commission (NKG) Working Group of Geoid and Height Systems.
- Aviso+. (n.d.). *Delay-Doppler / SAR altimetry*. Retrieved from Aviso+ Satellite Altimetry Data: <https://www.aviso.altimetry.fr/en/techniques/altimetry/principle/delay-doppler/-sar-altimetry.html>
- Baltic Marine Environment Protection Commission - Helsinki Commission. (n.d.). *Baltic Facts and Figures*. Retrieved from http://archive.iwlearn.net/helcom.fi/environment2/nature/en_GB/facts/index.html
- Birgiel, E., Ellmann, A., & Delpeche-Ellmann, N. (2019). Performance of Sentinel-3A SAR Altimetry Retracker: The SAMOSA Coastal Sea Surface Heights for the Baltic Sea. *International Association of Geodesy Symposia book series (IAG SYMPOSIA, volume 150)*. 150, pp. 23-32. Springer, Cham. doi:https://doi.org/10.1007/1345_2019_59
- BSHC Chart Datum Working Group. (n.d.). *Baltic Sea Hydrographic Commission*. Retrieved April 12, 2022, from <http://www.bshc.pro/working-groups/cdwg/>
- Bundesamt Für Seeschifffahrt und Hydrographie. (n.d.). *Ice reports and ice charts*. Retrieved April 16, 2022, from https://www.bsh.de/EN/DATA/Predictions/Ice_reports_and_ice_charts/ice_reports_and_ice_charts_node.html
- ECMWF Support Portal. (n.d.). *Sea level daily gridded data from satellite observations for the global ocean from 1993 to present*. Retrieved April 12, 2022, from <https://cds.climate.copernicus.eu/cdsapp#!/dataset/satellite-sea-level-global?tab=overview>
- EEA. (2021). *Global and European sea level rise*. European Environment Agency. Retrieved May 18, 2022, from <https://www.eea.europa.eu/ims/global-and-european-sea-level-rise>

- Egido, A., & Smith, W. (2017, January). Fully Focused SAR Altimetry: Theory and Applications. *IEEE Transactions on Geoscience and Remote Sensing*, 55(1), 392-406. doi:10.1109/TGRS.2016.2607122
- Emelyanov, E., Vallius, H., & Kravtsov, V. (2017). Heavy metals in sediments of the Gulf of Finland: A review. *Baltica*, 30(1), 47-54. doi:10.5200/baltica.2017.30.05
- eoPortal. (n.d.). *Sentinel-6 Michael Freilich*. Retrieved April 12, 2022, from <https://directory.eoportal.org/web/eoportal/satellite-missions/content/-/article/jason-cs>
- EOSSAR. (n.d.). *SAR Technology*. Retrieved April 12, 2022, from <https://eossar.com/technology/>
- Estonian Environmental Agency. (2018). *Hüdroloogiline aastaraamat 2018*. Estonian Environmental Agency.
- EUMETSAT. (2021). *Sentinel-6/Jason-CS ALT Level 2 Product Generation Specification (L2 ALT PGS)*. EUMETSAT.
- European Space Agency. (2021, November 29). *Sentinel-6 returning most precise data ever on sea level*. (PhysOrg) Retrieved April 12, 2022, from <https://phys.org/news/2021-11-sentinel-precise-sea.html>
- European Space Agency. (n.d.). *Data Products*. Retrieved April 12, 2022, from <https://sentinels.copernicus.eu/web/sentinel/missions/sentinel-6/data-products>
- European Space Agency. (n.d.). *Mission Objectives*. Retrieved April 12, 2022, from <https://sentinels.copernicus.eu/web/sentinel/missions/sentinel-3/mission-objectives>
- European Space Agency. (n.d.). *Mission Objectives*. Retrieved April 12, 2022, from <https://sentinels.copernicus.eu/web/sentinel/missions/sentinel-6/mission-objectives>
- European Space Agency. (n.d.). *Operating Modes*. Retrieved April 12, 2022, from <https://sentinels.copernicus.eu/web/sentinel/user-guides/sentinel-3-altimetry/overview/modes>
- European Space Agency. (n.d.). *Overview*. Retrieved April 12, 2022, from <https://sentinels.copernicus.eu/web/sentinel/missions/sentinel-6/overview>

- European Space Agency. (n.d.). *Re-Tracking Estimates*. Retrieved April 12, 2022, from <https://sentinels.copernicus.eu/web/sentinel/technical-guides/sentinel-3-altimetry/level-2/re-tracking-estimates>
- European Space Agency. (n.d.). *Sentinel Online*. Retrieved April 2022, 12, from <https://sentinels.copernicus.eu/web/sentinel/user-guides/sentinel-3-altimetry/resolutions>
- European Space Agency. (n.d.). *Sentinel Online*. Retrieved April 12, 2022, from <https://sentinels.copernicus.eu/web/sentinel/user-guides/sentinel-3-altimetry/resolutions/resolution-cells>
- European Space Agency. (n.d.). *Sentinel-6 returning most precise data ever on sea level*. Retrieved April 12, 2022, from https://www.esa.int/Applications/Observing_the_Earth/Copernicus/Sentinel-6/Sentinel-6_returning_most_precise_data_ever_on_sea_level
- Finnish Meteorological Institute. (n.d.). *Sea ice statistics*. Retrieved April 12, 2022, from <https://en.ilmatieteenlaitos.fi/icestatistics>
- Finnish Meteorological Institute. (n.d.). *Ice season in the Baltic Sea*. Retrieved April 12, 2022, from <https://en.ilmatieteenlaitos.fi/ice-season-in-the-baltic-sea>
- Finnish Meteorological Institute. (n.d.). *Theoretical mean water and geodetical height systems in Finland*. Retrieved April 12, 2022, from <https://en.ilmatieteenlaitos.fi/theoretical-mean-sea-level>
- Forsström, T., Haapaniemi, J., Holmroos, H., Humalisto, N., Kulha, N., Laamanen, L., . . . Saarinen, A. (2014). A Tentative Marine and Coastal Spatial Plan for the Gulf of Finland. *ResearchGate*. Retrieved from https://www.researchgate.net/publication/264081243_A_Tentative_Marine_and_Coastal_Spatial_Plan_for_the_Gulf_of_Finland
- GGOS. (n.d.). *How can the height of oceans be observed?* (G. G. System, Producer) Retrieved from Global Geodetic Observing System: <https://ggos.org/item/sea-surface-heights/#toggle-id-4>
- GOF Year 2014 Team. (2014). *Gulf of Finland Year 2014 - Assessment*. doi:<https://www.kik.ee/sites/default/files/5457.pdf>

- Grgic, M., & Bašić, T. (2021). *Radar Satellite Altimetry in Geodesy -Theory, Applications and Recent Developments*. London: IntechOpen Limited. doi:10.5772/intechopen.97349
- Guerova, G., & Simeonov, T. (2021). *Global Navigation Satellite System Monitoring of the Atmosphere* (Vol. 1st Edition). Elsevier.
- HELCOM. (2018). *Input of nutrients by the seven biggest rivers in the Baltic Sea region*. Retrieved from <https://helcom.fi/wp-content/uploads/2019/12/BSEP163.pdf>
- Hordoir, R., Axell, L., Höglund, A., Dieterich, C., Fransner, F., Gröger, M., . . . Jönsson, A. (2019). Nemo-Nordic 1.0: A NEMO based ocean model for Baltic & North Seas, research and operational applications. *Geoscientific Model Development*, *12*, 363-286. doi:<https://doi.org/10.5194/gmd-12-363-2019>
- isardSAT. (n.d.). *Sentinel-6 L1 GPP*. Retrieved from <https://www.isardsat.space/project/s6-poseidon-4-gpp>
- Jahanmard, V., Delpeche-Ellmann, N., & Ellmann, A. (2021, June 1). Realistic dynamic topography through coupling geoid and hydrodynamic models of the Baltic Sea. *Continental Shelf Research*, *222*. doi:<https://doi.org/10.1016/j.csr.2021.104421>
- Kollo, K., & Ellmann, A. (2019). Geodetic Reconciliation of Tide Gauge Network in Estonia. *Geophysica*.
- Lagemaa, P., Elken, J., & Kõuts, T. (2011). Operational sea level forecasting in Estonia. *Estonian Journal of Engineering*, *17(4):301*. doi:10.3176/eng.2011.4.03
- Mostafavi, M., Delpeche-Ellmann, N., & Ellmann, A. (2021, September 17). Accurate Sea Surface heights from Sentinel-3A and Jason-3 retracers by incorporating High-Resolution Marine Geoid and Hydrodynamic Models. *Journal of Geodetic Science*, *11(1)*, 58-74. doi:<https://doi.org/10.1515/jogs-2020-0120>
- NASA (Director). (2020). *Sentinel-6 Micheal Freilich Satellite Family Tree* [Motion Picture]. Retrieved May 25, 2022, from nasa.gov/sentinel-6/videos
- National Aeronautics and Space Administration. (n.d.). *Jason-3*. Retrieved April 12, 2022, from <https://sealevel.jpl.nasa.gov/missions/jason-3/summary>
- National Oceanic and Atmospheric Administration. (n.d.). *Altimetric Bathymetry*. (Laboratory for Satellite Altimetry) Retrieved April 12, 2022, from <https://www.star.nesdis.noaa.gov/socd/Isa/AltBathy/>

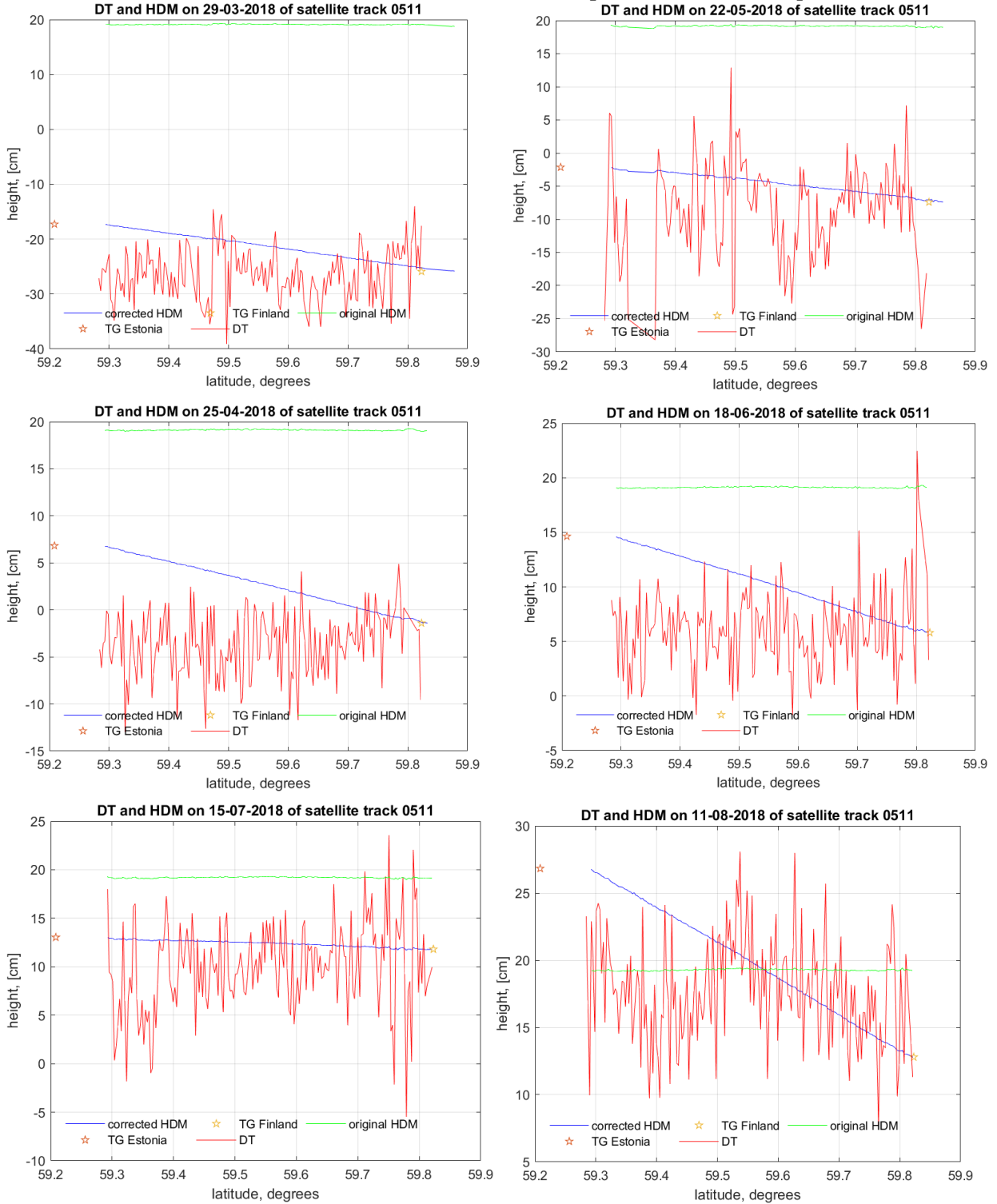
- Nietosvaara, V., & Prieto, J. (2018, March 27). *Ice melting in the Baltic Sea*. (EUMETSAT) Retrieved April 16, 2022, from <https://www.eumetsat.int/ice-melting-baltic-sea>
- NOAA. (n.d.). *How are satellites used to observe the ocean?* (N. O. Administration, Producer, & National Ocean Service website) Retrieved April 12, 2022, from <https://oceanservice.noaa.gov/facts/satellites-ocean.html>
- NOAA. (n.d.). *National Ocean Service*. (N. O. Administration, Producer, & National Ocean Service website) Retrieved April 12, 2022, from <https://oceanservice.noaa.gov/facts/sealevel.html>
- Passaro, M., Müller, F. L., Abulaitjiang, A., Andersen, O. B., Dettmering, D., Høyer, J. L., . . . Tuomi, L. (2020). *Using the Baltic Sea to advance algorithms to extract altimetry-derived sea-level data from complex coastal areas, featuring seasonal sea-ice*. 22nd EGU General Assembly, held online 4-8May, 2020, id.6773. doi: 10.5194/egusphere-egu2020-6773
- Passaro, M., Müller, F., Dettmering, D., Abulaitjiang, A., Rautiainen, L., Scarrott, R., & Chalçon, E. (2021). *Baltic SEAL: Product Handbook, Version 1.1*. doi:<http://doi.org/10.5270/esa.BalticSEAL.PH1.1>
- Public Broadcasting of Latvia. (n.d.). *Baltic Sea water levels rising fast*. Retrieved April 12, 2022, from <https://eng.lsm.lv/article/society/society/baltic-sea-water-levels-rising-fast.a342960/>
- Pujol, M.-I., Schaeffer, P., Faugère, Y., Raynal, M., Dibarboure, G., & Picot, N. (2018, May 16). Gauging the Improvement of Recent Mean Sea Surface Models: A New Approach for Identifying and Quantifying Their Errors. *Journal of Geophysical Research: Oceans*, Volume 123(Issue 8), 5889-5911. doi:<https://doi.org/10.1029/2017JC013503>
- Rjazin, J., Hordoir, R., & Pärn, O. (2019). EVALUATION OF THE NEMO-NORDIC MODEL BY COMPARING THE SEAICE CONCENTRATION VALUES IN THE BALTIC SEA. *The Journal of Ocean Technology*, 14(2), 183. Retrieved from https://www.researchgate.net/publication/334431905_EVALUATION_OF_THE_NEMO-NORDIC_MODEL_BY_COMPARING_THE_SEA-ICE_CONCENTRATION_VALUES_IN_THE_BALTIC_SEA
- Siegel, H., & Gerth, M. (2018). *Sea Surface Temperature in the Baltic Sea 2018*. Leibniz Institute for Baltic Sea Research Warnemünde (IOW). Retrieved from

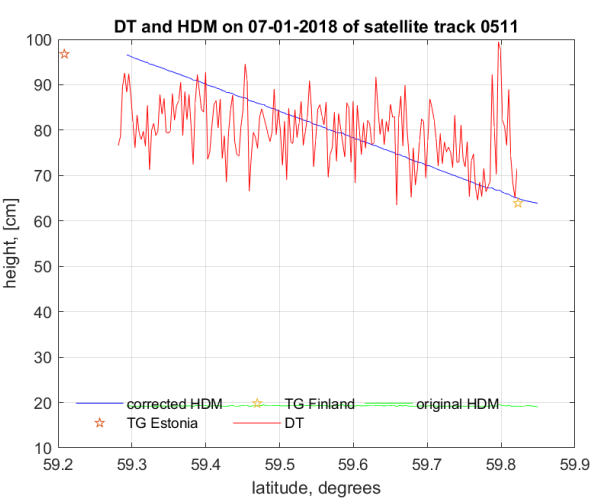
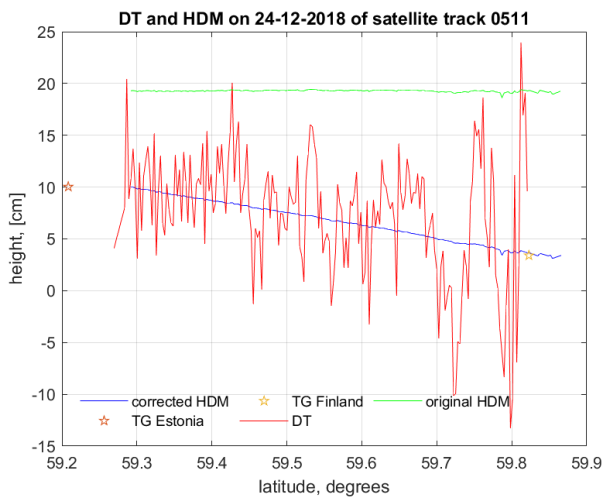
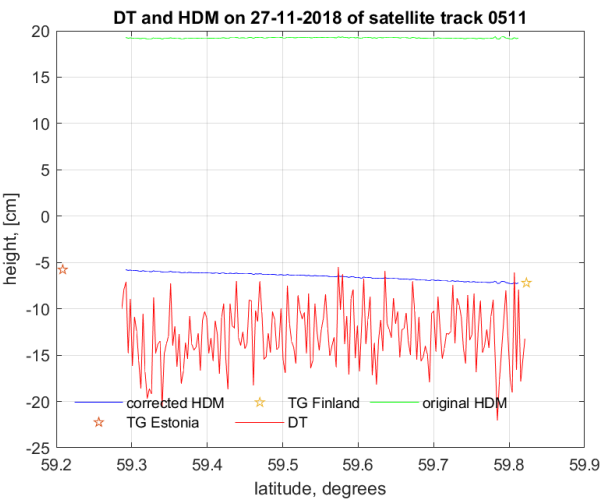
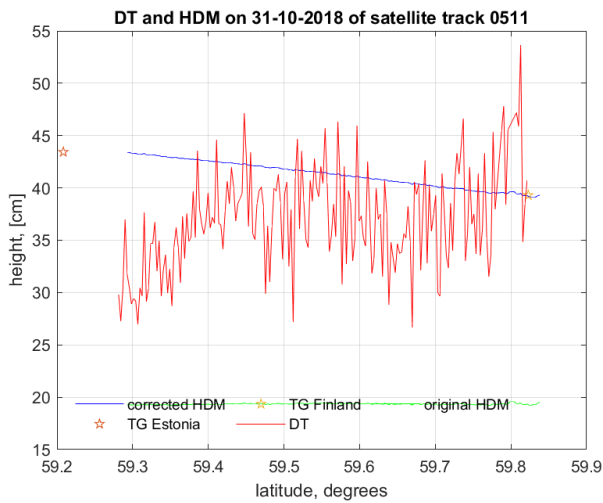
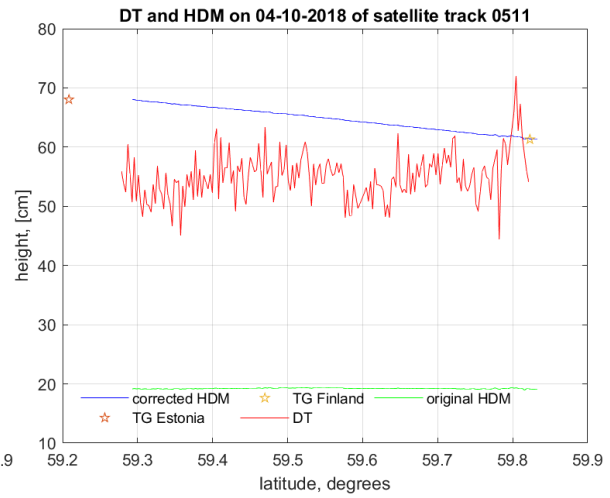
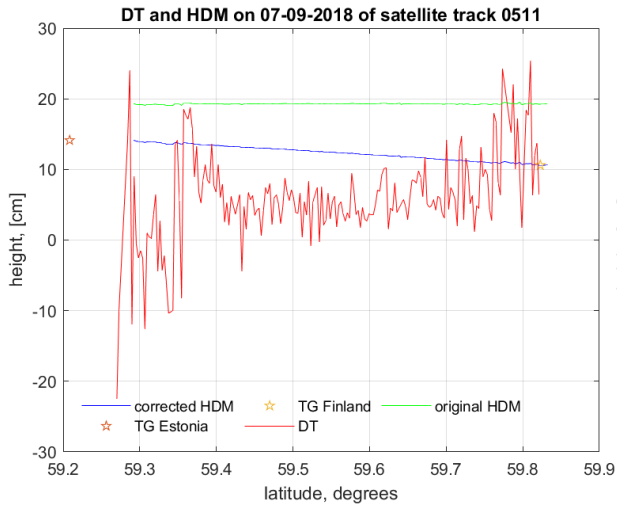
<https://helcom.fi/wp-content/uploads/2020/07/BSEFS-Sea-Surface-Temperature-in-the-Baltic-Sea-2018.pdf>

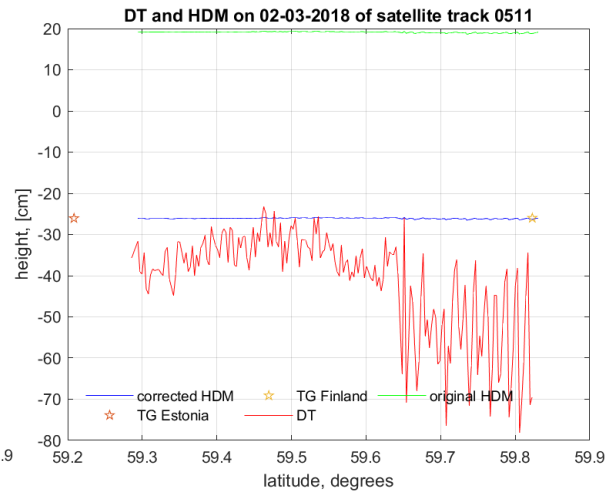
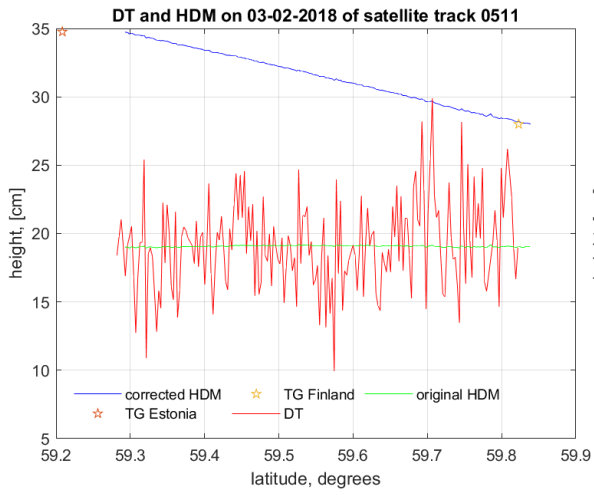
- Snaith, H., Scharoo, R., & Naeije, M. (2006). JUST-IN-TIME ALTIMETRY: INTERNATIONAL COLLABORATION IN PROVISION OF ALTIMETRY DATASETS. Retrieved from https://www.researchgate.net/publication/237299642_JUST-IN-TIME_ALTIMETRY_INTERNATIONAL_COLLABORATION_IN_PROVISION_OF_ALTIMETRY_DATASETS
- Soomere, T., Behrens, A., Tuomi, L., & Nielsen, J. (2008). Wave conditions in the Baltic Proper and in the Gulf of Finland during windstorm Gudrun. *Nat Hazards Earth Syst. Sci*, 8, 37-46. doi:<https://doi.org/10.5194/nhess-8-37-2008>
- The European Space Agency. (n.d.). *Sentinel-6 - Charting sea level for Copernicus*. Retrieved from https://www.esa.int/Applications/Observing_the_Earth/Copernicus/Sentinel-6
- Varbla, S., Ågren, J., Ellmann, A., & Poutanen, M. (2022). Treatment of Tide Gauge Time Series and Marine GNSS Measurements for Vertical Land Motion with Relevance to the Implementation of the Baltic Sea Chart Datum 2000. *Remote Sensing*, 14(4). doi:<https://doi.org/10.3390/rs14040920>
- Varbla, S., Liibus, A., & Ellmann, A. (2022). Shipborne GNSS-Determined Sea Surface Heights Using Geoid Model and Realistic Dynamic Topography *remote sensing*, 14(10). doi:<https://doi.org/10.3390/rs14102368>
- Vestøl, O., Ågren, J., Steffen, H., Kierulf, H., Lidberg, M., Oja, T., . . . Tarasov, L. (2016). *NKG2016LU, an improved postglacial land uplift model for Noridc-Baltic region*. Nordic Geodetic Commission (NKG) Working Group of Geoid and Height Systems.
- Vignudelli, S., Kostianoy, A., Cipollini, P., & Benveniste, J. (2011). *Coastal Altimetry*. Springer Berlin, Heidelberg. doi:<https://doi.org/10.1007/978-3-642-12796-0>
- Wolski, T., Wiśniewski, B., Giza, A., Kowalewska-Kalkowska, H., Boman, H., Grabbi-Kaiv, S., . . . Lydeikaitė, Ž. (2014). Extreme sea levels at selected stations on the Baltic Sea coast. *Oceanologia*, 56(2), 259-290. doi:<https://doi.org/10.5697/oc.56-2.259>
- Zwaly, H. J., & Berner, A. C. (2001). Ice sheet dynamics and mass balance. *Academic Press*, Chapter 9. doi:[https://doi.org/10.1016/S0074-6142\(01\)80154-6](https://doi.org/10.1016/S0074-6142(01)80154-6)

15. Appendices

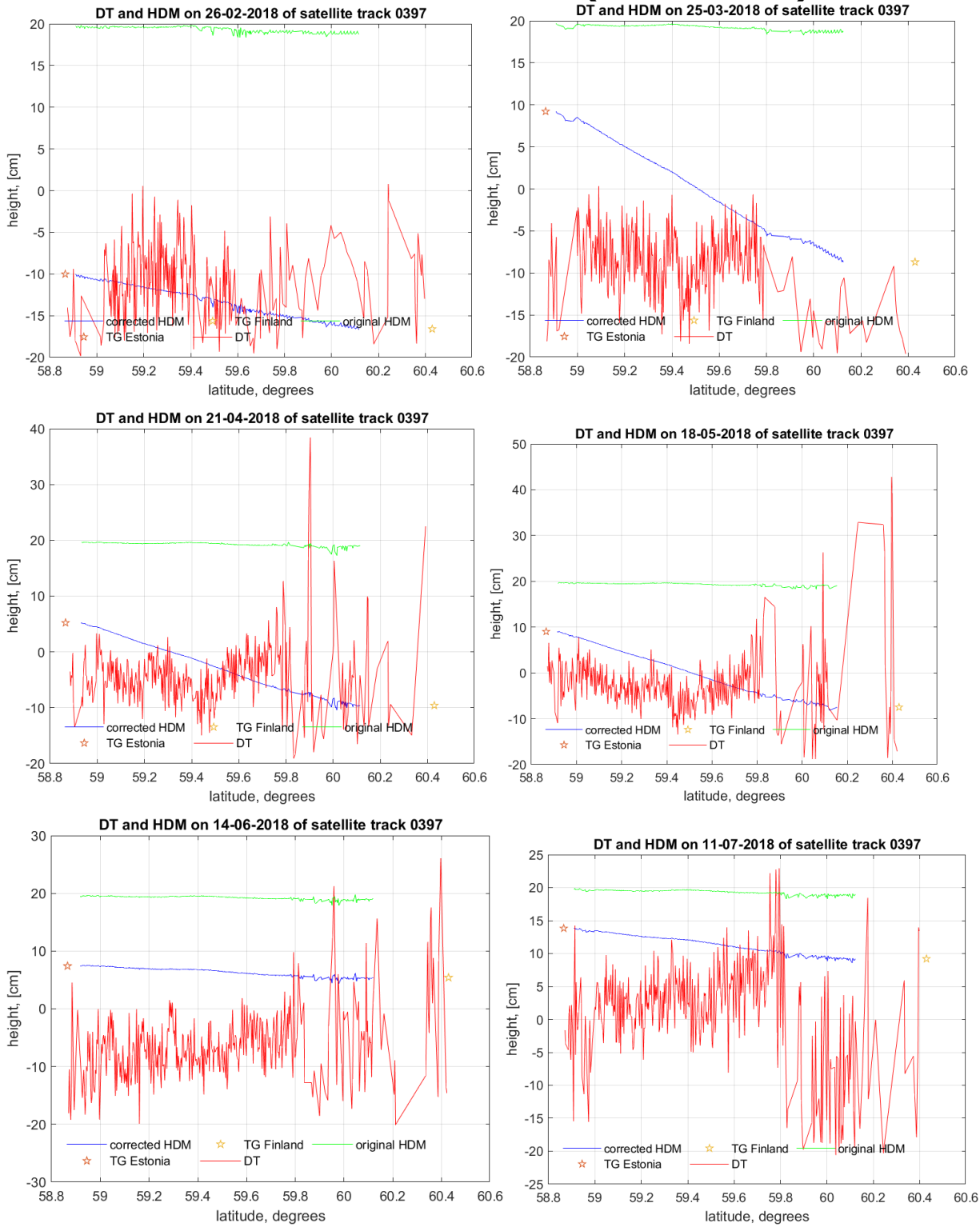
15.1 Results for the track of 0511 (Sentinel-3A)

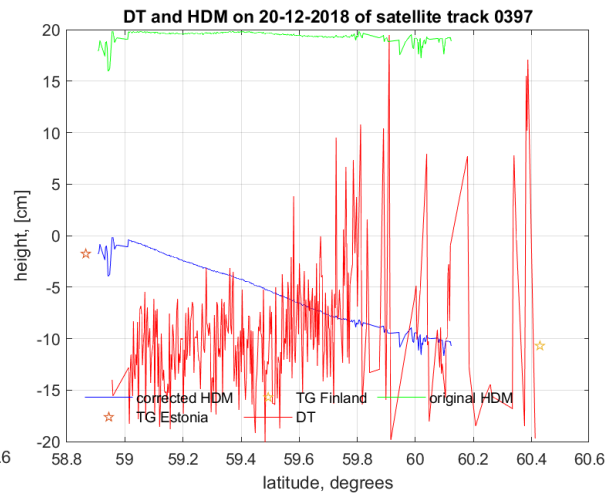
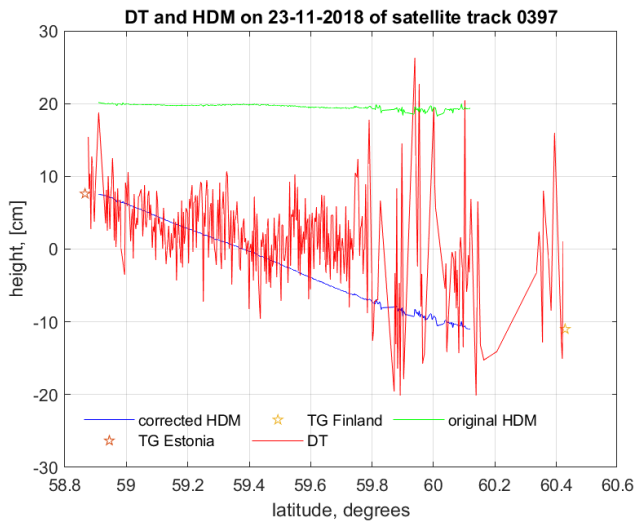
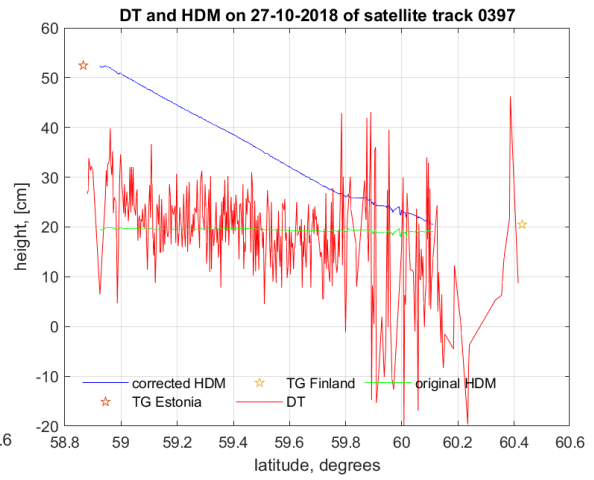
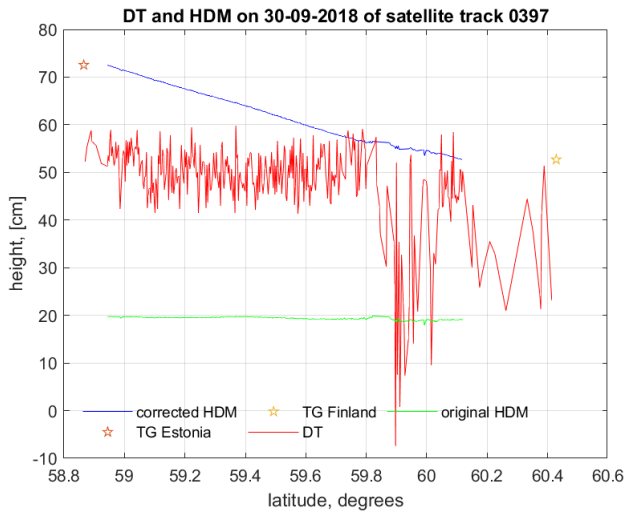
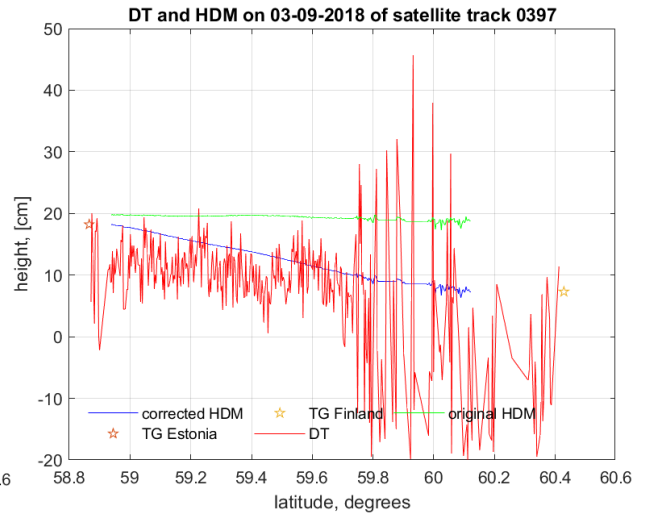
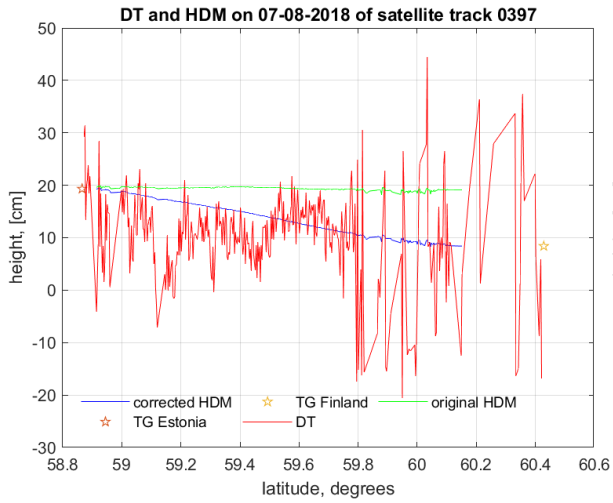


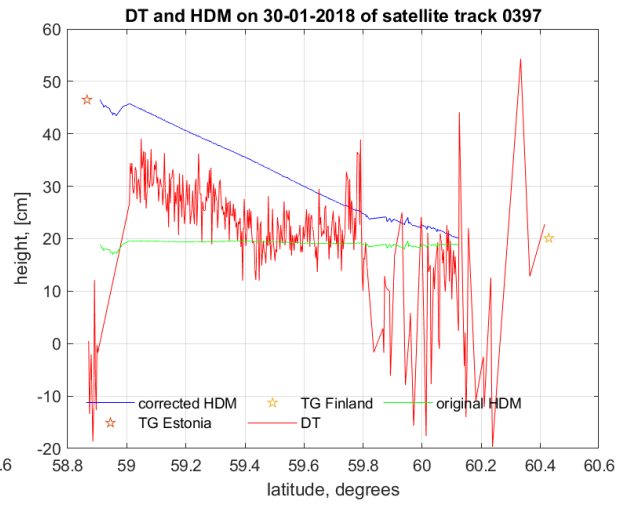
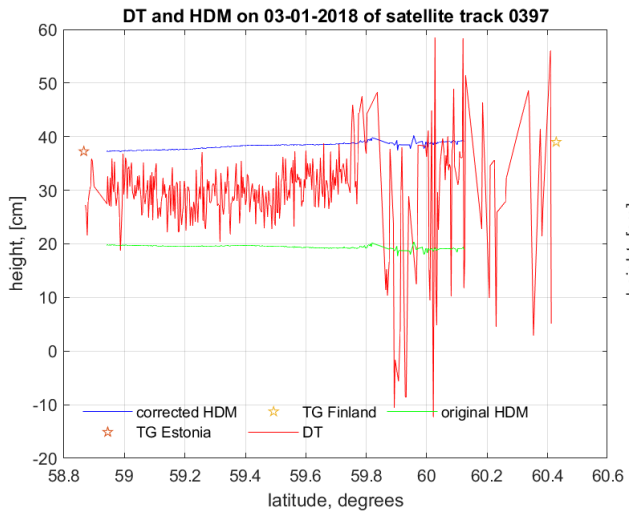




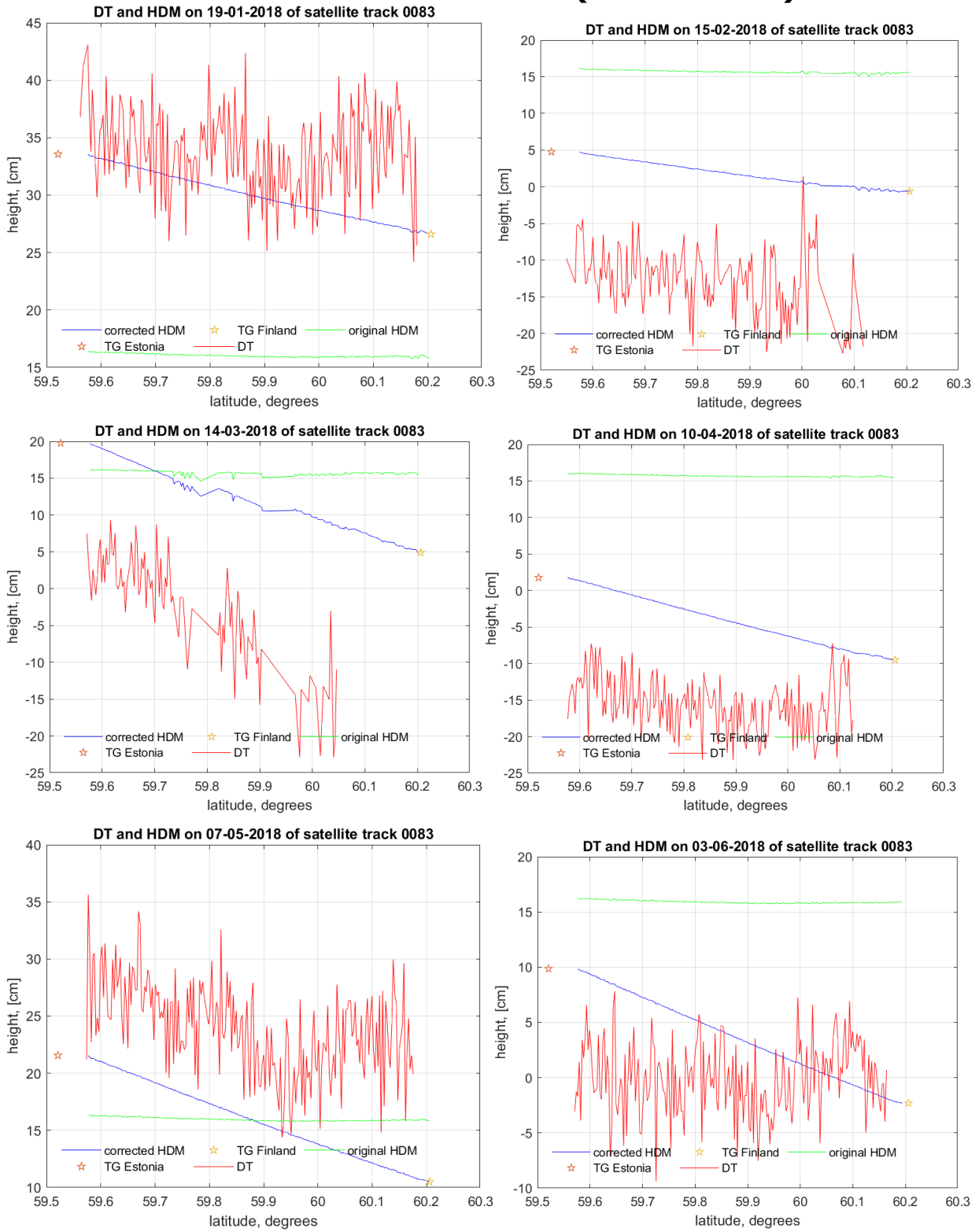
15.2 Results for the track of 0397 (Sentinel-3A)

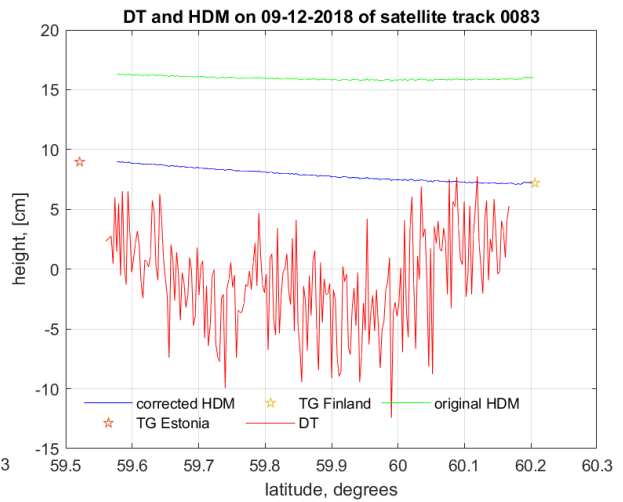
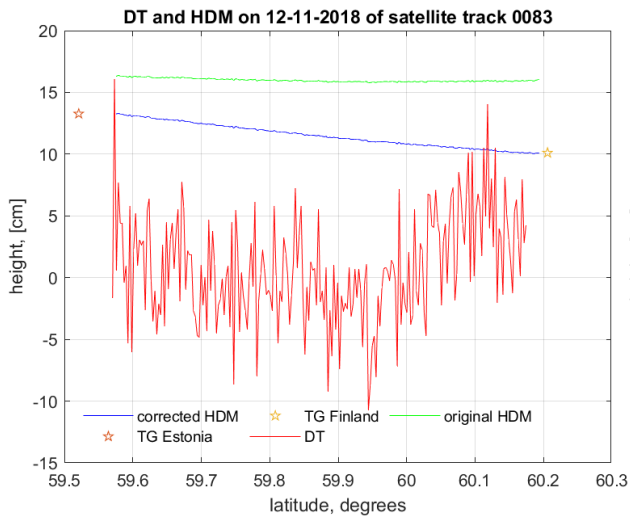
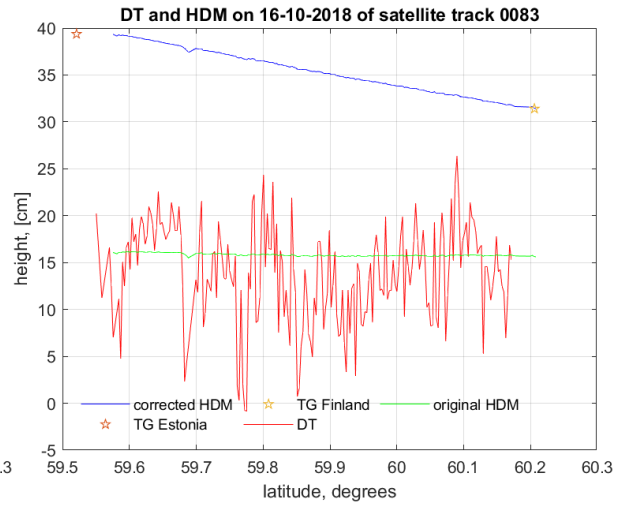
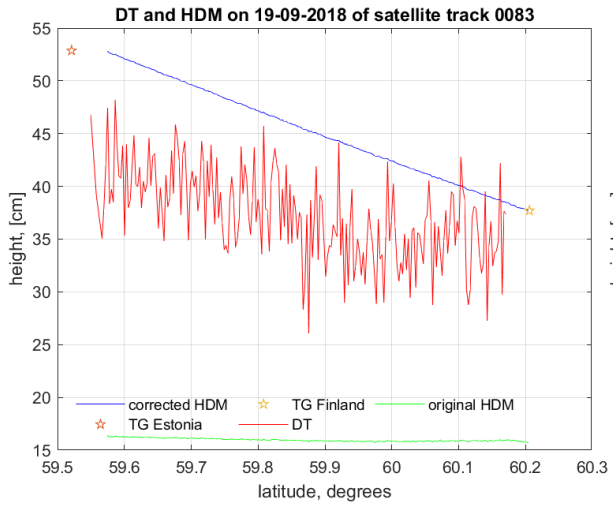
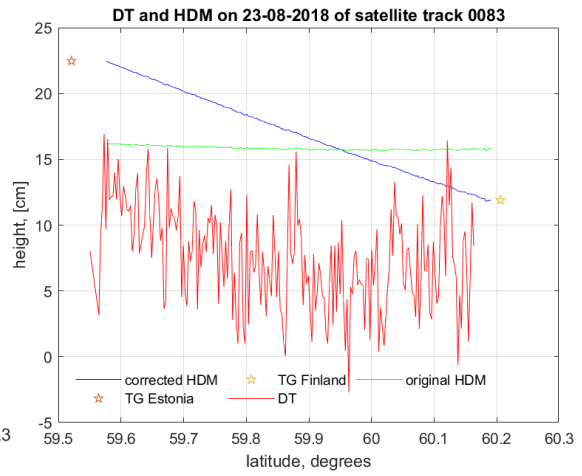
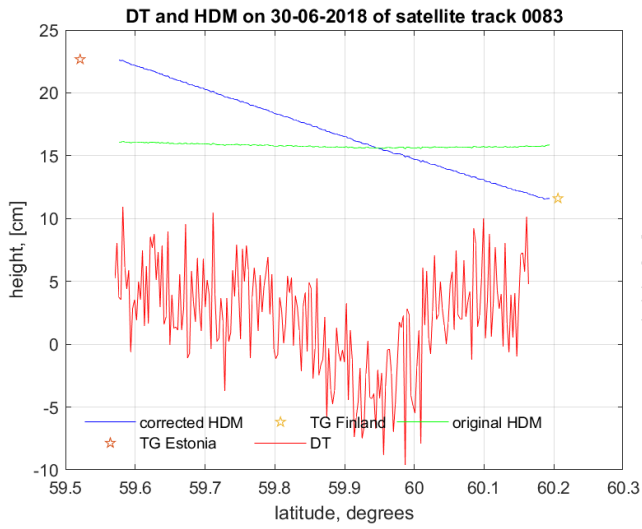




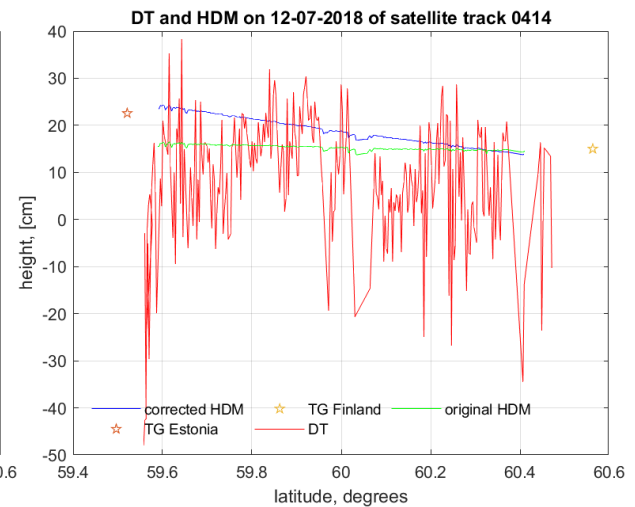
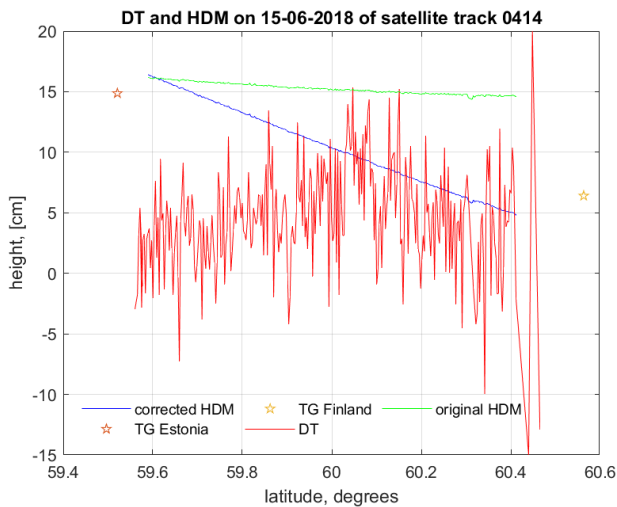
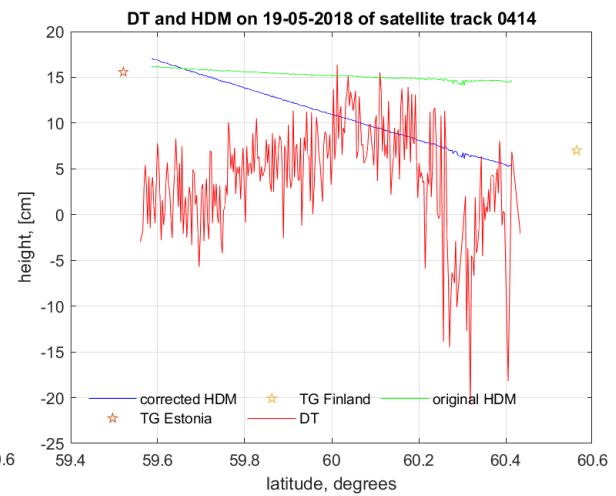
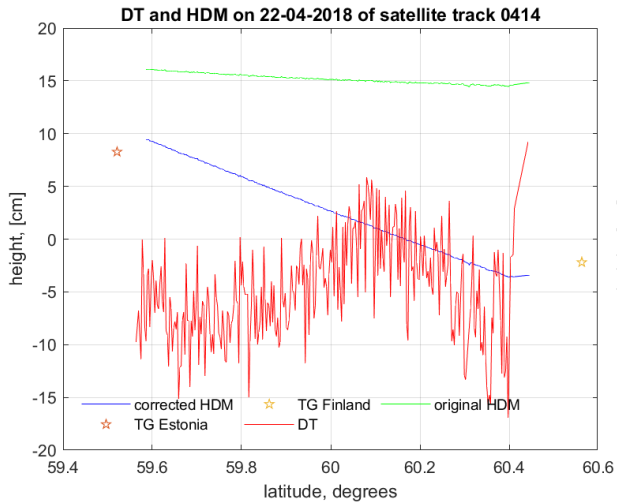
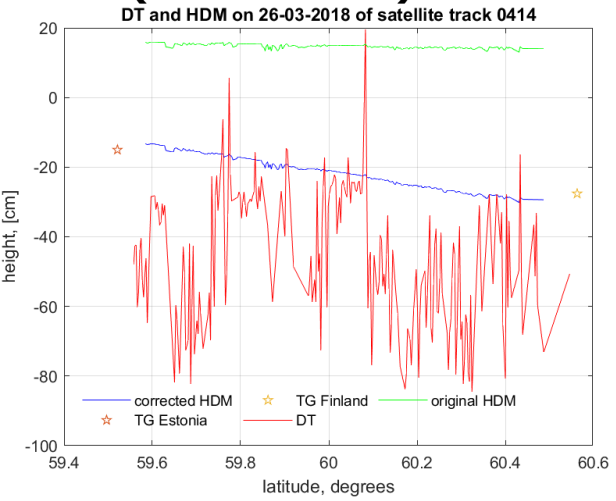
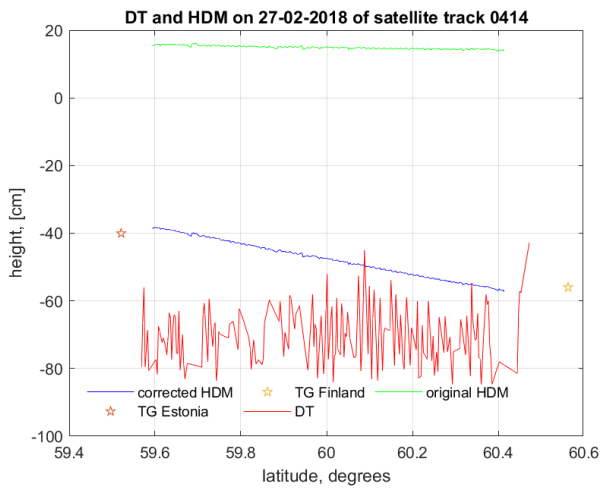


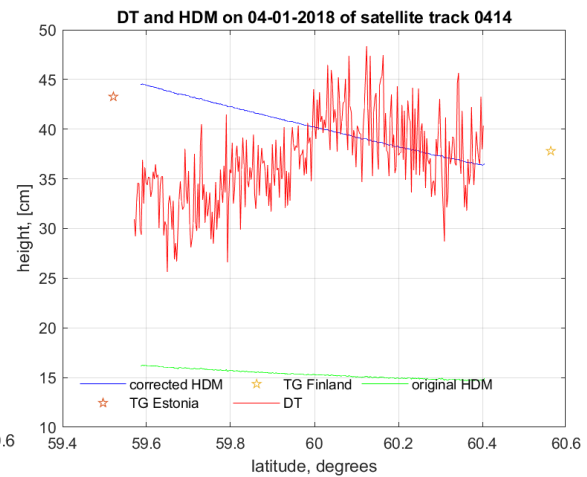
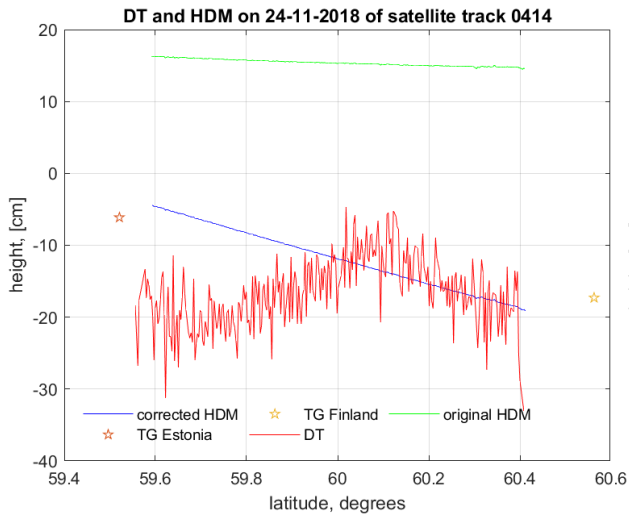
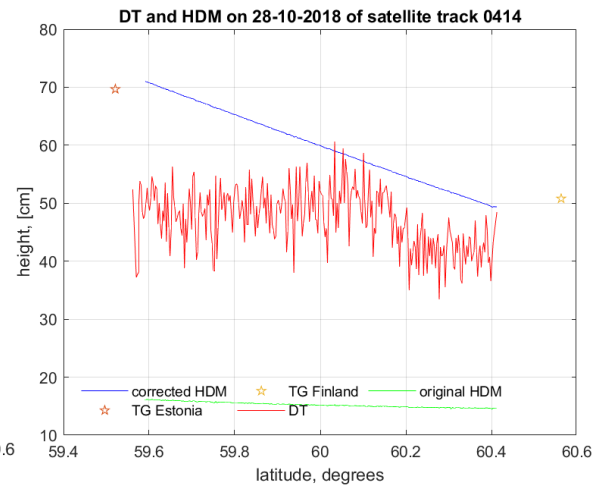
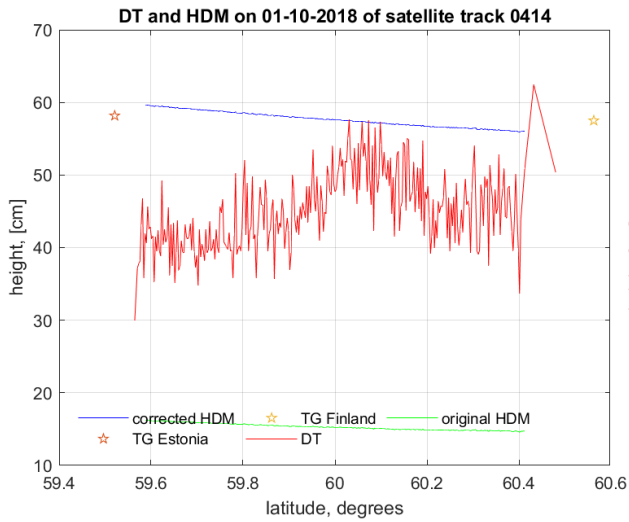
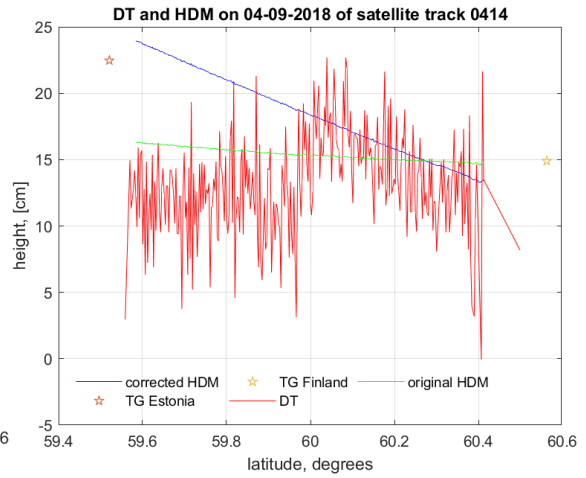
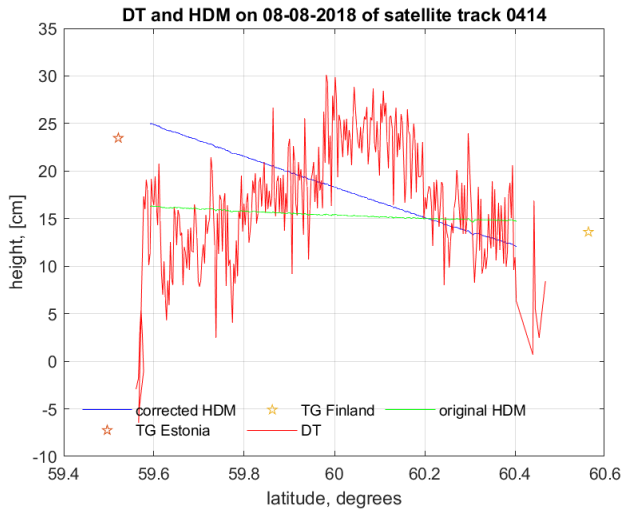
15.3 Results for the track of 0083 (Sentinel-3A)

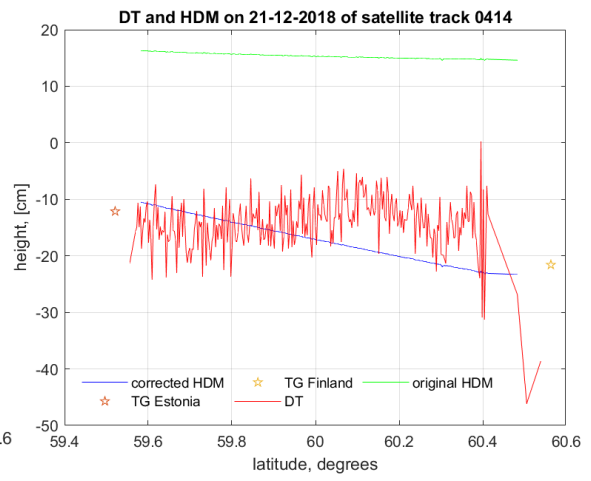
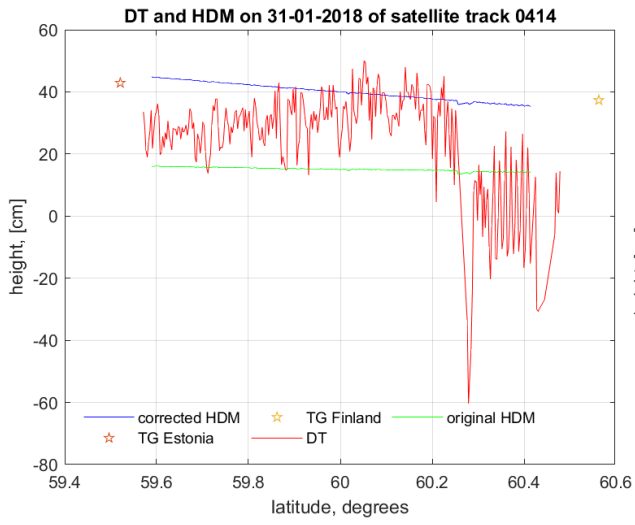




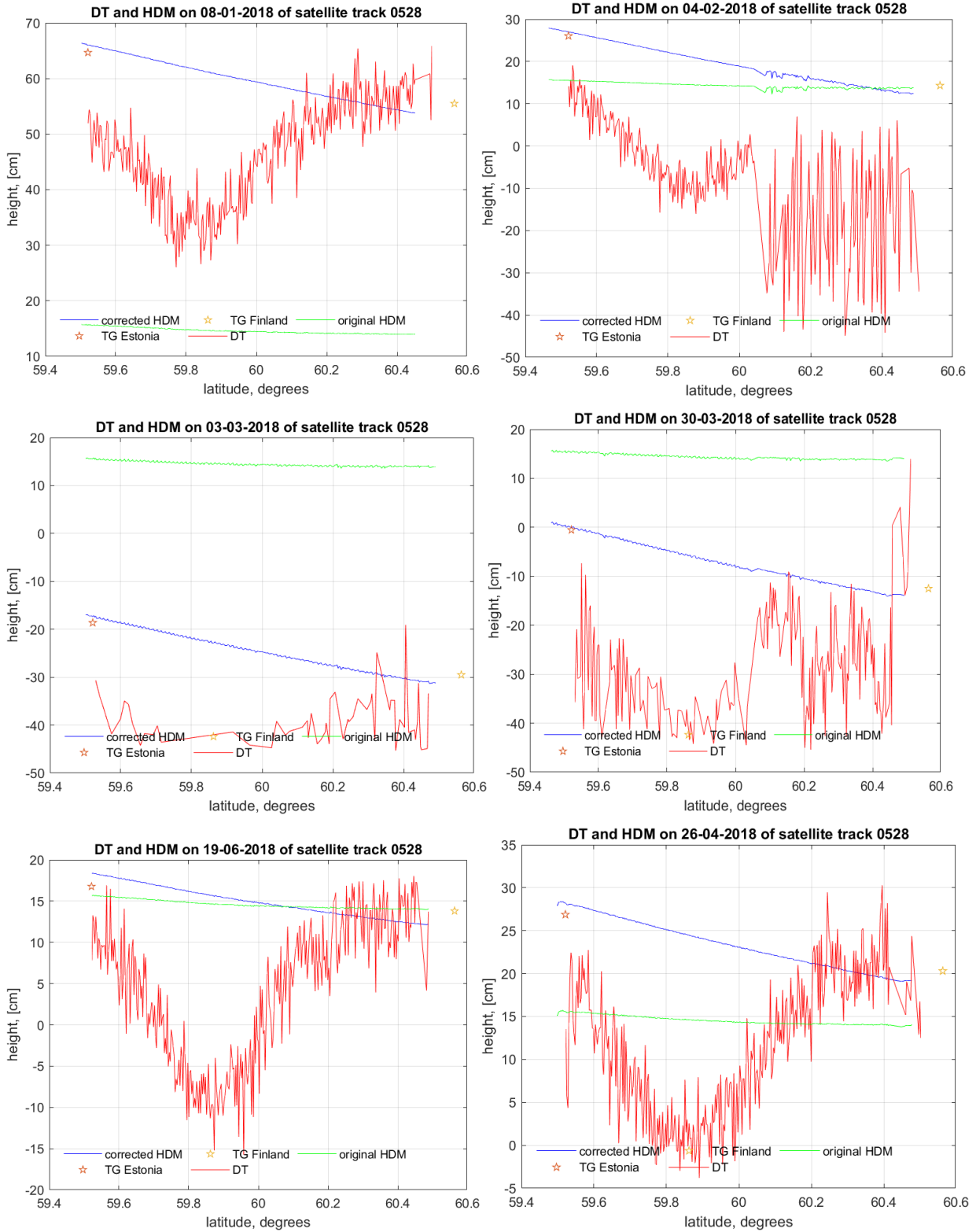
15.4 Results for the track of 0414 (Sentinel-3A)

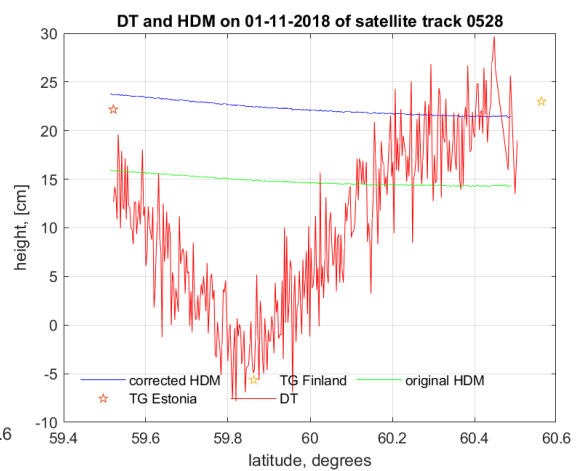
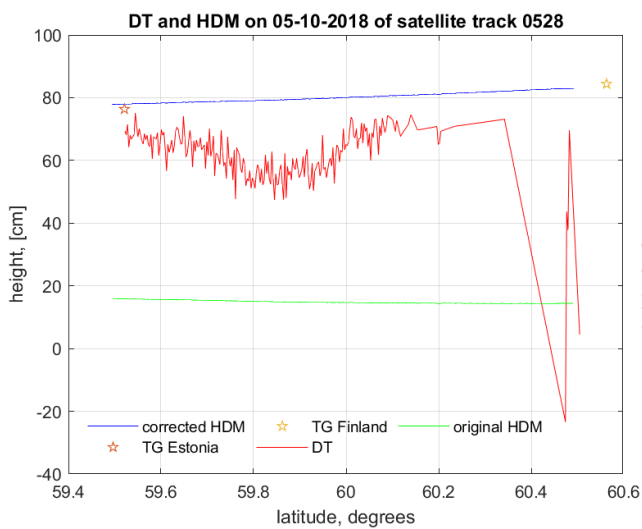
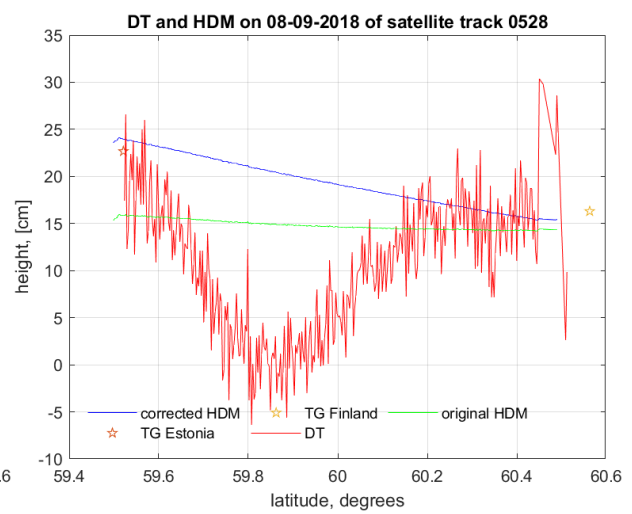
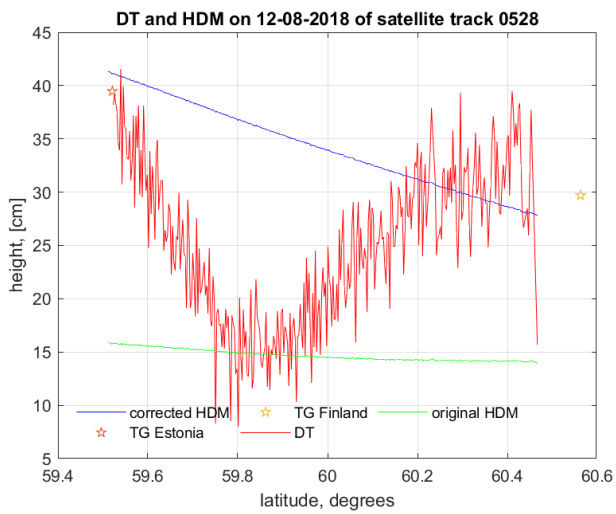
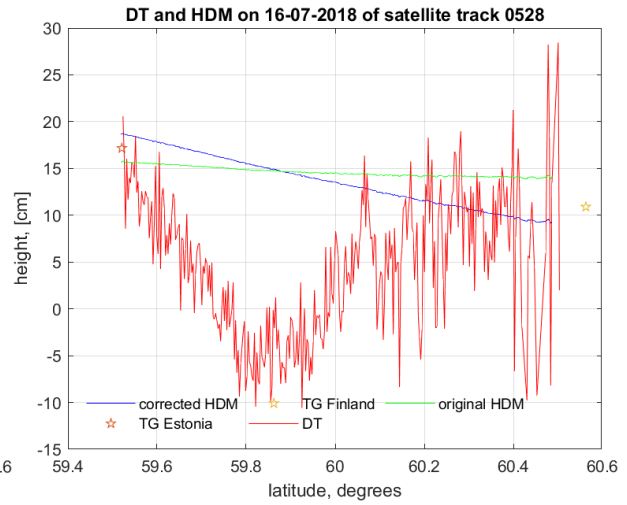
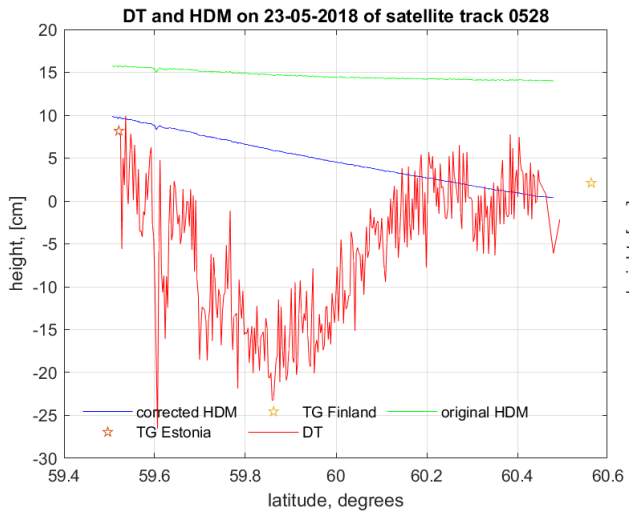


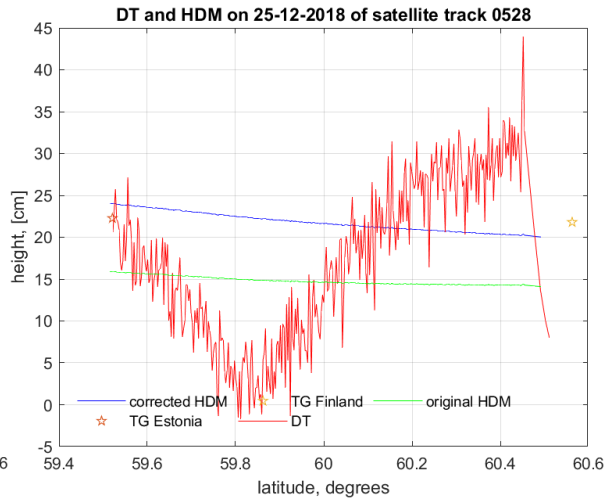
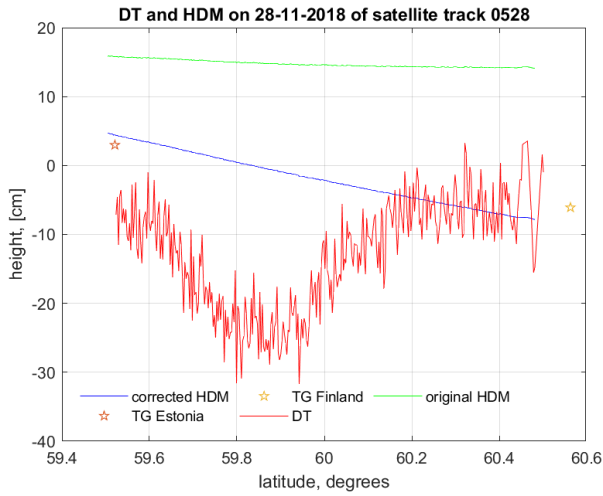




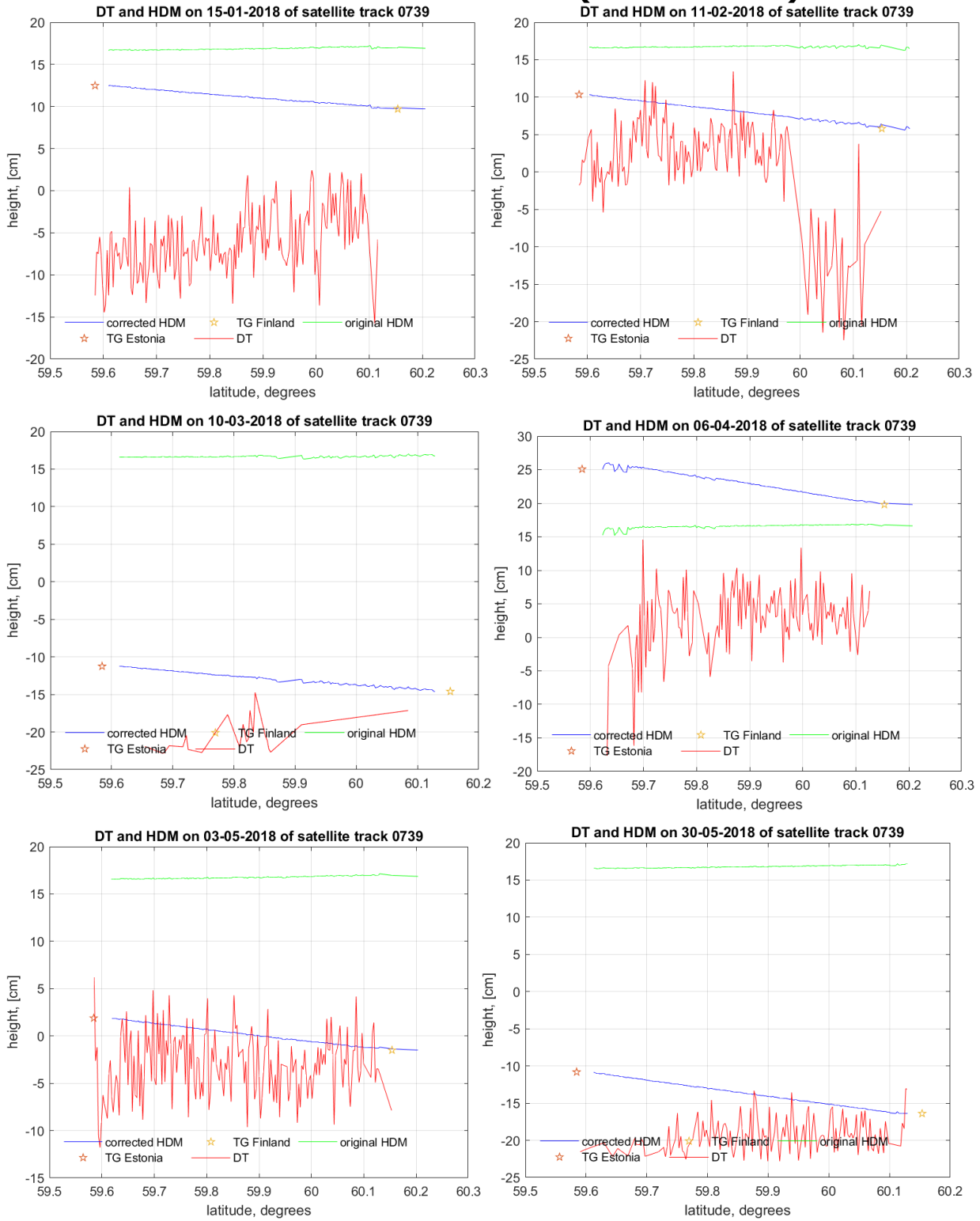
15.5 Results for the track of 0528 (Sentinel-3A)

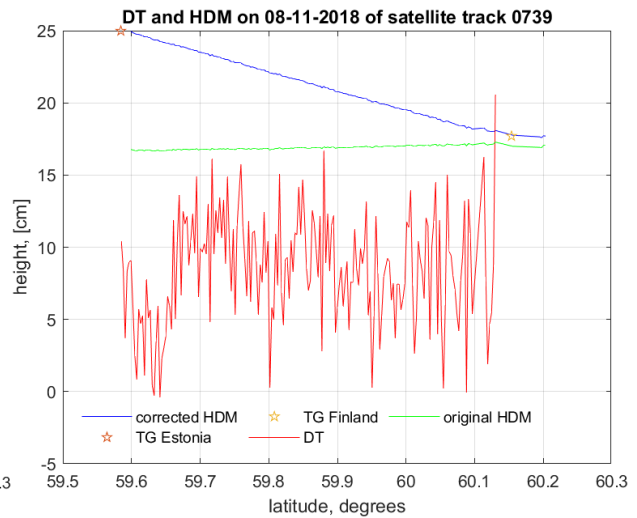
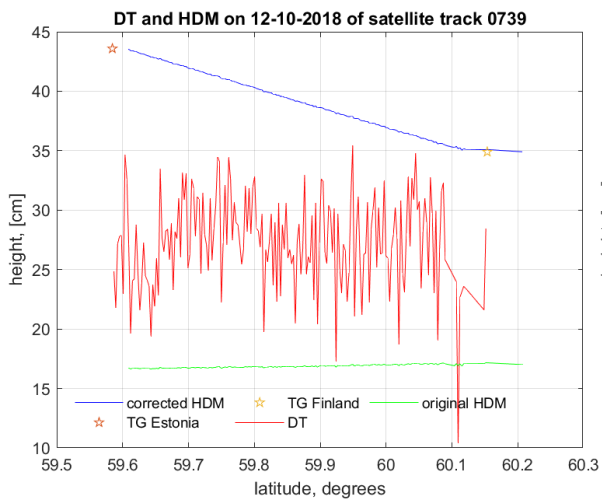
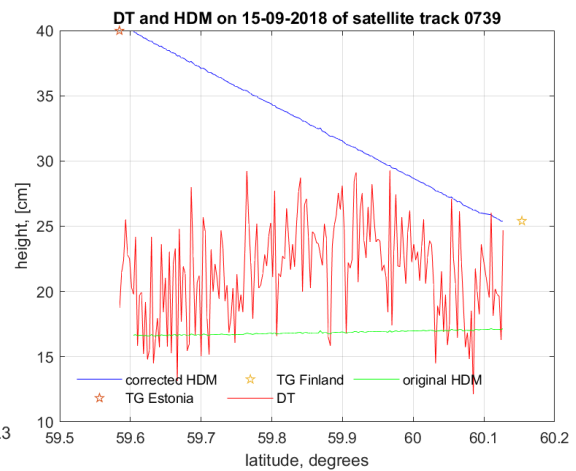
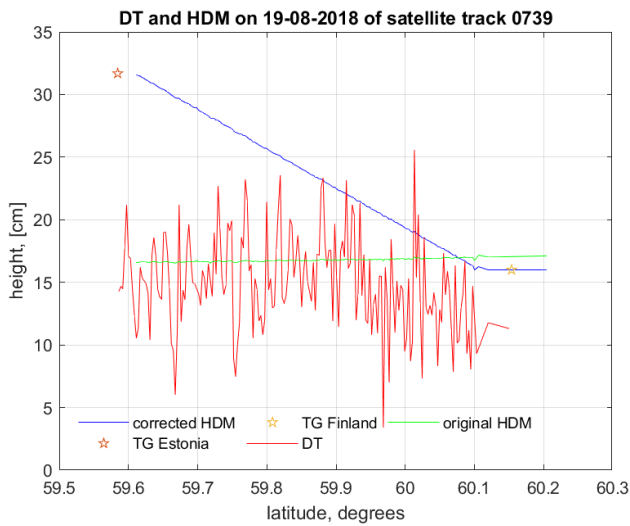
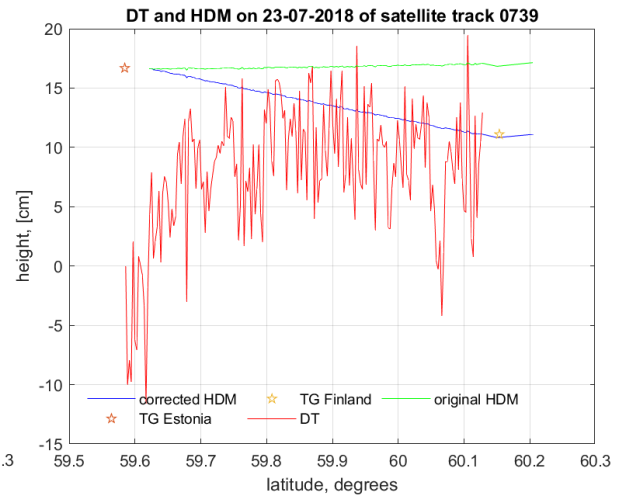
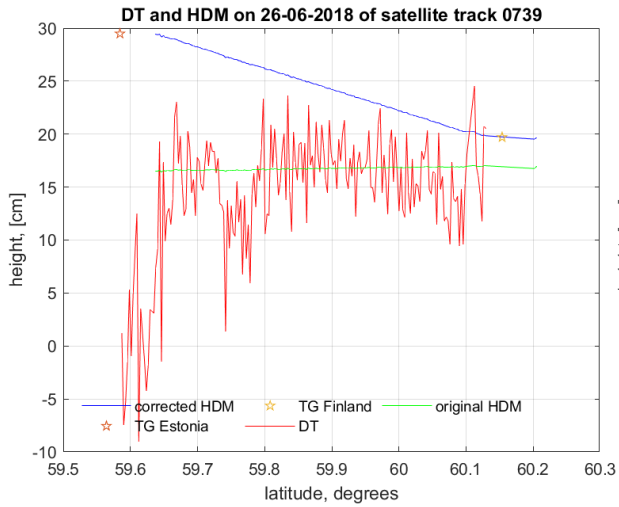


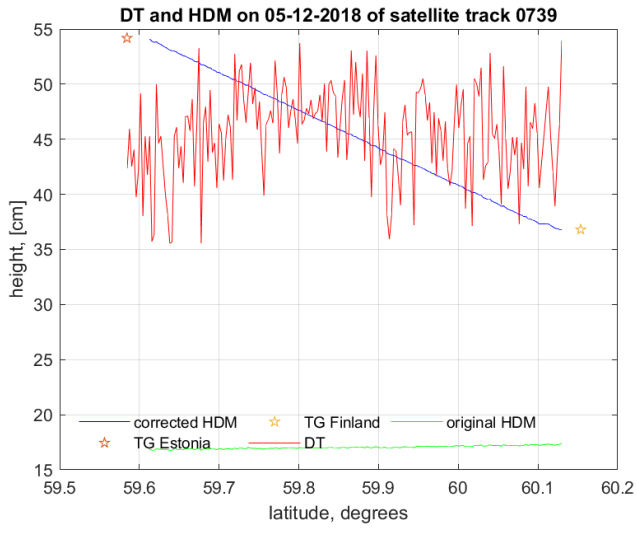




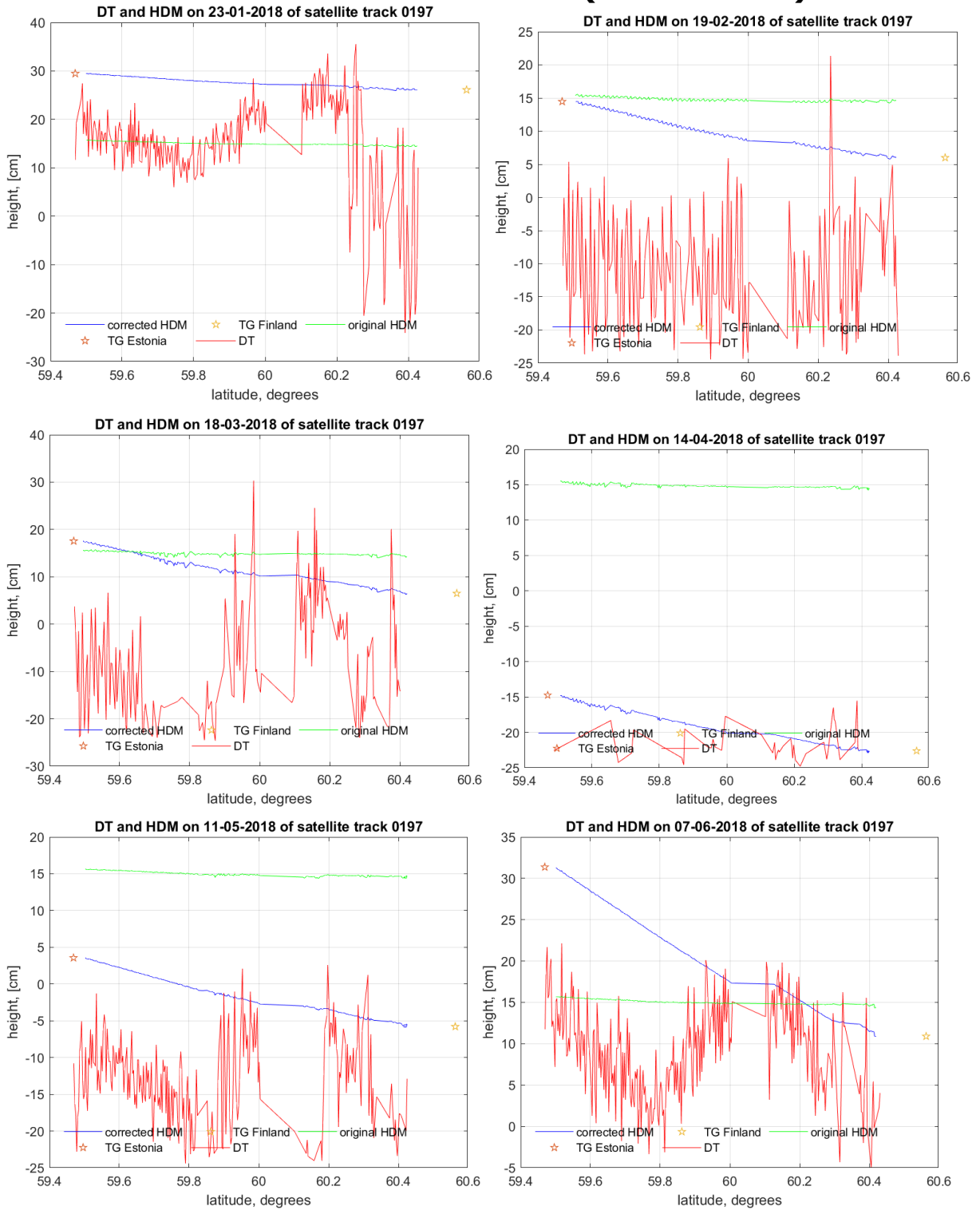
15.6 Results for the track of 0739 (Sentinel-3A)

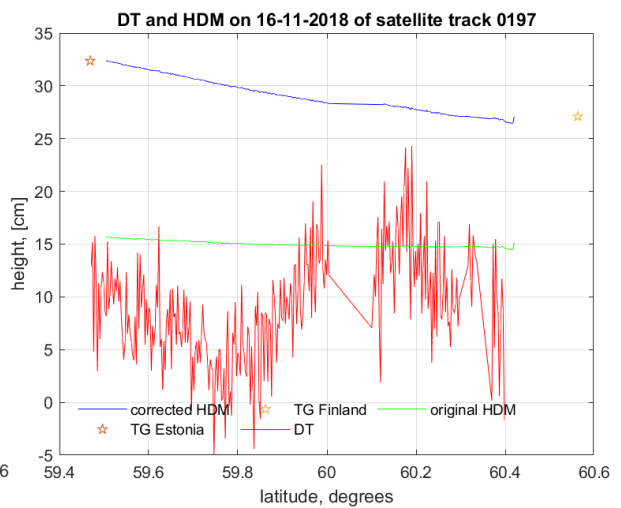
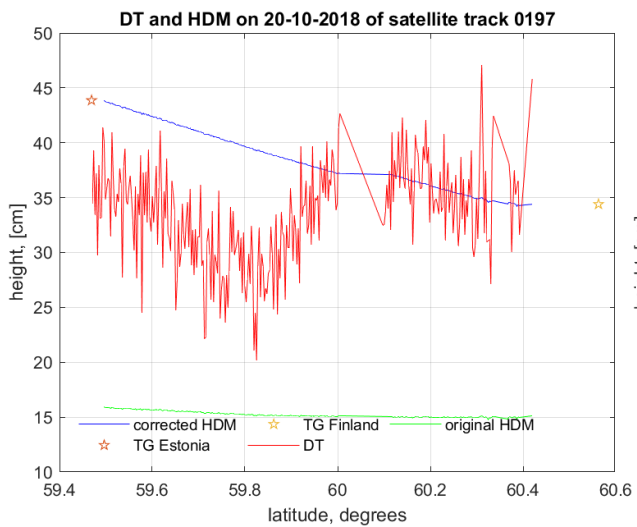
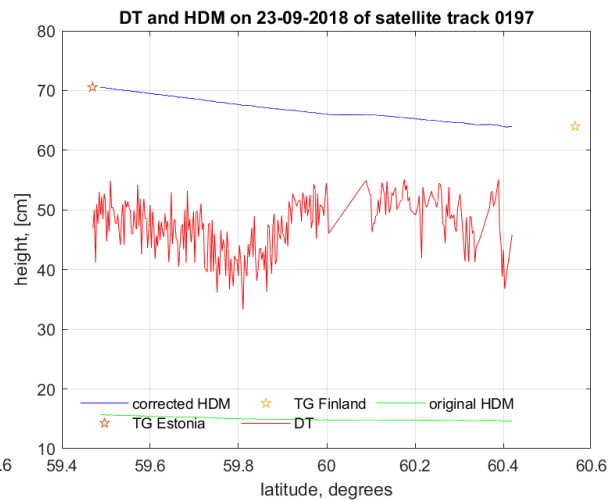
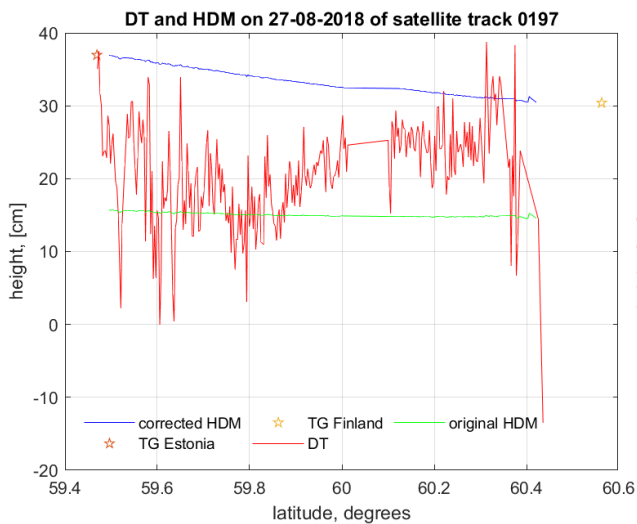
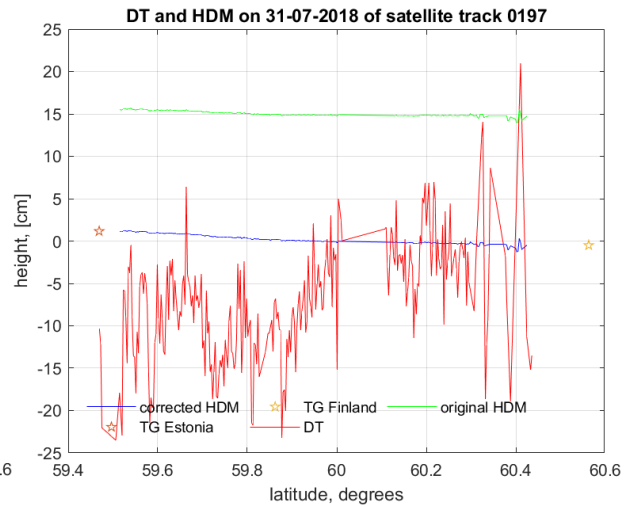
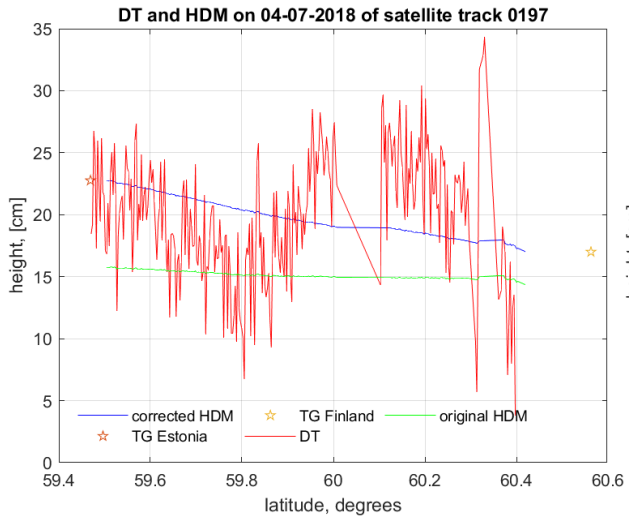


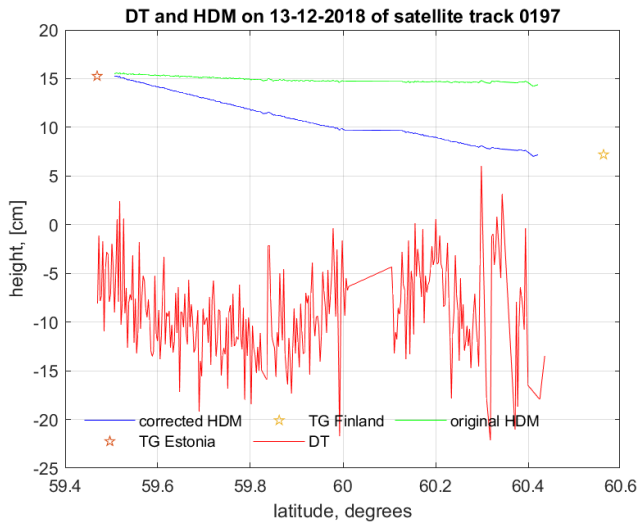




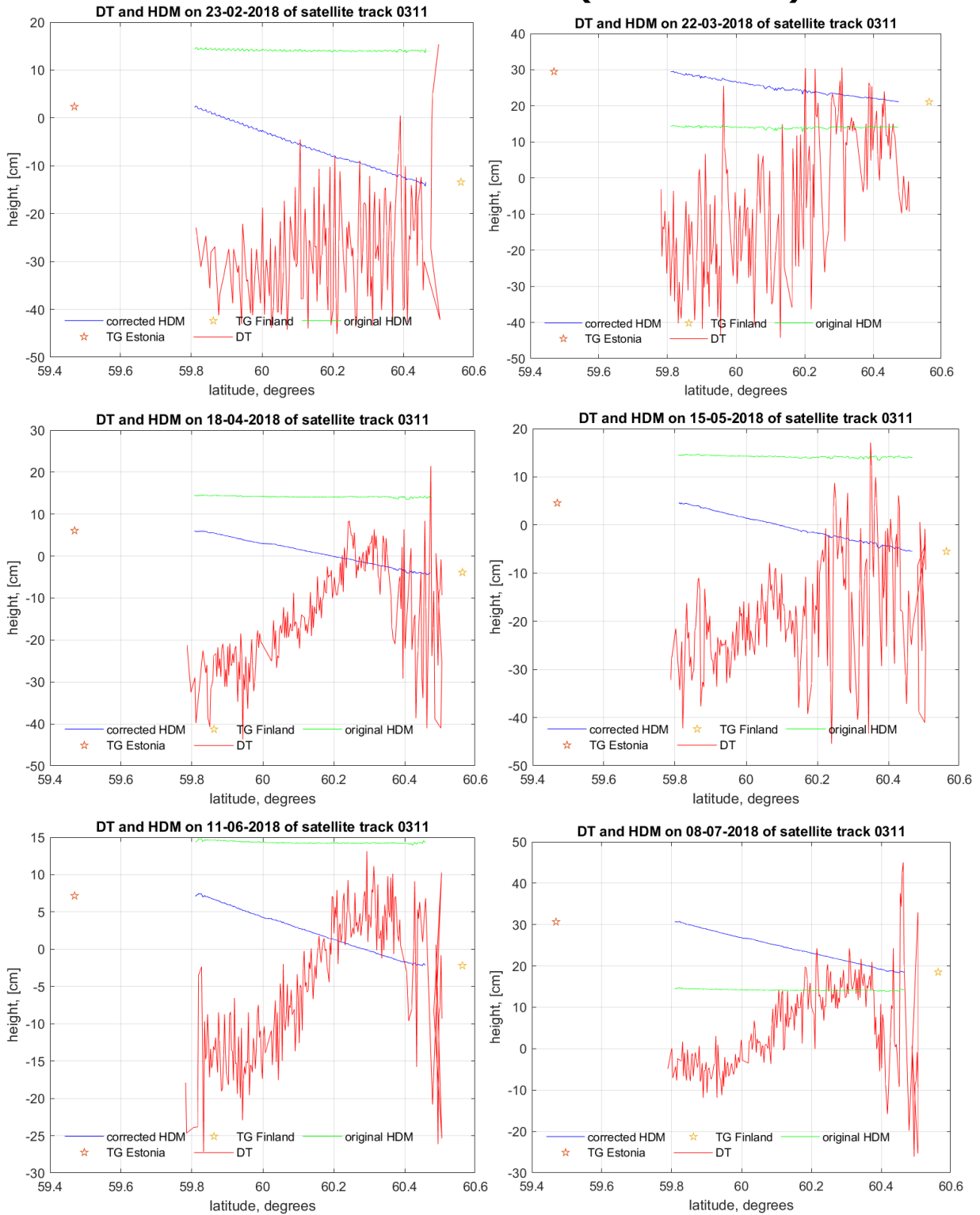
15.7 Results for the track of 0197 (Sentinel-3A)

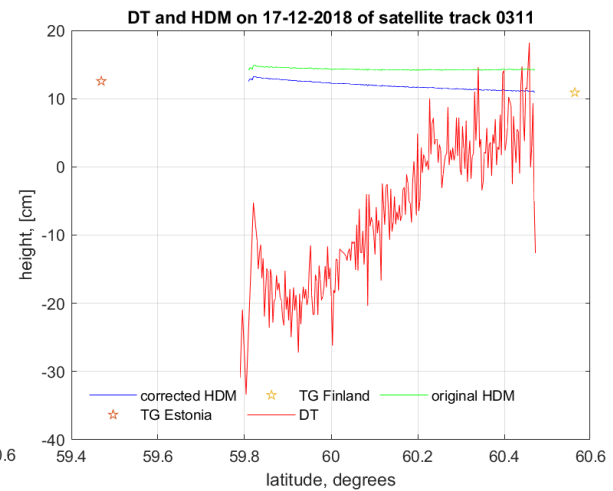
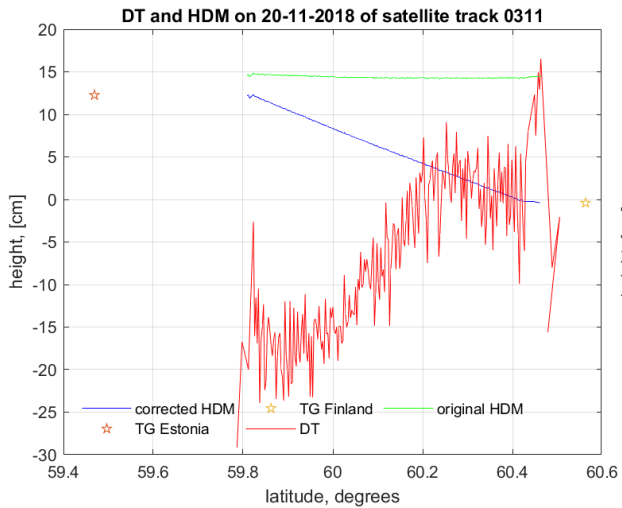
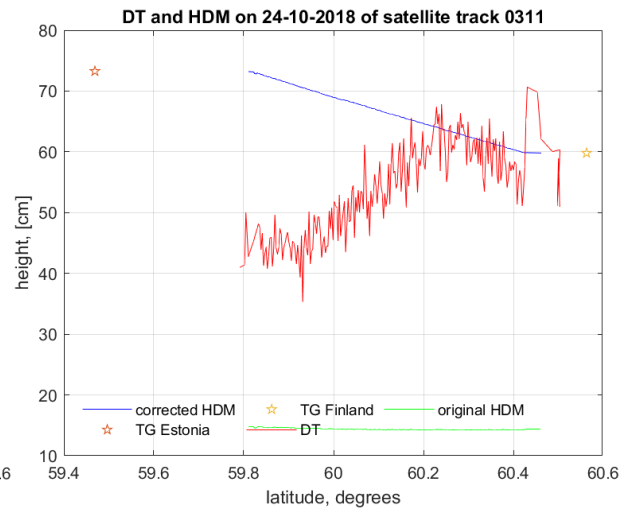
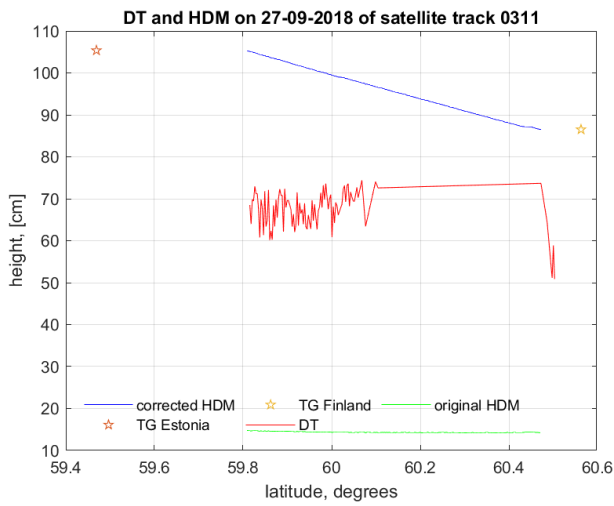
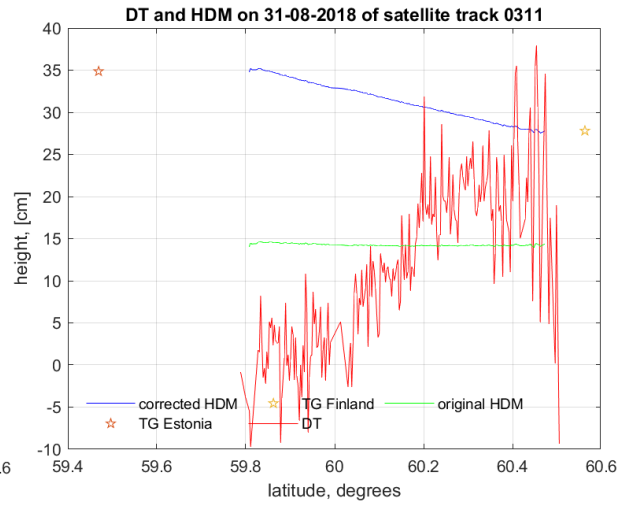
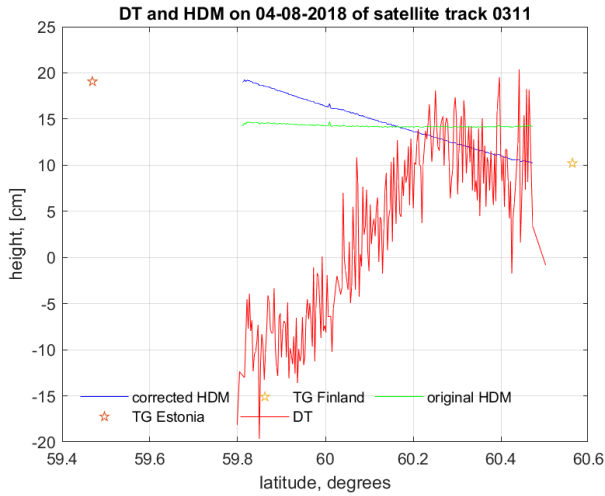


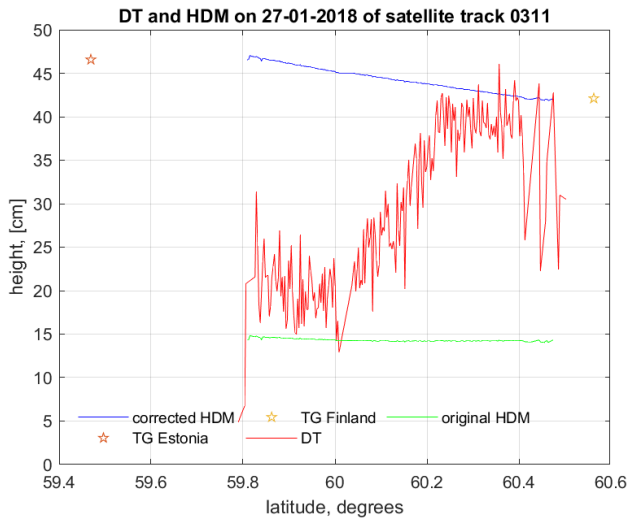




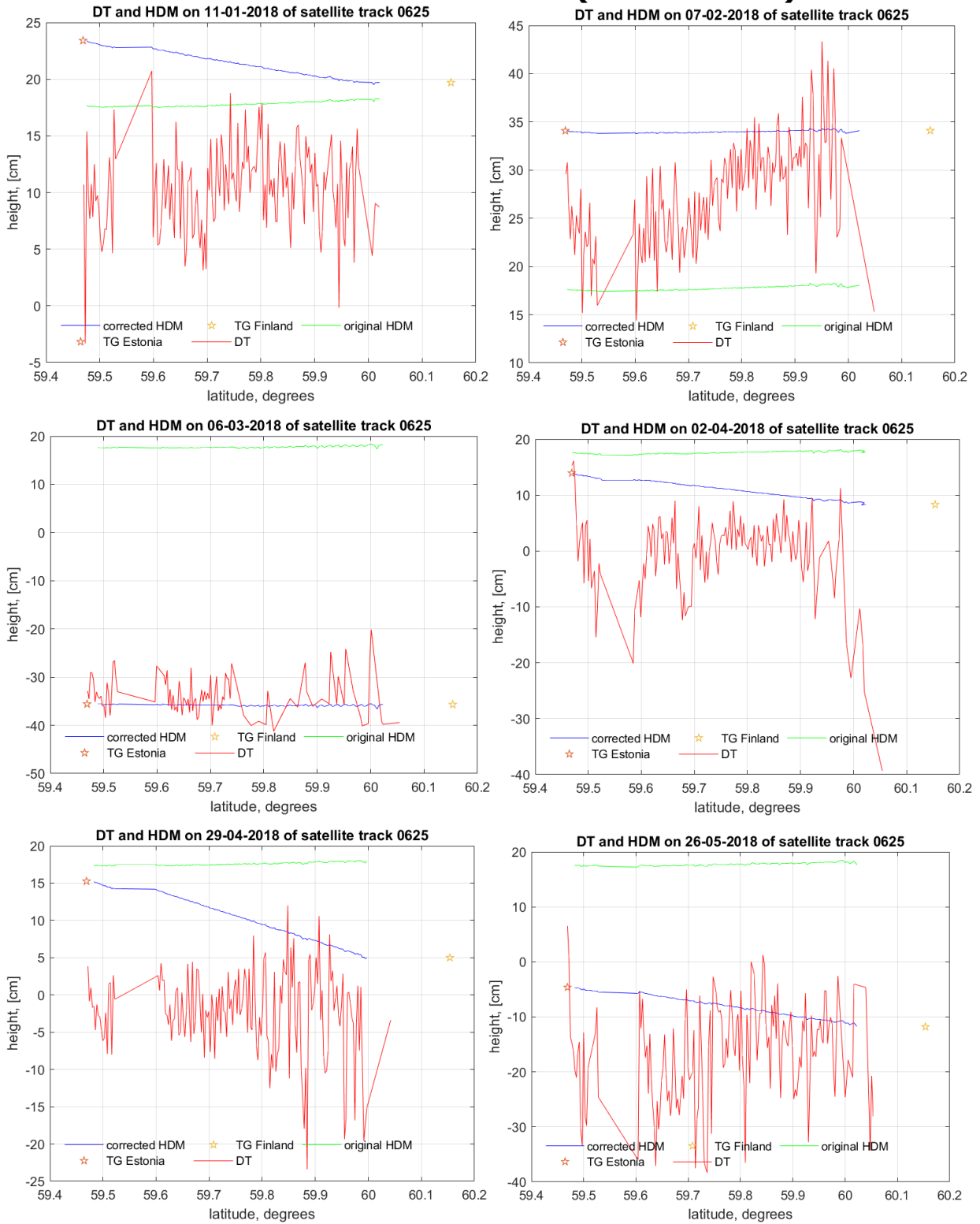
15.8 Results for the track of 0311 (Sentinel-3A)

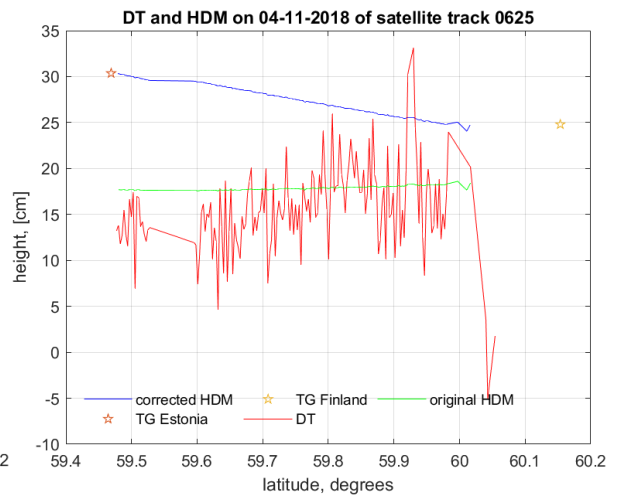
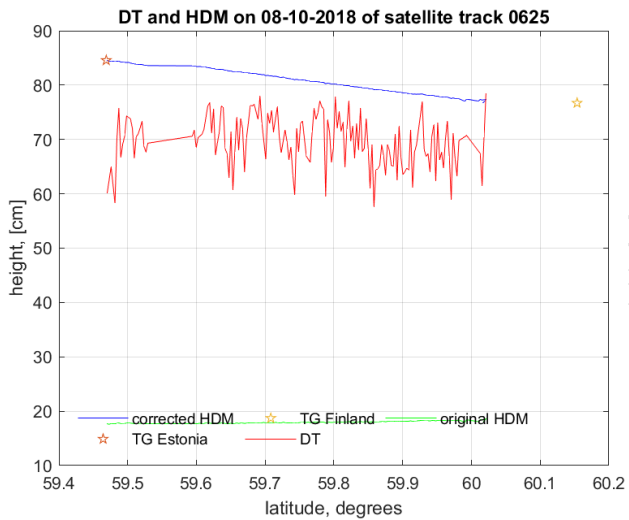
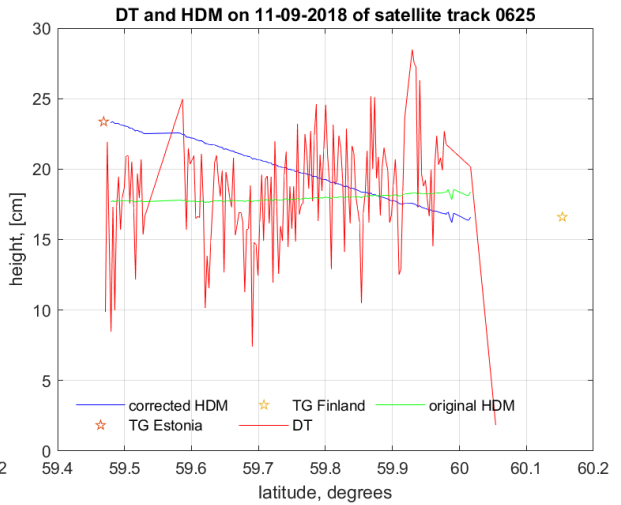
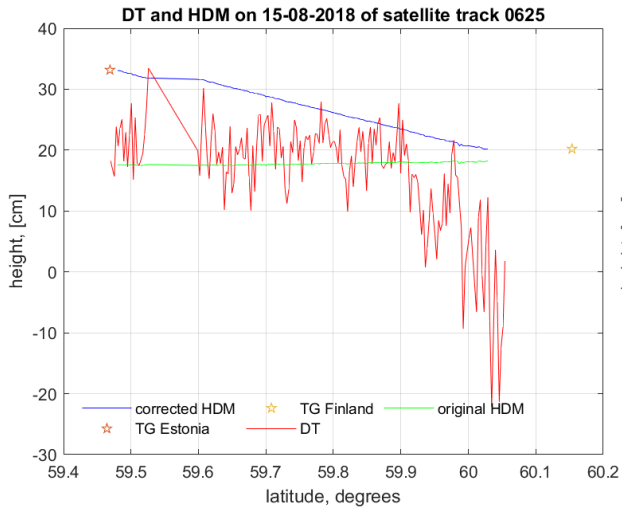
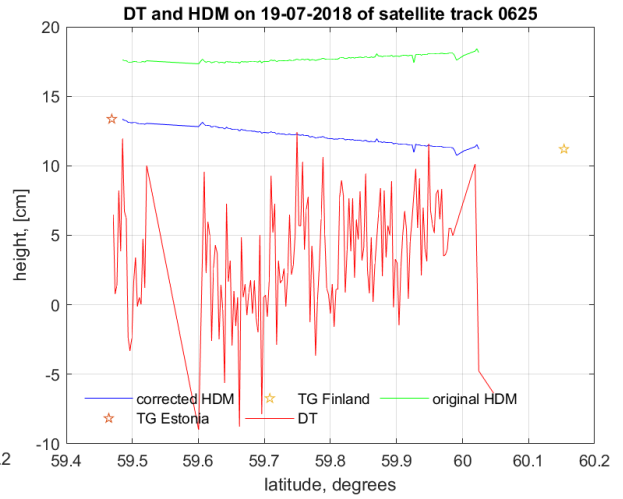
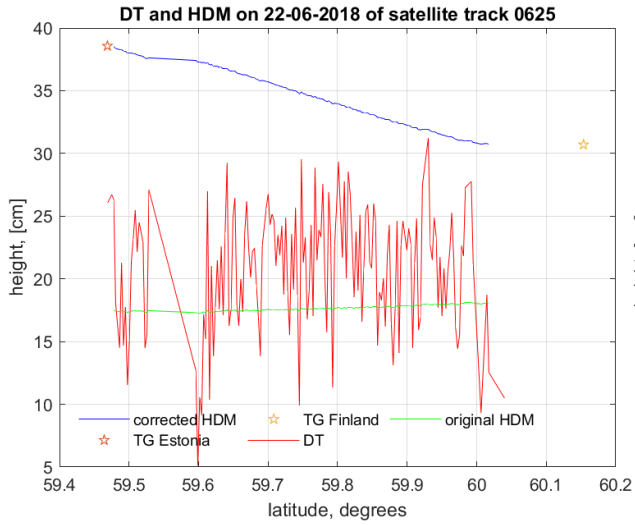


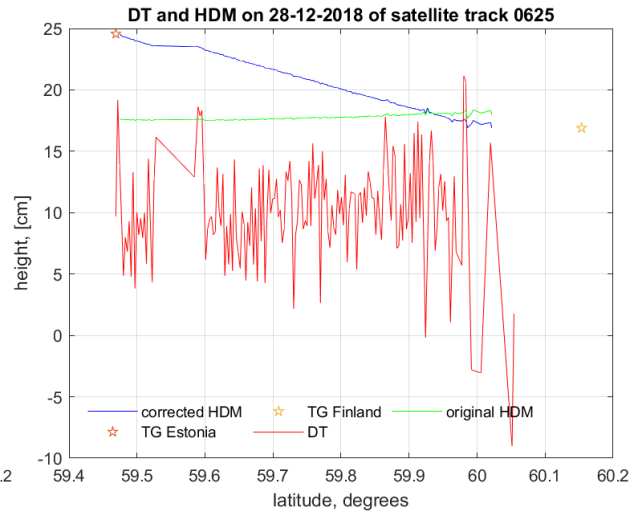
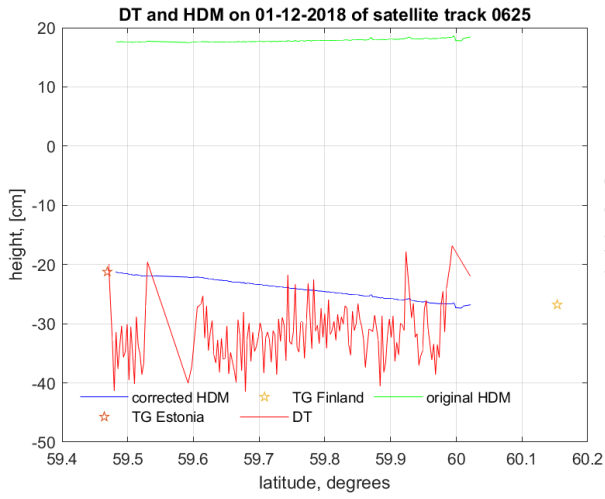




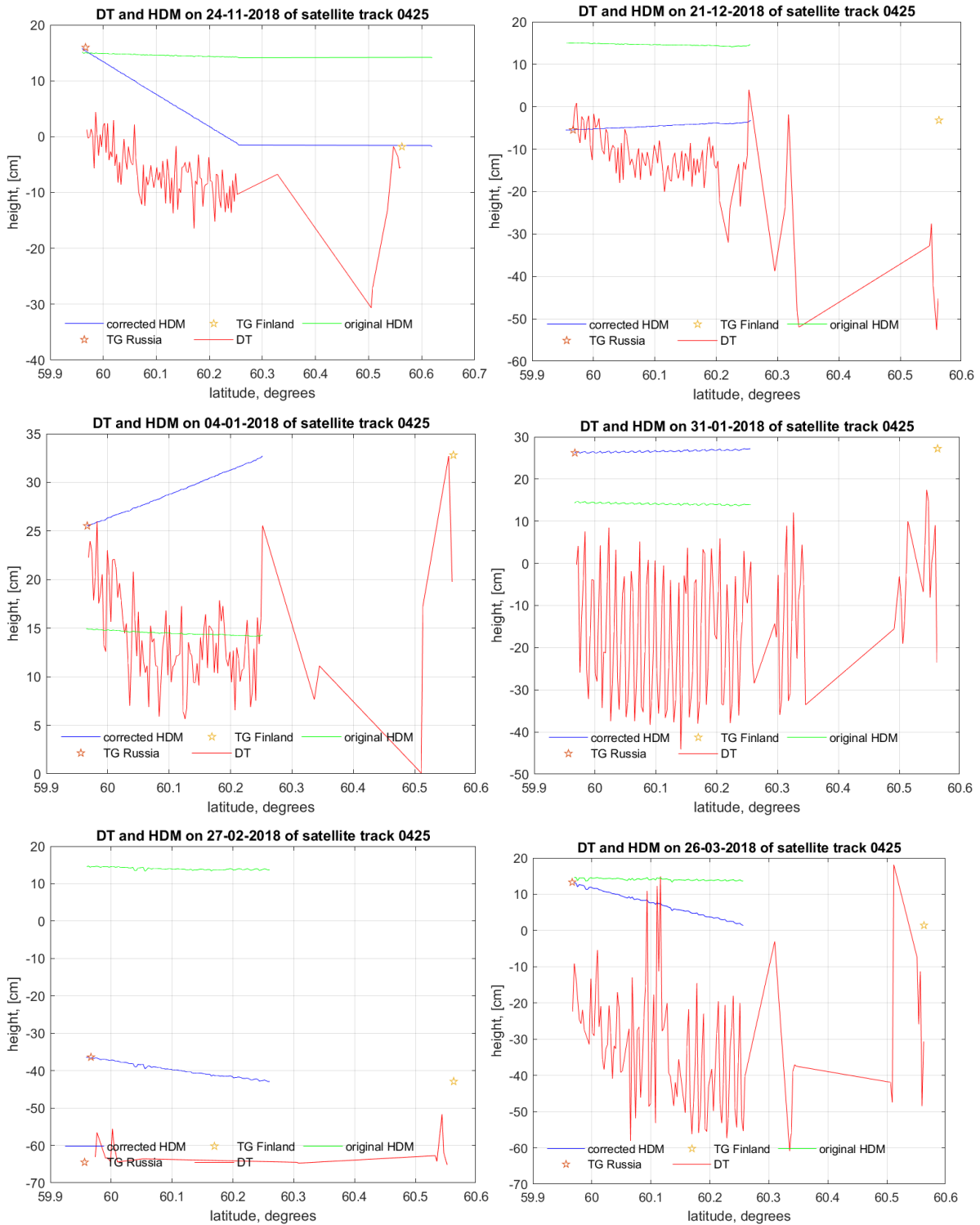
15.9 Results for the track of 0625 (Sentinel-3A)

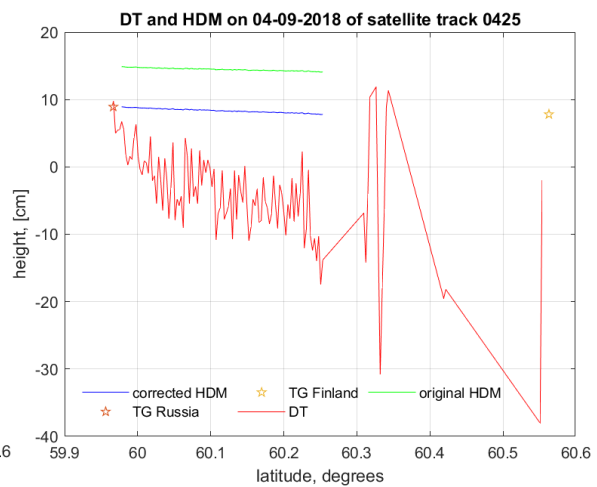
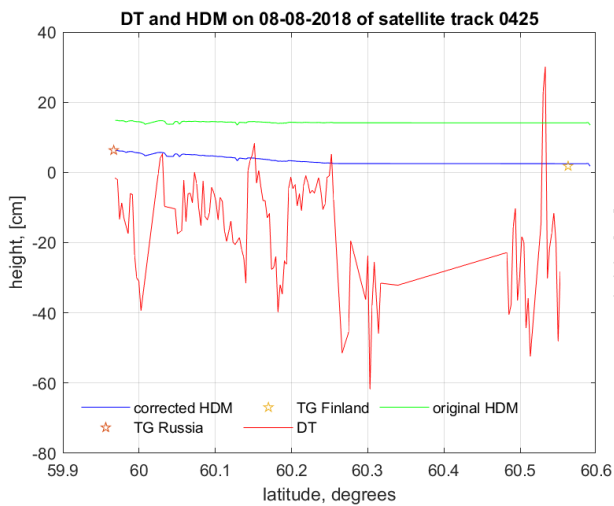
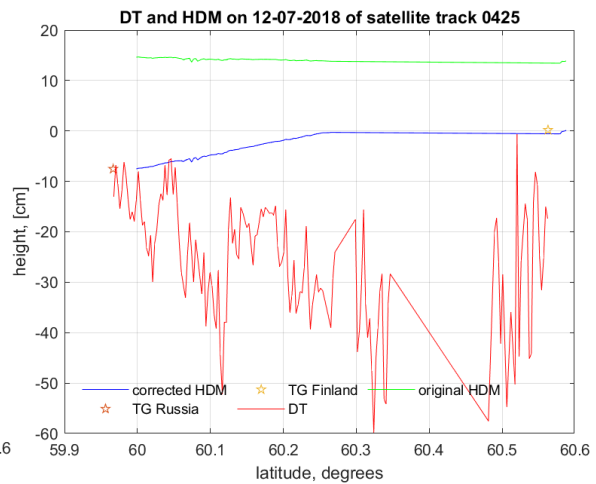
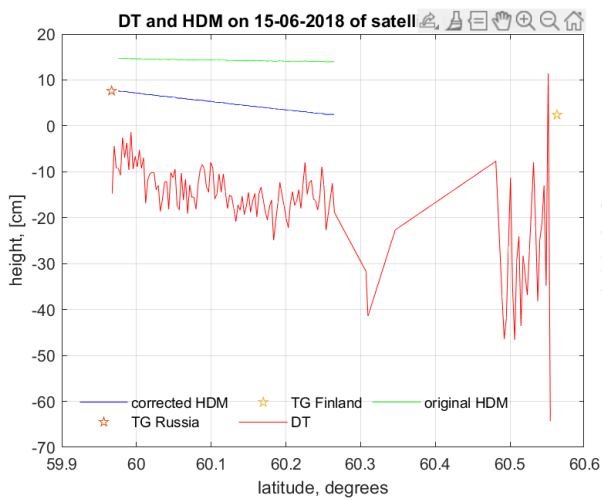
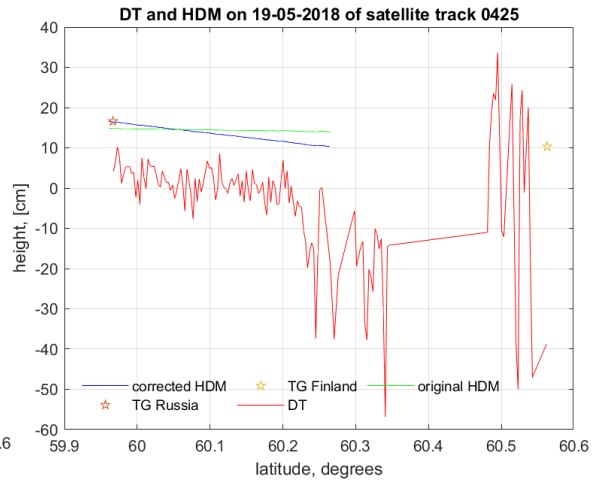
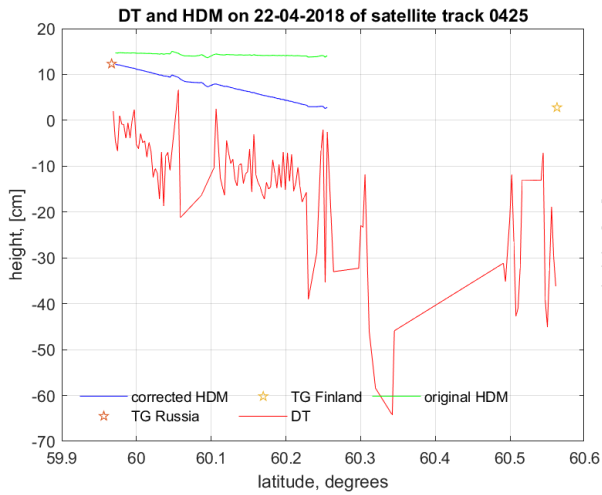


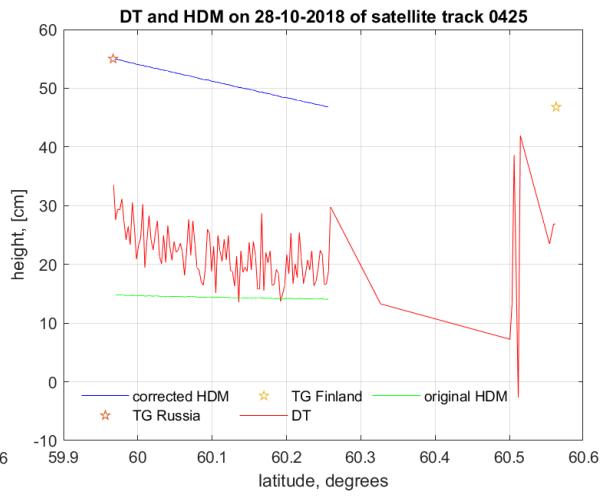
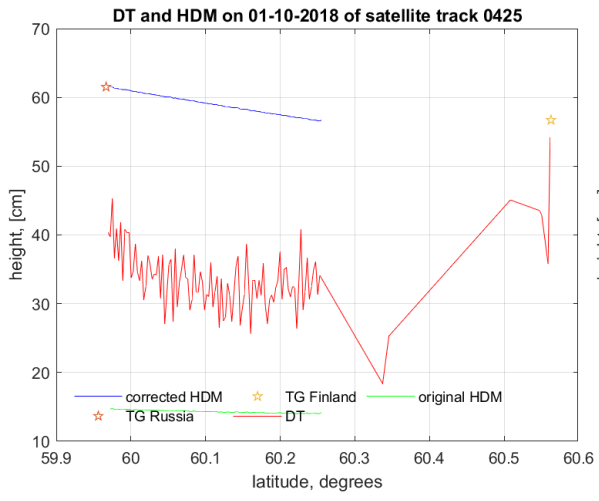




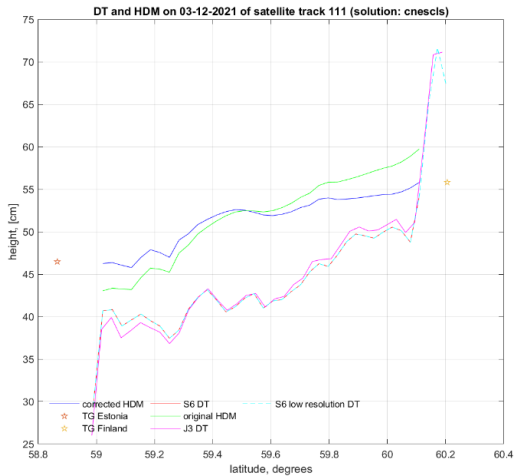
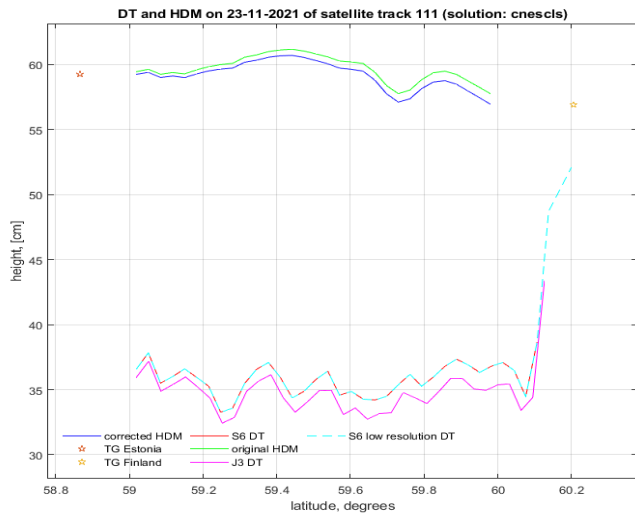
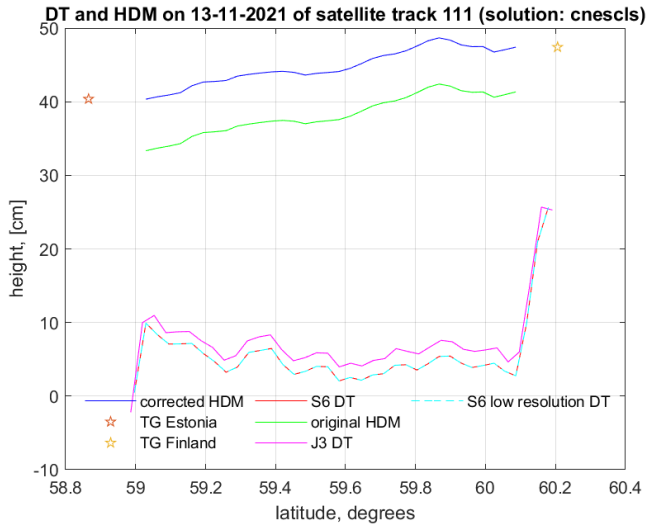
15.10 Results for the track of 0425 (Sentinel-3A)

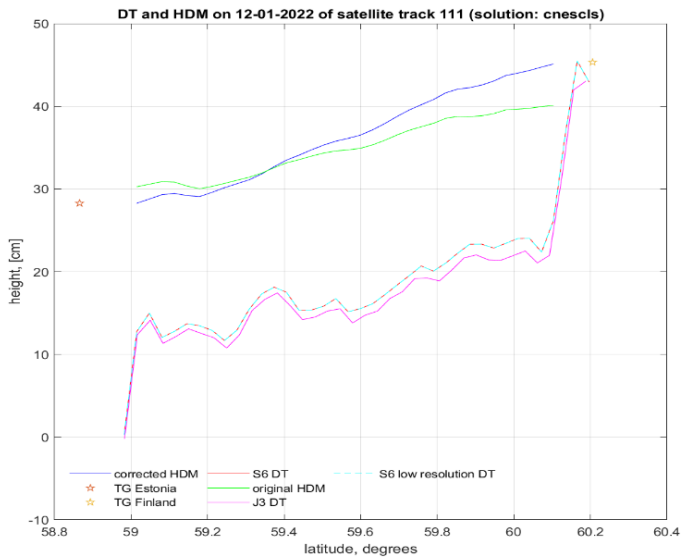
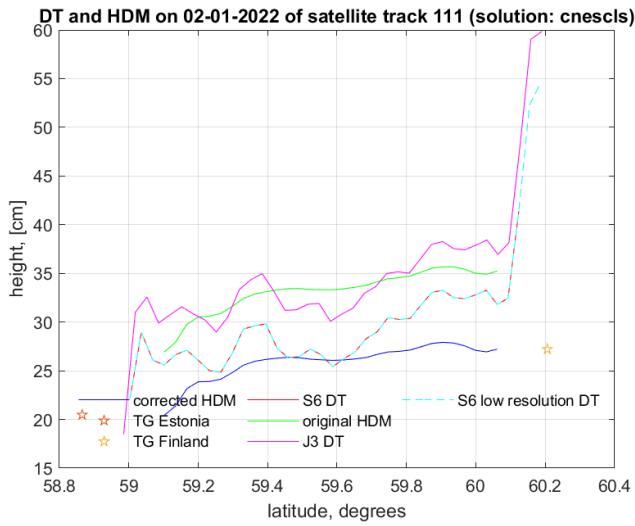
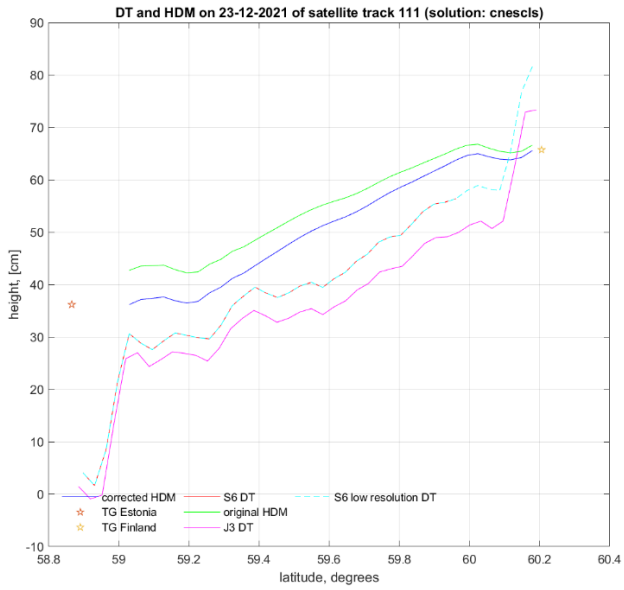


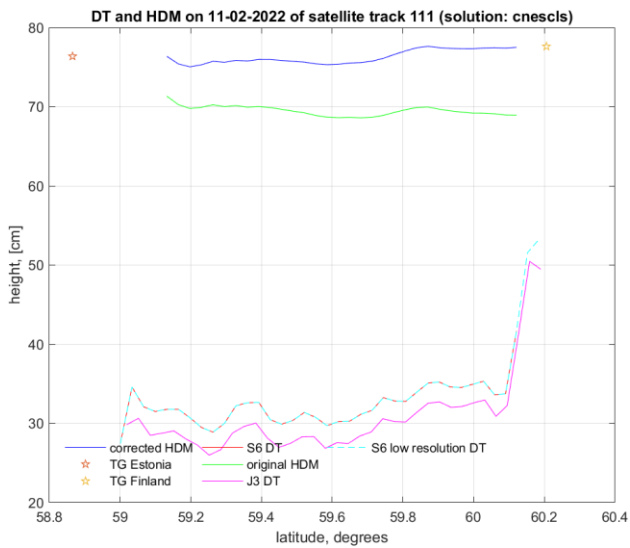
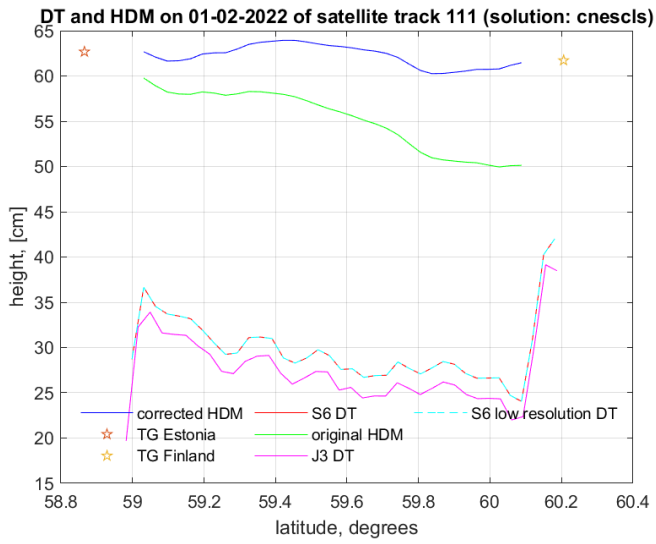
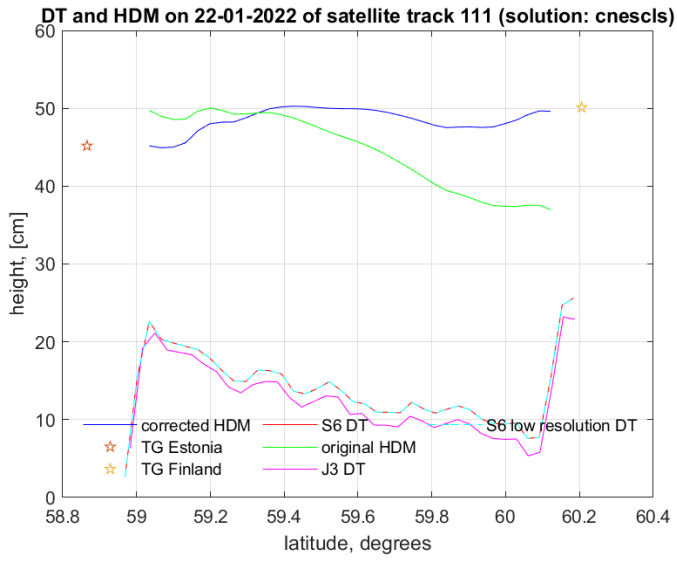


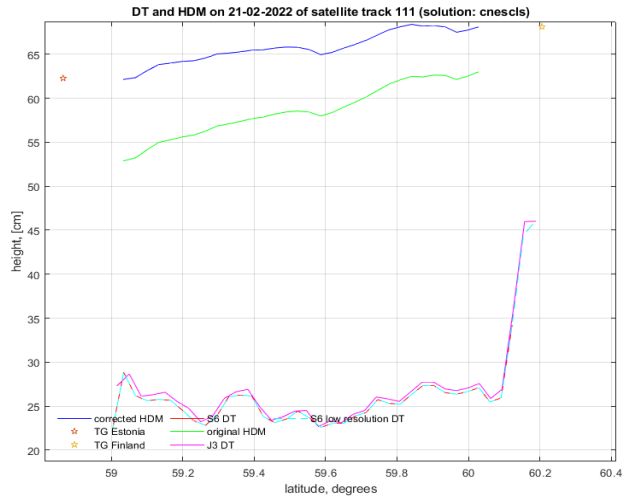


15.11 Results for the track of 0111 (Sentinel-6A and Jason-3)

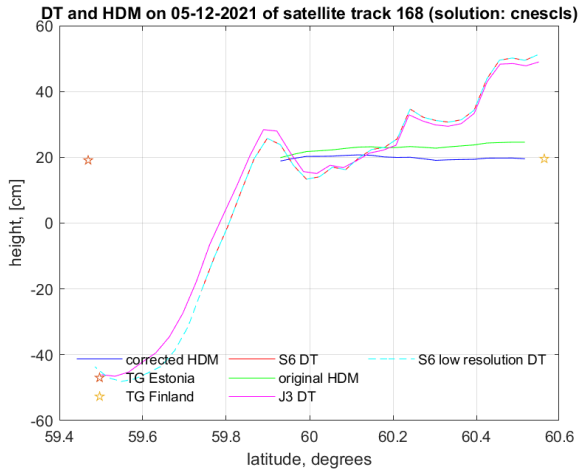
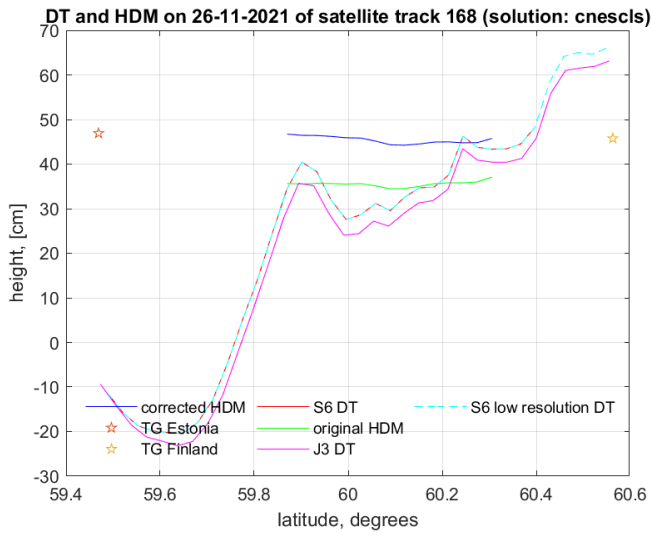
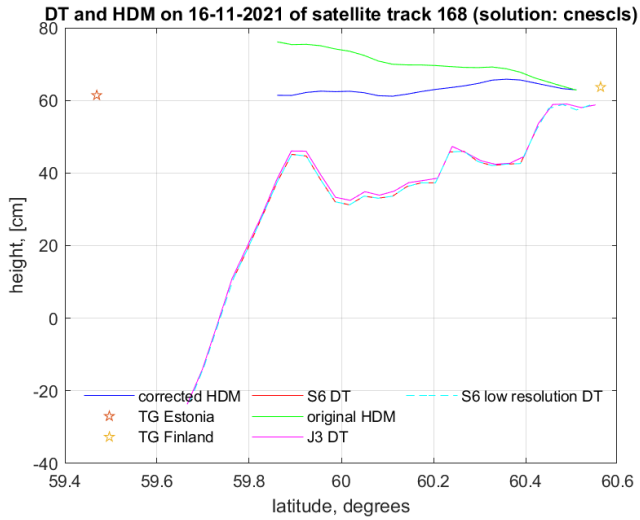


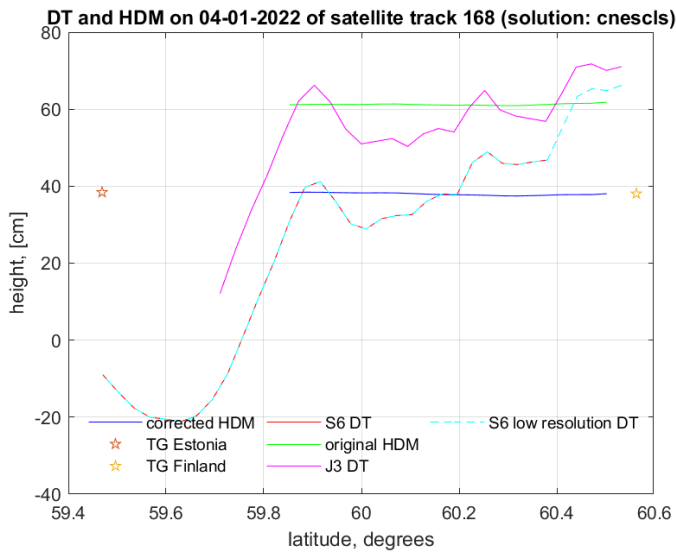
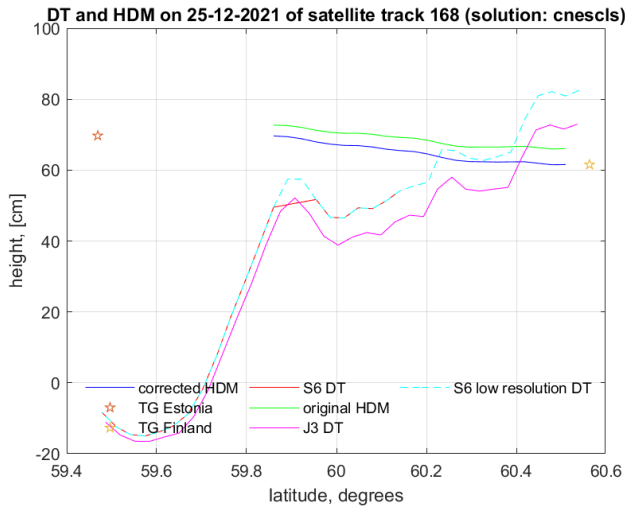
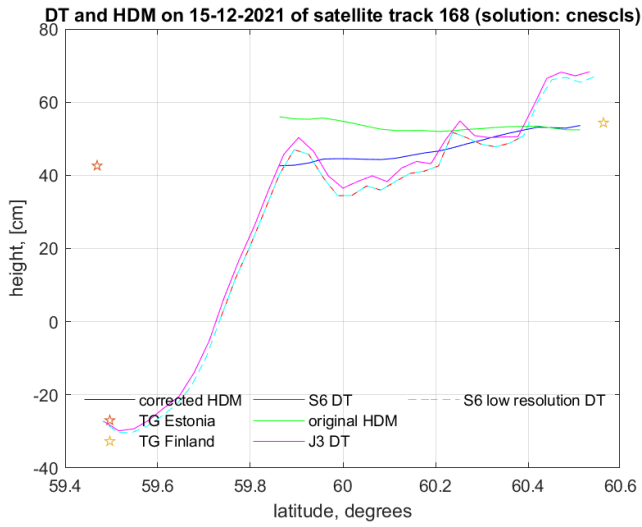


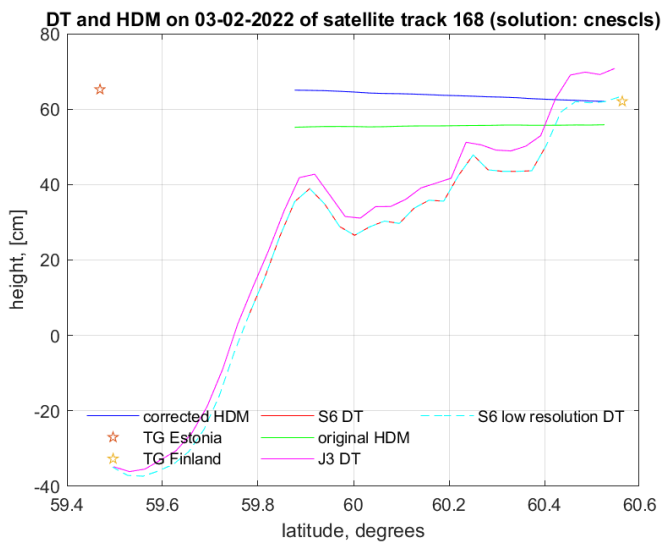
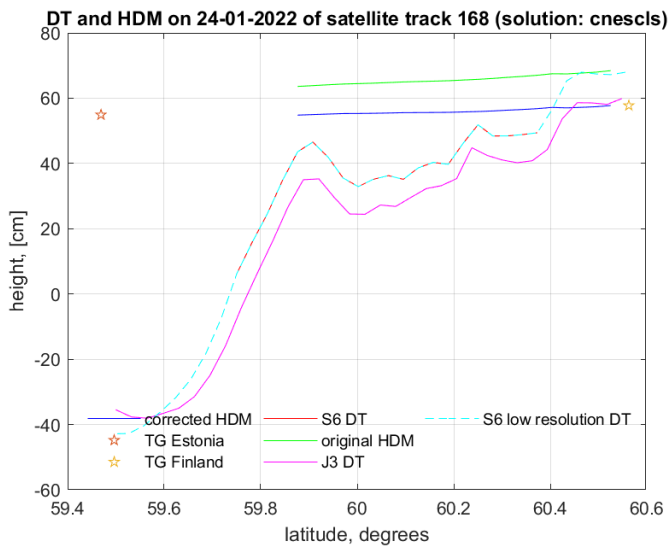
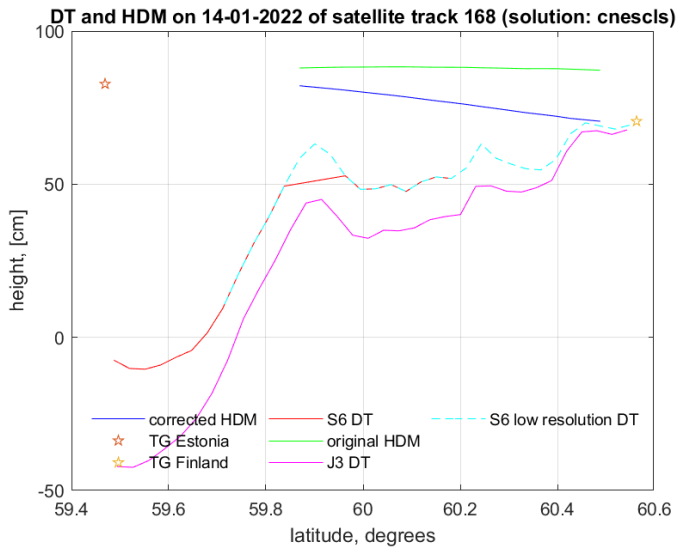


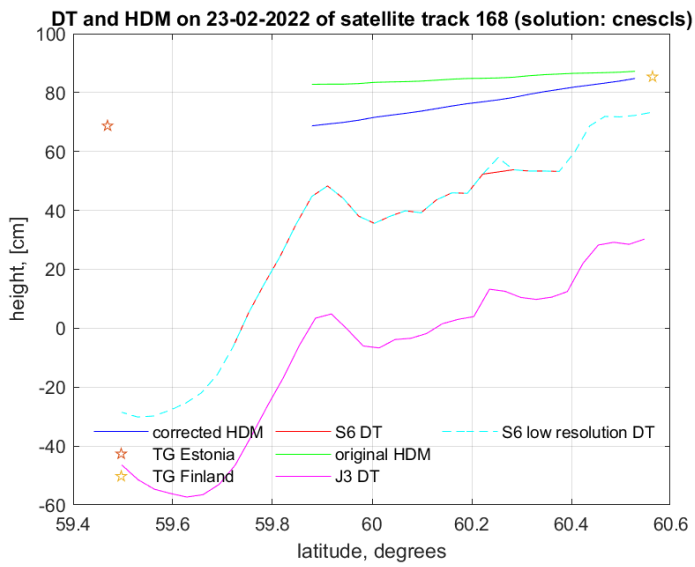
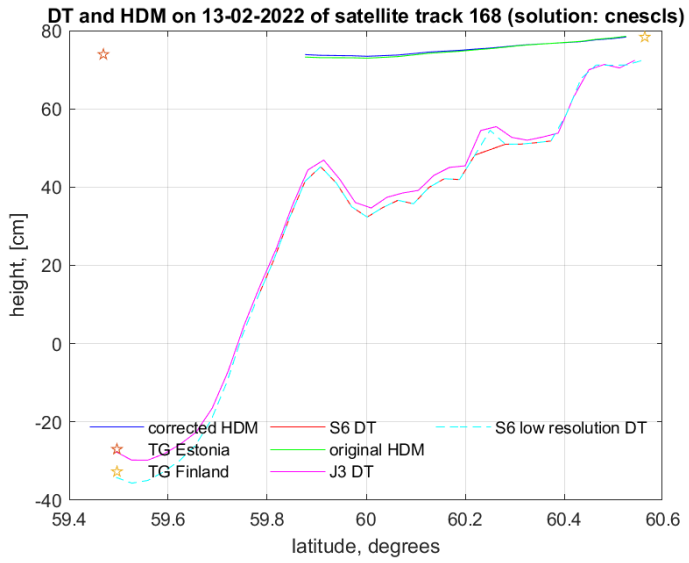


15.12 Results for the track of 0168 (Sentinel-6A and Jason-3)

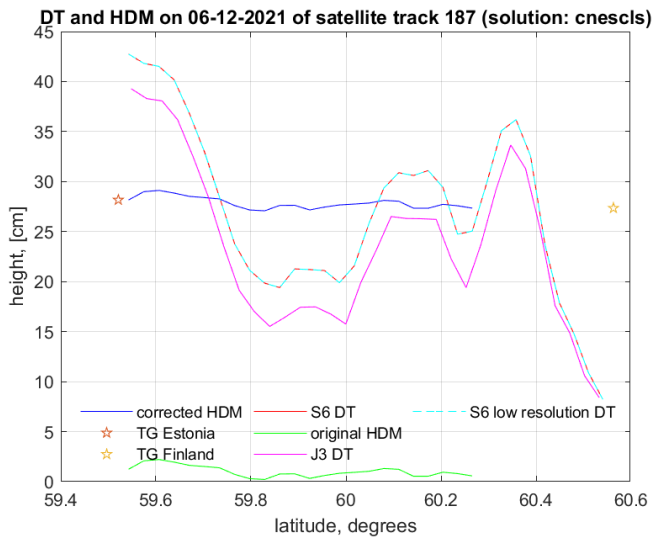
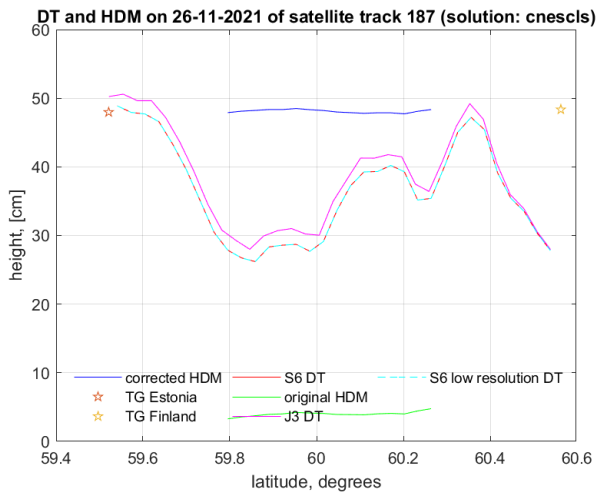
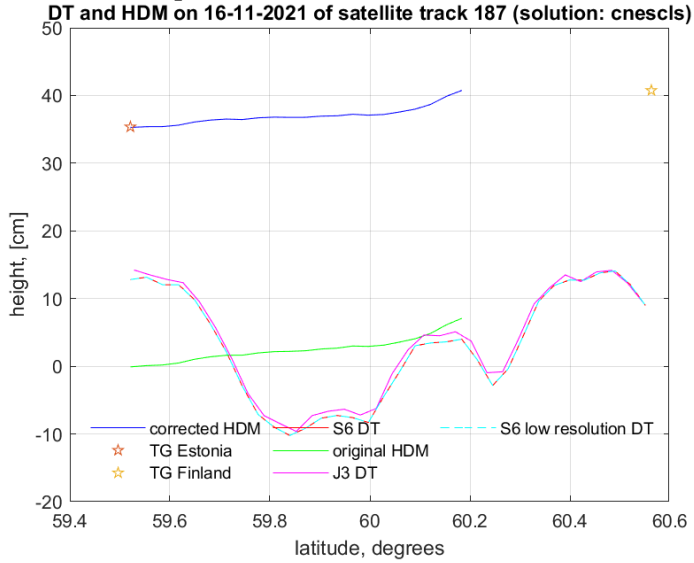


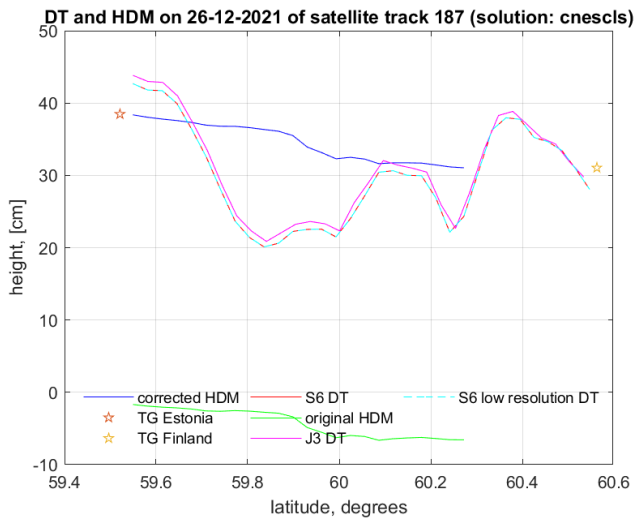
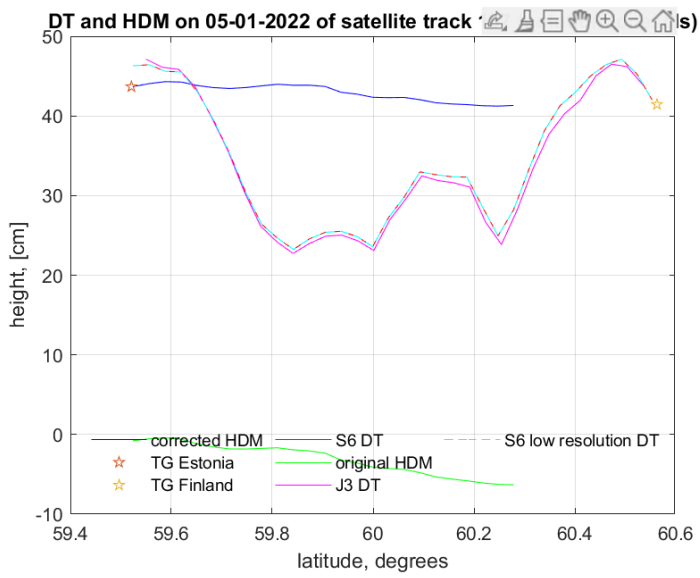
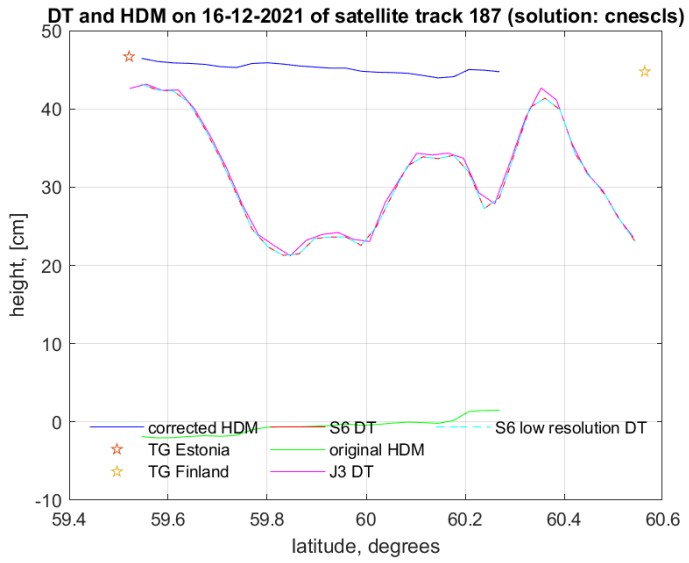


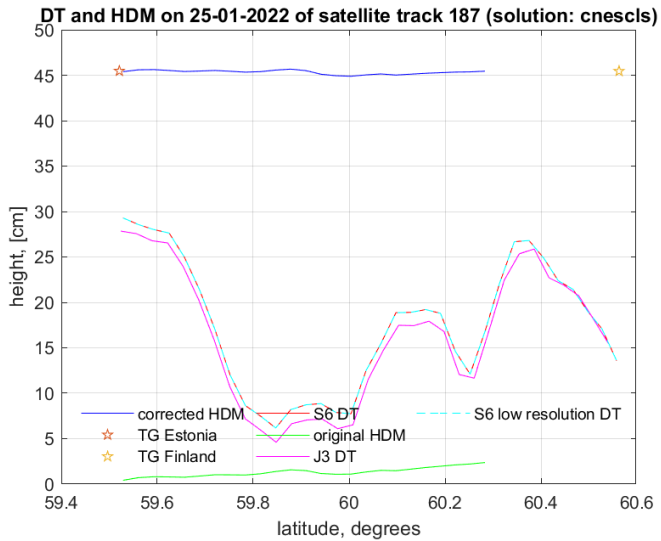
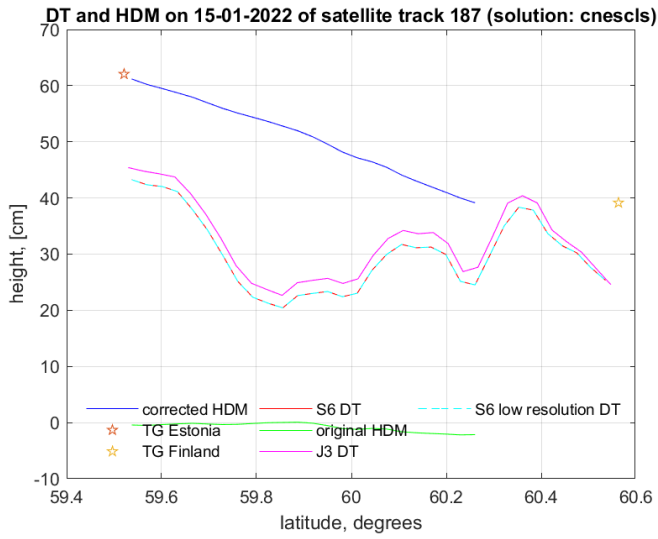
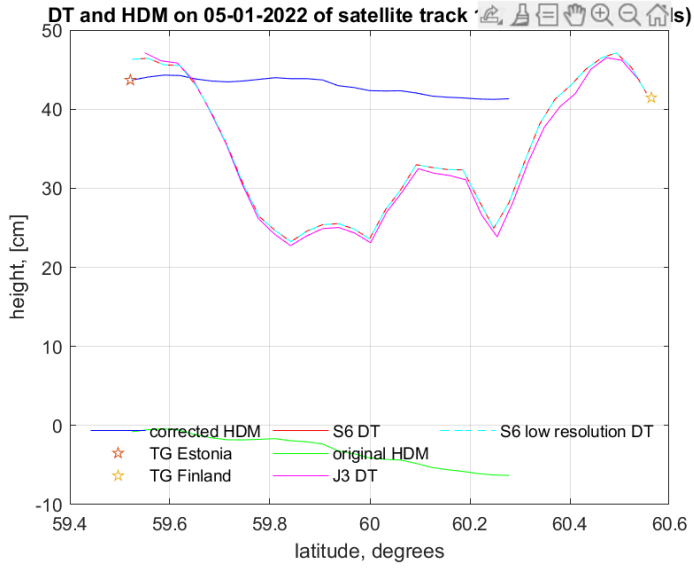


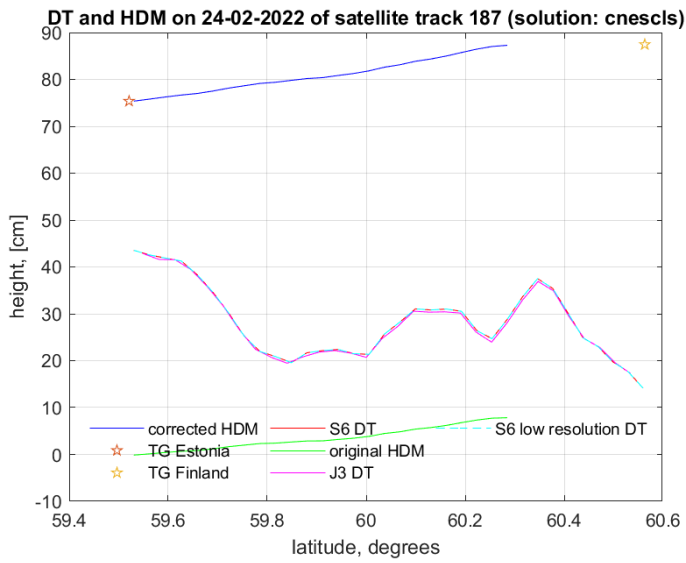
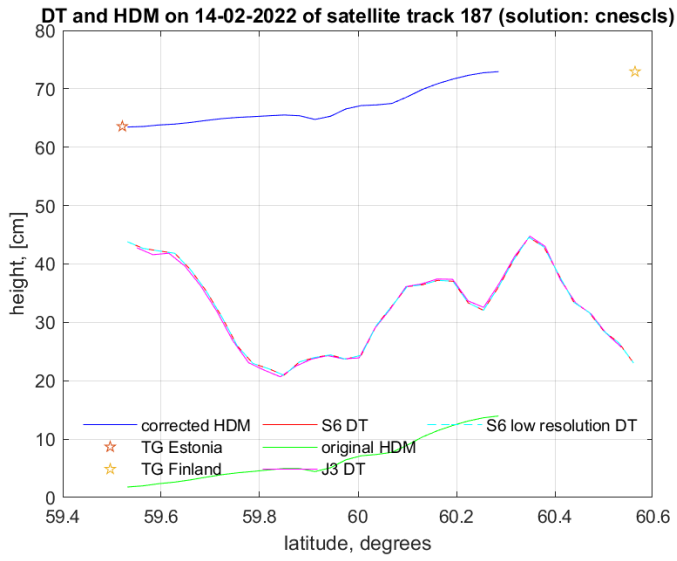


15.13 Results for the track of 0187 (Sentinel-6A and Jason-3)

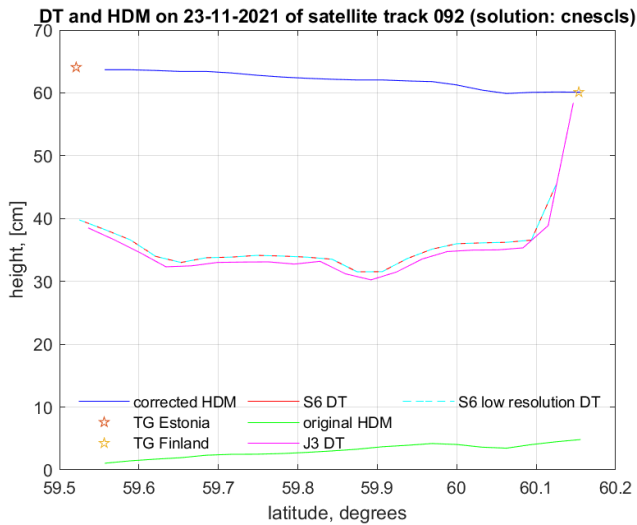
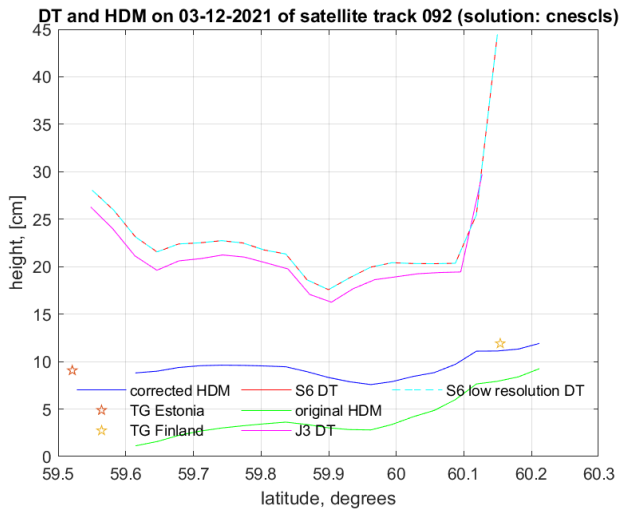
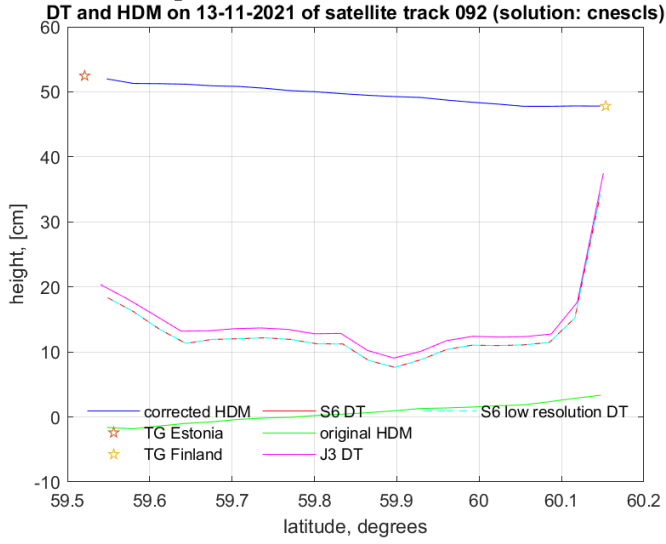


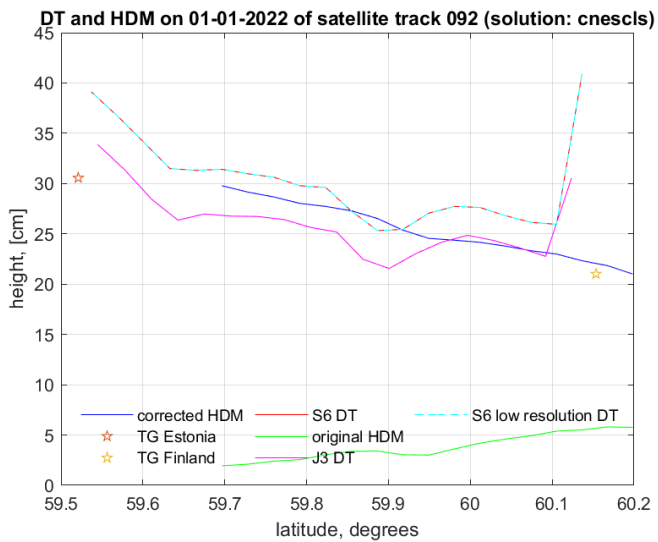
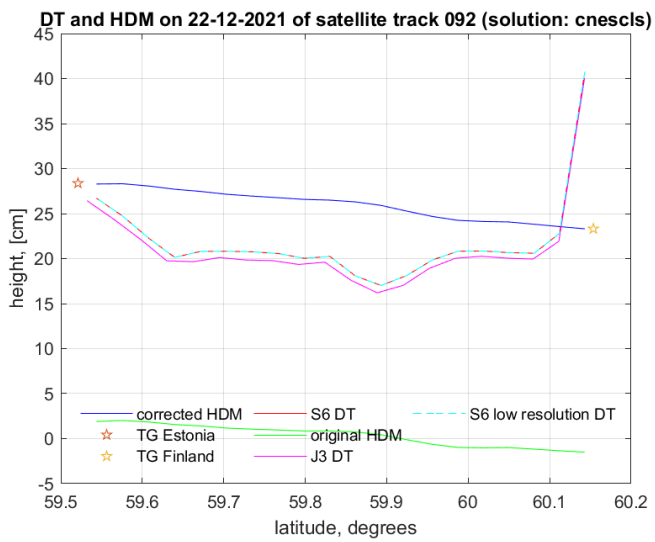
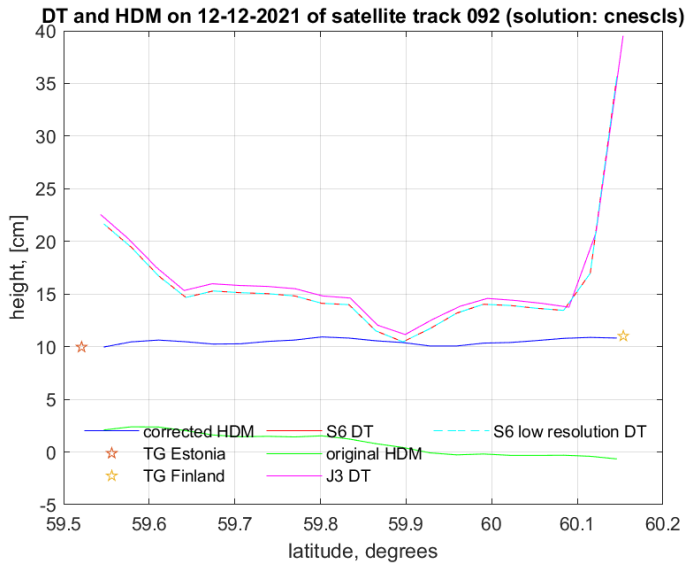


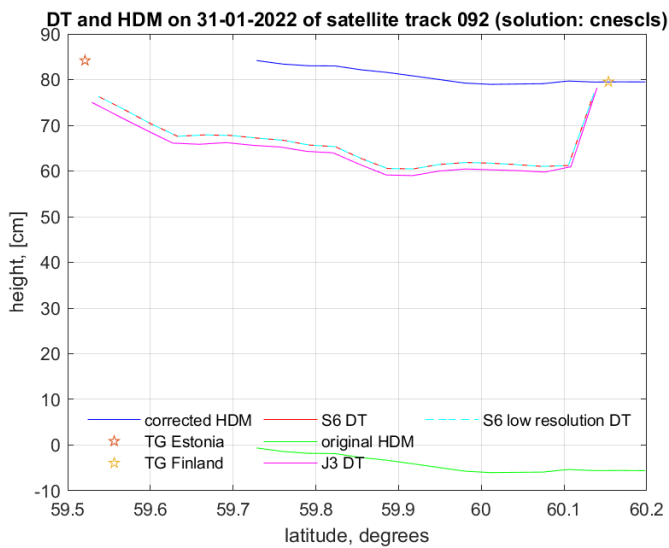
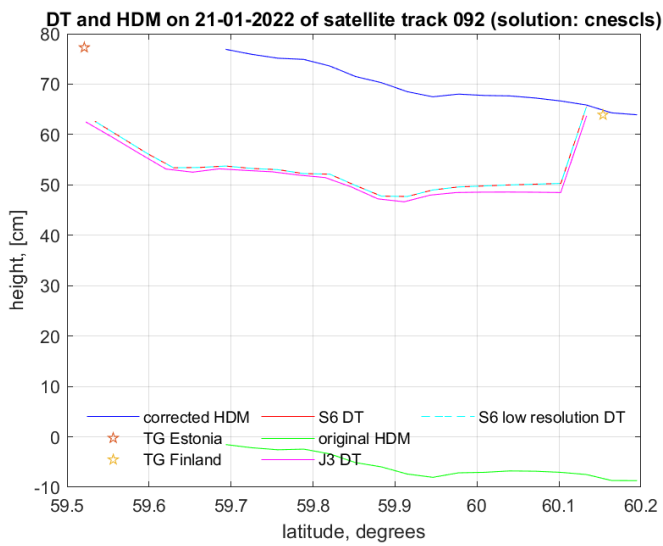
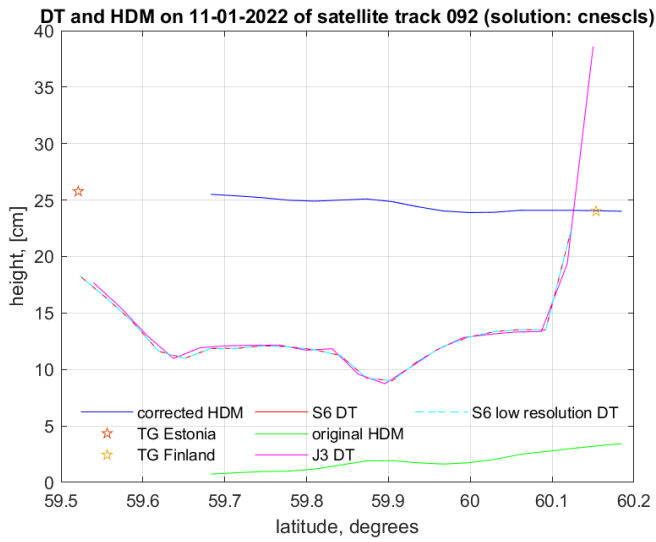


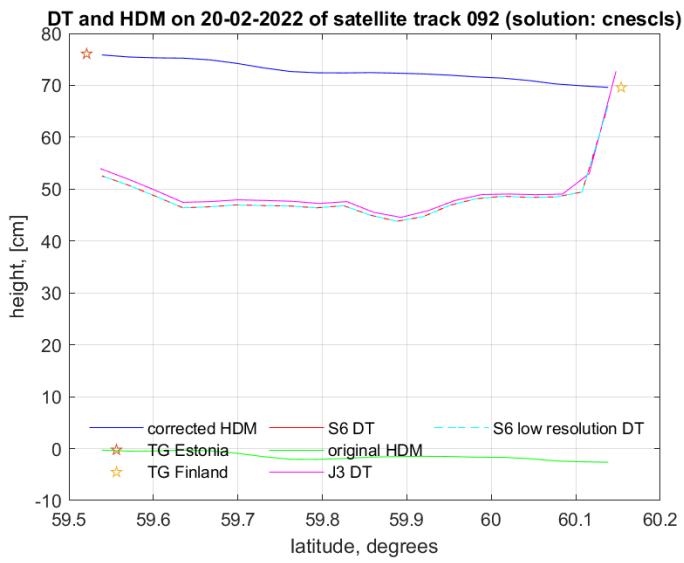
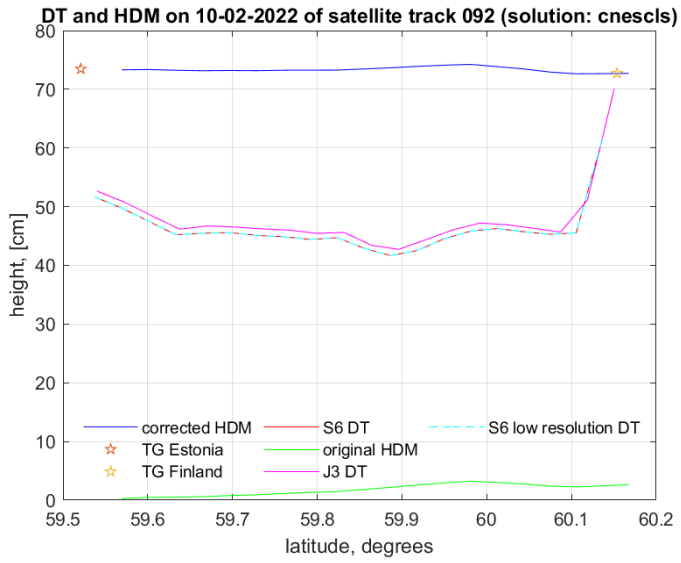


15.14 Results for the track of 0092 (Sentinel-6A and Jason-3)









15.15 Results for the track of 0016 (Sentinel-6A and Jason-3)

